

(NASA-CR-137660) PIONEER PROBE MISSION WITH  
ORBITER OPTION (TRW Systems Group) 153 p.  
HC \$6.25 CSDL 22A

N75-20439

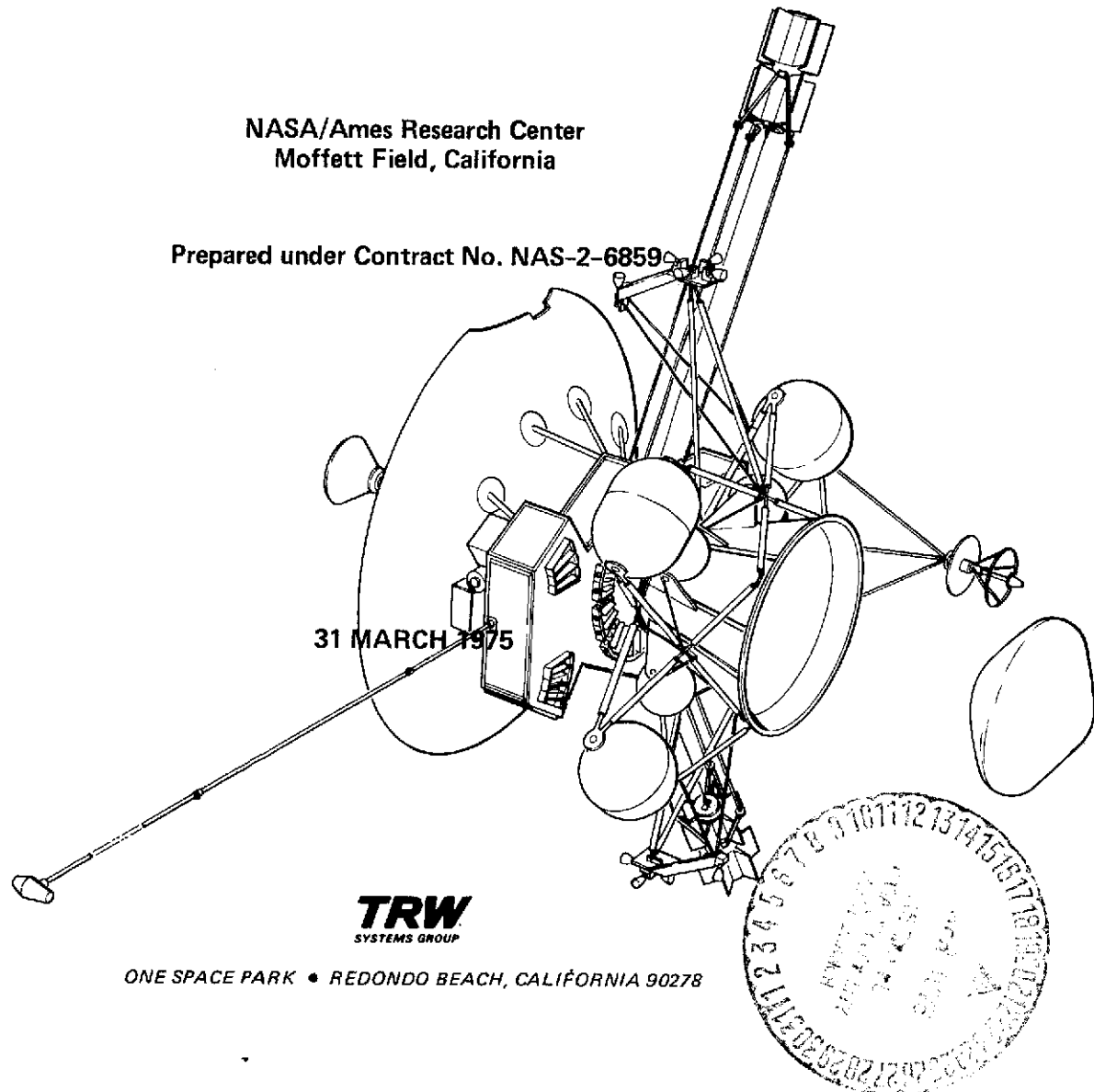
Unclas

63/15 18217

# PIONEER PROBE MISSION WITH ORBITER OPTION

NASA/Ames Research Center  
Moffett Field, California

Prepared under Contract No. NAS-2-6859



## ABSTRACT

Among the possible missions which are logical extensions of the Pioneer 10 and 11 flybys of the planet Jupiter are atmospheric entry probe missions and orbiter missions of outer planets. A particularly attractive mission is one in which a probe is delivered to Jupiter, and the spacecraft bus enters an orbit about the same planet. This single orbiter-probe mission (PJO<sub>p</sub>) is a feasible extension of current Pioneer technology.

This report, prepared by TRW Systems Group for NASA/Ames Research Center, describes the mission, its scientific objectives, and the spacecraft designs (particularly in terms of the modifications to the Pioneer 10 and 11 spacecraft) appropriate to accomplish the mission.

## CONTENTS

	Page
1. INTRODUCTION	1-1
1.1 Organization of the Report	1-1
1.2 Mission Summary	1-2
1.3 Related Documentation	1-3
1.4 Conclusions	1-5
2. SCIENCE OBJECTIVES	2-1
2.1 Scientific Background — The Importance of Jupiter Exploration	2-1
2.1.1 Implications of the Pioneer 10, 11 Results	2-2
2.1.2 Results Anticipated from Mariner - Jupiter-Saturn '77	2-7
2.2 Scientific Objectives of the Pioneer Orbiter Mission	2-9
2.2.1 Magnetospheric Science and the "Flower" Orbit	2-10
2.3 Probe Science Objectives	2-12
2.4 Science Instruments	2-12
2.4.1 Orbiter Instruments	2-12
2.4.2 Probe Instruments	2-16
3. MISSION ANALYSIS	3-1
3.1 Mission Profile	3-1
3.2 Mission Characteristics	3-4
3.2.1 Launch	3-4
3.2.2 Interplanetary	3-7
3.2.3 Orbiter Deflection	3-12
3.2.4 Probe Entry	3-16
3.2.5 Probe Communications	3-16
3.2.6 Orbit Selection	3-23

## CONTENTS (Continued)

	Page
3. 2. 7 Orbit Insertion	3-24
3. 2. 8 Raising Periapsis	3-26
3. 2. 9 Orbit Shaping by Satellite Encounters	3-27
3. 2. 10 Daylight Entry Options (Type 11 Trajectory)	3-29
3. 2. 11 Summary Propulsive Requirements and Performance	3-35
4. SUMMARY PROBE DESCRIPTION	4-1
5. SPACECRAFT DESCRIPTION	5-1
5.1 System	
5.1.1 Configuration and Summary of Requirement Changes from Pioneer 10 and 11	5-1
5.1.2 Mass Properties	5-6
5.1.3 Electrical Power Requirements	5-13
5.2 Subsystems	5-13
5.2.1 Structure	5-13
5.2.2 Thermal Control	5-17
5.2.3 Electrical Power	5-19
5.2.4 Attitude Control	5-22
5.2.5 Propulsion	5-27
5.2.6 Communications	5-33
5.2.7 Command and Data Handling	5-40
6. RADIATION EXPOSURE	6-1
6.1 Estimated Electron and Proton Fluences Experienced by Orbiter and Probe	6-1
6.2 Degradation Effects Due to Radiation Exposure	6-5
6.2.1 Probe Degradation	6-6
6.2.2 Orbiter Degradation	6-7
6.2.3 Recovery Effects	6-9
6.3 Radiation Summary	6-12

CONTENTS (Continued)

	Page
7. SCHEDULE	7-1
APPENDIX A - EQUIPMENT STATUS	A-1
APPENDIX B - TRW'S MULTIMISSION BIPROPELLANT PROPULSION SYSTEM	B-1

## ILLUSTRATIONS

		Page
2-1	Pioneer 10 Encounter Trajectory and Model Jupiter Magnetosphere	2-4
2-2	Sample "Flower" Orbit (a Jovian Particles-and- Fields Tour)	2-10
2-3	Probe Instrument Accommodation	2-17
2-4	Probe Data Collection Sequence	2-18
3-1	Mission Profile	3-1
3-2	Launch Vehicle Capability	3-5
3-3	Near-Earth Trajectory	3-6
3-4	Earth-Jupiter Trajectory Characteristics (1980). $C_3$ , $V_\infty$ .	3-8
3-5	Earth-Jupiter Trajectory Characteristics (1980). $C_3$ , DLA, ZAP.	3-9
3-6	Interplanetary Trajectory and Orbital Operations	3-13
3-7	Velocity Increment to Separate Spacecraft's Approach Trajectory from Probe's	3-14
3-8	Probe and Spacecraft Approach to Jupiter	3-17
3-9	Probe Entry Profiles. Nominal Atmosphere	3-18
3-10	Pressure vs Temperature for the Jupiter Model Atmosphere	3-19
3-11	Descent Profiles of the Probe	3-20
3-12	Probe Communication Geometry	3-21
3-13	Definition of Aspect Angles	3-22
3-14	Nominal Initial Orbit about Jupiter	3-23
3-15	Orbit Insertion $\Delta V$ . Ideal Transfer	3 25
3-16	$\Delta V$ at Apoapsis	3-27
3-17	Trajectory Quantities vs Arrival Date	3-30
3-18	Local Time at Probe Entry and Descent	3-31

## ILLUSTRATIONS (Continued)

		Page
3-19	Probe and Spacecraft Approach to Jupiter (Type II Trajectory)	3-32
3-20	Probe Communication Geometry (Type II Trajectory)	3-33
4-1	Probe Configuration	4-1
4-2	Carbon Phenolic Heat Shield Requirements	4-2
4-3	Mass Properties	4-3
5-1	Spacecraft Configuration	5-2
5-1	Spacecraft Configuration (Repeated for Reference)	5-16
5-2	Allowable Effective Blockage of the Pioneer 10, 11 Louver System vs Internal Spacecraft Dissipation	5-18
5-3	PJO <sub>p</sub> Shunt Regulator Diagram	5-20
5-4	Comparison of Total Shunt Power Dissipation	5-20
5-5	Pioneer 10 Maneuver Control Modes	5-23
5-6	Sun Precession and Auto-Spin Logic Block Diagram	5-25
5-7	Radial Thruster Control (PJO <sub>p</sub> )	5-26
5-8	Radial Thruster Program Logic	5-26
5-9	Pseudoperiod Logic Block Diagram	5-27
5-10	Five-Pound Thrust Biopropellant Engine	5 28
5-11	Five-Pound Thrust Propellant Engine	5-29
5-12	AJ10-181-1 Engine	5-30
5-13	Pulse Mode Performance - AJ10-181-1	5-31
5-14	Steady-State Performance - AJ10-181-1	5-31
5-15	New S/X Feed System	5-33
5-16	ALTAIR Scale-Model FSS Subreflector	5 34

## ILLUSTRATIONS (Continued)

		Page
5-17	Corrigated Horn Feed Used for DSCS-II Spot Beam Antenna	5-35
5-18	Uplink Communications Performance	5-36
5-19	Downlink Communications Performance	5-37
5-20	X-Band Beacon Link Margin Versus Range and Range Versus Time in Orbit	5-39
5-21	PJO <sub>p</sub> Command and Data Handling Equipment	5-41
6-1	Jupiter High Energy Particle Flux in Equatorial Plane	6-2
6-2	Jupiter Orbiter Fluence	6-3
6-3	Jupiter Probe Fluence 7-Degree Entry Angle — Equatorial Plane	6-4
6-4	Pioneer 10 Recovery of Telemetered RTG Parameters	6-10
6-5	Pioneer 10 Recovery of Oscillator Frequency Changes	6-11
6-6	Pioneer 10 Recovery of Telemetered TWTA Parameters	6-11
7-1	PJO <sub>p</sub> Spacecraft Schedule (Coordinated with Probe Schedule)	7-2

## TABLES

		Page
2-1	PJO Orbiter Model Payload	2-13
2-2	JPL Line-Scan Image System Characteristics	2-15
3-1	Major PJO <sub>p</sub> Mission Events	3-3
3-2	Criteria in Selection of Sample Trajectories	3-10
3-3	Inner Five Satellites of Jupiter	3-10
3-4	Compositions of Models of Jupiter's Atmosphere	3-19
5-1	Design Drivers Arising from New Mission	5-3
5-2	Pioneer Jupiter Orbiter Plus Probe Launch Weight	5-7
5-3	PJO <sub>p</sub> Mass Properties – Pioneer Jupiter Orbiter with Probe	5-8
5-4	Basic Spacecraft Subsystem Weight Summary	5-9
5-5	Basic Spacecraft Subsystem Details	5-10
5-6	Retropropulsion Unit Subsystem Weight	5-12
5-7	PJO <sub>p</sub> Power Requirements	5-14
5-8	Backup Sun Seeking Mode	5-22
5-9	Automatic Spin-Up/Spin-Down	5-24
5-10	RCS Propulsion - Engine SN 2 MIB Repeatability	5-32
5-11	X-Band Beacon Link Budget	5-38
5-12	PJO <sub>p</sub> Command and Data Handling Unit	5-42
5-13	Source of New Requirements	5-42
6-1	Criteria for Degradation Analysis	6-5
6-2	Probe Worst Case Equivalent of 3 MeV Electron Fluence and Degradation Fluence	6-6
6-3	Worst Case Dose at Components in Probe and Degradation Dose	6-7

TABLES (CONTINUED)

		Page
6-4	Equivalent 3 MeV Electron Fluence at Components for Orbiter ( $R_p/R_J = 1.8$ and Degradation Fluence	6-8
6-5	Orbital Dose ( $R_p/R_J = 1.8$ and Degradation Dose	6-8

## 1. INTRODUCTION

This document describes a spacecraft based on Pioneer 10, 11 and existing propulsion technology which can transport and release a probe for entry into Jupiter's atmosphere and subsequently maneuver to place the spacecraft in orbit about Jupiter. Orbital operations last 3 years and include maneuvers to provide multiple close satellite encounters which allow the orbit to be significantly changed to explore different parts of the magnetosphere.

### 1.1 ORGANIZATION OF THE REPORT

This introduction provides a mission summary, a guide to related documents, and conclusions.

Section 2 provides background information about Jupiter and its environment, and anticipates Mariner Jupiter Saturn results as it relates to the objectives of a Pioneer Jupiter Orbiter with Probe (PJO<sub>p</sub>) mission. It then develops these objectives, reflecting the conclusions of the joint ESRO-NASA PJO working group. Finally, brief descriptions of sample payloads for both probe and orbiter are given.

Section 3 covers mission analysis over the complete mission profile. It includes launch, interplanetary flight, probe release and orbit deflection, probe entry, orbit selection, orbit insertion, periapsis raising, orbit shaping maneuver capability, and a discussion of an alternate profile (Type II trajectory) which allows daylight entry of the probe.

Section 4 provides a probe description overview abstracted from studies performed by the McDonnell Douglas Corporation.

Section 5 provides a spacecraft description at both the system and subsystem levels. Emphasis is placed upon changes to the Pioneer 10, 11, the new retropropulsion stage and its derivation from the TRW Multimission Bipropellant Propulsion System, and the probe interface.

Section 6 discusses the effects of Jupiter's radiation belt on both the orbiter and the probe, and highlights potential problem areas.

Section 7 gives a brief discussion of the schedule associated with a 1980 launch.

Appendix A documents the status of residual Pioneer 10, 11 hardware, and Appendix B is a descriptive brochure about the Multimission Propulsion Stage.

## 1.2 MISSION SUMMARY

### Pioneer Jupiter Orbiter and Entry Probe Mission

Launch date	6 December 1980
Jupiter arrival date	14 February 1983
Probe entry life	30 minutes
Orbital lifetime	3 years
Injected mass (orbiter and probe)	1092 kg
Probe mass	150 kg
Probe instrument mass	20.4 kg
Orbiter instrument mass	50 kg
Launch vehicle	Titan 3E/Centaur/D-1T/ TE-364-4

### Objectives

To conduct comprehensive exploration of Jupiter, its atmosphere, physical environment and its satellites by combined observations from the orbiting spacecraft bus and an atmospheric entry probe designed to survive a descent to 10 bars or more. The long-life maneuverable spacecraft bus can operate at orbit inclinations ranging from equatorial to high latitudes, with repeated close encounters at the planet's Galilean satellites.

### Typical Science Investigations

#### Probe

- Atmospheric composition
- Hydrogen/helium ratio
- Cloud structure and opacity
- Temperature, pressure, density profiles
- Thermal energy balance
- Near planet radiation environment

## Orbiter

- Multispectral line-scan camera (imaging)
- Magnetosphere mapping
- Solar plasma interaction with Jupiter's magnetosphere
- Trapped particle detection and radiation belt mapping
- IR radiometry and spectrometry
- UV photometry
- Plasma wave/radio emissions
- Micrometeoroid detection
- Celestial mechanics observations (Jupiter and satellites)
- Radio physics (X-band beacon) (Jupiter and satellites)

## Mission Description

A combination entry probe/orbiter mission at modest cost is particularly attractive because of the complementary nature of probe and orbiter information. The probe concentrates on a physical and chemical description of the atmosphere and the orbiter on its time and latitude variability.

The orbiter also explores the environment around Jupiter, the magnetosphere, and its interaction with the solar wind. Further, multiple satellite encounter techniques developed by the JPL Advanced Projects Group, particularly Beckman, Roberts, Uphoff and Friedman, allow changing the orbit as well as providing close looks at the Galilean satellites.

A Pioneer line-scan imager has been studied by JPL. It provides 160 detector elements and takes a picture with 160 x 640 pixels. The pixel size is 0.1 mrad and, from typical satellite approach distances of less than 5000 km, will give pictures with higher resolution than earth-based astronomy of the moon.

### 1.3 RELATED DOCUMENTATION

Over recent years a number of studies and reports have been done which provide additional information. The following listing provides insight into the more significant of these:

- 1) "Pioneer F/G Spacecraft Operational Characteristics Study" Final Report, TRW Systems Report 71-7531-9-14, 23 April 1971. A comprehensive document on design features and operational characteristics of Pioneer F/G.
- 2) "The Pioneer Mission to Jupiter," NASA Report SP-268, Washington, 1971. A brief description of the Pioneer F/G missions, the scientific objectives, payload instruments, and the spacecraft and its support system.
- 3) "Study of Follow-On Pioneer Missions to Jupiter," TRW Systems Report 20406-6006-RO-00, 13 August 1971. A preliminary study which explores alternate design approaches for a Jupiter Orbiter without probe.
- 4) "Outer Planets Pioneer Spacecraft," NASA/Ames Research Center Report, 23 March 1973, and Revision 1, 15 April 1974. A document describing the design of advanced Pioneer spacecraft for outer planet flyby, orbiter, and probe missions. This document (Revision 1) also contains updated characteristics of Pioneer 10, 11.
- 5) "Extended Life Outer Planets Pioneer Spacecraft," NASA/Ames Research Center Report, 5 March 1974. A comprehensive review document of recommended approaches to extend mission life of Pioneer F/G type spacecraft as required for outer planet missions exceeding the basic 2.5-year mission life requirement of the baseline spacecraft.
- 6) "Pioneer Outer Planets Orbiter," NASA/Ames Research Center Report, 10 December 1974. A comprehensive study of Jupiter and Saturn orbiters (without probe). Basically an update of item 3), but including Saturn.
- 7) Draft of "Final Report, Pioneer Jupiter Orbiter," prepared by TRW for the 11 November 1974 meeting at NASA/Ames which discussed the possible ESRO participation in the mission.
- 8) Draft of "Pioneer Jupiter Orbiter Probe Mission - 1980, Probe Description," prepared by McDonnell Douglas Corporation for the 11 November 1974 meeting at NASA/Ames.
- 9) "Jupiter Orbiter - Study of Critical Aspects of a Joint ESA/NASA Project," prepared by Messerschmitt-Bolkow-Blohm GMBH-Space Division, MBB Report No. URU-77(74), December 1974. MBB study report about possible ESA (was ESRO) participation in the Jupiter Orbiter Mission, with emphasis on science integration, retropropulsion unit, and spacecraft integration.
- 10) "Pioneer Jupiter Orbiter and Probe Report on the Mission Definition Study" prepared by ESRO, MS(74)33, 30 December 1974. The official document used in determining whether there

would be European participation in the program. It summarizes material from items 7), 8) and 9) with the addition of the Mission Definition Group recommendations.

#### 1.4 CONCLUSIONS

This mission will fully characterize Jupiter's atmosphere using probe instrumentation, and because of the orbiter's long life and orbit flexibility (through satellite gravity swingbys) it will provide both temporal and position information about the magnetosphere and environment about Jupiter. Further characterization of atmospheric long term motions and cycles will be obtained by the visual images and UV and IR sensors.

The mission is cost effective and its Pioneer 10, 11 hardware base can lead to further cost savings.

Further study is recommended for the following items:

- Preparation of a definitive spacecraft/probe interface document.
- The navigation problem associated with obtaining multiple satellite encounters. In particular, the possible improvements in Galilean satellite ephemerides, DSN tracking capabilities, and the merit of onboard sensing of satellite directions.
- Cost comparisons between using domestic or European propulsion components. Also on the merit of using residual Apollo (LEM attitude control) engines for the main thruster.
- Further definition of the possible need for radiation hardening and investigations of annealing of radiation-damaged components.
- Preparation of detailed development plans for probe and orbiter.

## 2. SCIENCE OBJECTIVES

### 2.1 SCIENTIFIC BACKGROUND – THE IMPORTANCE OF JUPITER EXPLORATION

Shortly after the time when spacecraft started to make direct measurements of the earth's radiation belts (Van Allen, 1958), it became evident that Jupiter also has an extensive radiation belt, and that synchrotron radiation from the energetic electrons is responsible for the Jovian decimetric radiation (Drake and Hvatum, 1959). Since that time, the measurements of intense decametric bursts from Jupiter (Burke and Franklin, 1955) have also been discussed in terms of mechanisms and processes that are thought to be operative in the earth's magnetosphere and auroral regions. Moreover, the discovery of the striking effect of the orbital position of Jupiter's satellite Io upon the decametric emission (Bigg, 1964) indicated years ago that these satellites can interact very strongly with the Jupiter magnetosphere, and the observations suggested that the satellite interactions can directly affect the coupling between the ionosphere and magnetosphere.

Well before the Pioneer encounters these radiometric observations indicated that Jupiter's magnetic field was considerably stronger than the earth's field; since Jupiter is immersed in the low density solar wind at 5.2 AU, this clearly meant that the Jupiter magnetosphere would be enormous in comparison to that of earth (Carr and Gulkis, 1969). Minimum particle fluxes for trapped inner belt electrons at relativistic energies were also deduced from the decimetric observations (Warwick, 1970), and it was widely accepted that the Jovian radiation belts contained considerably higher electron fluxes than the earth's belts.

Another unique feature of Jupiter's magnetosphere is related to the very high rotation rate of the planet. In recent years, Piddington (1967), Brice and his coworkers (Brice and Ioannidis, 1970; Ioannidis and Brice, 1971; Brice and McDonough, 1973), and others, pointed out that centrifugal forces would dominate the plasma configuration, and their theories strongly suggested that Jupiter's magnetosphere would not resemble that of earth. In fact, even before the initial Pioneer 10 measurements, these

theoretical speculations indicated that the Jovian magnetosphere might have properties similar to those of pulsars and other astrophysical objects (see Michel, 1969; Michel and Sturrock, 1974), and this astrophysical comparison was supported by recent analyses suggesting that Jupiter emits detectable levels of cosmic rays (Pizella and Venditti, 1973).

The concept that study of the magnetospheres of Jupiter and earth would lead to understanding of significant astrophysical questions was also widely accepted long before the Pioneer 10, 11 encounters. In a 1968 report of a study by the Space Science Board of the U.S. National Academy of Sciences ("Physics of the Earth in Space," p. 2), the following general arguments were used to support the need for detailed exploration of the magnetospheres of earth and Jupiter:

"Among the objects of greatest astrophysical interest today are pulsars, quasars, and x-ray stars. Most models proposed for such bodies involve concepts of intensified magnetic fields attached to collapsed and rapidly rotating stars, with twisted field lines subject to tearing and reconnection, perhaps forming closed magnetospheres in which particles may be accelerated by hydromagnetic or stochastic processes. The processes of particle acceleration characteristic of magnetized plasmas also appear in laboratory beam plasmas; in solar flares, supernovae, radio galaxies, quasars; and probably operate at the sources of cosmic rays."

For all of these reasons, it has been concluded that Jupiter missions (including orbiters and an entry probe) must have very high priorities. The 1971 report of a study by the Space Science Board of the U.S. National Academy of Sciences ("Priorities for Space Research 1971-1980," p. 9) contains the statement "We concluded, however, that a thorough study of Jupiter is, for the near future, the most rewarding objective among the outer planets and will contribute to the experience needed for successful missions to more distant planets at a later time."

### 2.1.1 Implications of the Pioneer 10, 11 Results

#### Jupiter Flyby Data

The successful Pioneer 10, 11 flybys of the Jupiter magnetosphere in December 1973, 1974 provided direct first-order information on the

planetary magnetic dipole moment, the trapped radiation population, and the overall configuration of the magnetosphere out to about  $150 R_J$ . In addition, the observations show indirectly but conclusively that plasma physics phenomena actually control the entire magnetosphere. The basic phenomena revealed by the Pioneer 10 and 11 (see Science, 183, 301-325, 1974; J. Geophys. Res., 79, 3487-3694, 1974) observations can be summarized as follows:

- 1) The magnetic dipole moment is only about  $4 \text{ gauss} \cdot R_J^3$ , rather than the  $(10-12) \text{ gauss} \cdot R_J^3$  value previously estimated, but the orientation and offset are similar to the values deduced by radio astronomers.
- 2) Despite the small value of the surface field, the Jupiter magnetosphere is much larger than anticipated, because some unmeasured "thermal" plasma drags the field outward and causes it to be distorted into a sun-like radial spiral. The  $\beta \approx (1)$  plasma may involve energized photoelectrons or secondaries from the Jovian atmosphere, and the variable interaction with the solar wind (over the range 50 to  $100 R_J$ ) may involve two-stream instabilities, as conjectured by Michel and Sturrock (1974). The planetary field lines can merge with the interplanetary field over the entire outer region, with current-driven plasma instabilities providing the dissipation mechanism. Some idea of the vast extent of the Jupiter magnetosphere is indicated in Figure 2-1 where the earth-to-Venus distance and the solar disk are shown on the Pioneer 10 trajectory plot, along with Van Allen's sketch of the possible magnetodisk configuration.
- 3) Within about  $20 R_J$ , the trapped energetic electron levels are much greater than those found on earth, and up to a hundred times greater than predicted by the Radiation Belt Workshop upper limit model. The Pioneer 10 data suggested that there could be a problem in accounting for the observed decimetric radiation pattern because these measured particle fluxes appear to be too high, but the Pioneer 11 results indicate that this problem might be resolved when experimental uncertainties are taken into account.
- 4) The Pioneer 10 trapped proton fluxes fell off strongly within  $L \approx 3.6$ , suggesting that an electrostatic or magnetic ion cyclotron instability might be very effective at low L-values. However, Pioneer 11 data show that the fluences rise again on even lower L-shells, and satellite effects or plasma instabilities could account for the flux ripples.
- 5) There is evidence for collisionless local acceleration (to MeV energies) of electrons and protons throughout the magnetosphere out to the bow shock, and intense fluxes of usually energetic particles were observed over vast upstream distances.

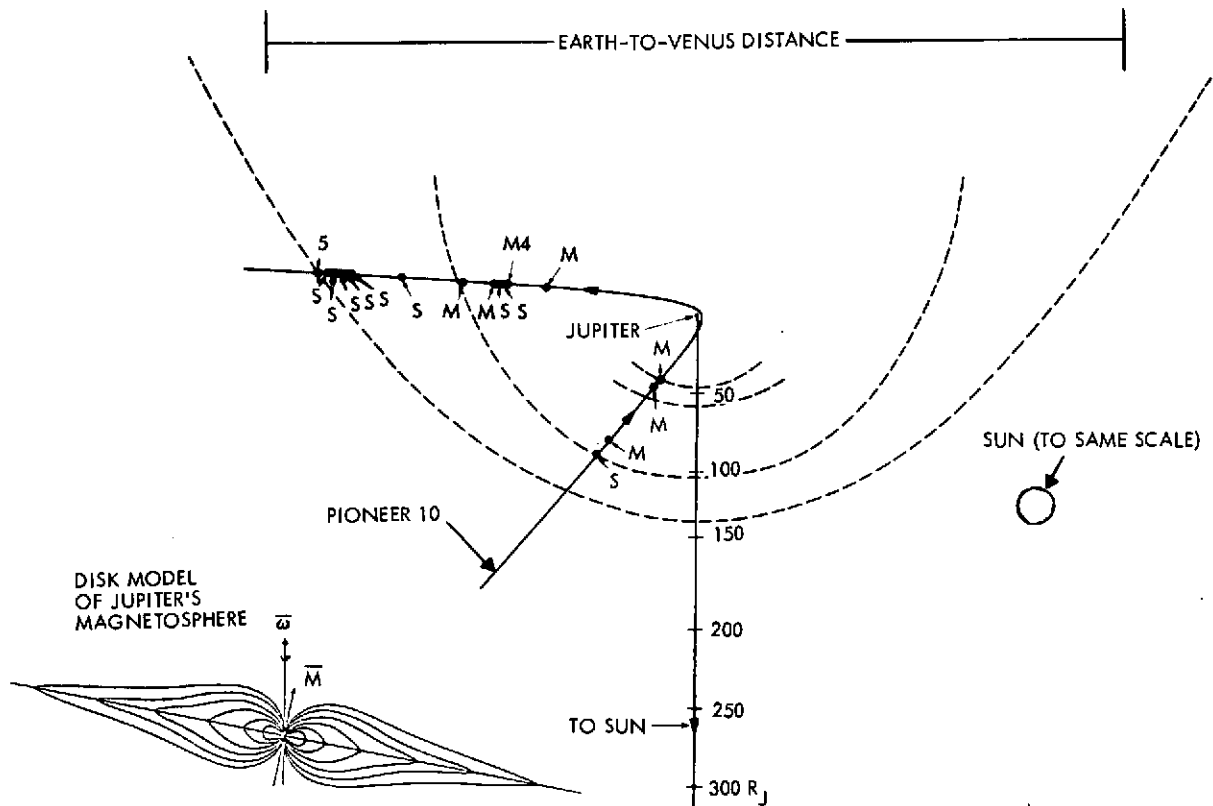


Figure 2-1. Pioneer 10 Encounter Trajectory and Model Jupiter Magnetosphere

- 6) The Pioneer 10, 11 spacecraft could have charged to large potentials during the encounter; the measured fluxes near  $L = 12$  were comparable to expected photoemission fluxes. Some spacecraft anomalies and false commands were detected on Pioneer 10 and 11 near  $L = 12-13$ ; these might be attributed to impulses associated with sheath fluctuations. However, there was not an unambiguous (sheath-independent) measurement of  $N$  (thermal), so that one cannot determine the sheath conditions or the magnitude of the sheath correction with certainty.
- 7) The origin of the Jupiter ionosphere is somewhat obscure because the observed trapped particle fluxes are so close to the expected stable trapping limits [for nominal  $N$  (thermal)-values] that the precipitating particle flux may well control the ionization, as it does in the earth's polar ionosphere.
- 8) Since the observed dipole field strength is so low, it may be very difficult to explain the decametric radiation in terms of ionospheric gyrofrequency radiation. However, if magnetospheric wave-particle interactions provide enough precipitation to enhance the ionospheric density above about  $5 \times 10^6 \text{ cm}^{-3}$ ,

electrostatic emissions at  $(n + 1/2) f_c^e$  can couple strongly to the radiation field and account for the observed decametric spectrum. On the other hand, large higher order moments (suggested by one Pioneer 11 magnetometer experimenter) could account for large  $f_c^e$ -values within the ionosphere.

- 9) The cloud top temperatures determined by the Pioneer 10, 11 IR radiometers agree with expectations based on remote measurements from earth, but the radio occultation data provide a very different temperature versus pressure profile for the upper atmosphere.
- 10) Pioneer 10 found that Io has an atmosphere and an ionosphere, and that it emits a torus of hydrogen. There is evidence from Pioneer 10 and 11 that the inner Galilean satellites and Amalthea interact strongly with the magnetospheric plasma and energetic particle population.

#### Radiation Belt Data

Pioneer 10, 11 also enabled us to draw the following conclusions regarding preencounter theoretical ideas on the radiation belts:

- 1) Radial diffusion is probably operative in the Jovian radiation belts.
- 2) There is inferential evidence that plasma turbulence may cause electron losses in the region  $10 < L < 20$ . There the particle fluxes above 100 KeV have a magnitude consistent with that required to stimulate whistler turbulence. In addition, they depend much more weakly upon  $L$  than the  $L^{-4.5}$  or  $L^{-6}$  required for loss-free radial diffusion. The electrons, if they precipitate, will carry a heat flux of 0.1-1 erg/cm<sup>2</sup>sec to Jupiter's upper atmosphere, and thus will be comparable at least with solar UV as an ionizing source. In addition, Van Allen argued, on the basis of Pioneer 11 results, that whistler-mode instabilities control the many MeV electron fluxes within  $L \approx 7$ .
- 3) Sweep-up losses at Io and Europa were less severe than anticipated by some. However, the radiation belts at these  $L$ -shells are sufficiently intense that significant energy fluxes to the satellite surfaces, and/or to Io's ionosphere are expected. Whether the satellites can also energize particles is unclear, but plausible interactions involving the satellite plasma sheaths have been suggested.

From the point of view of theory, Pioneer 10, 11 left several important puzzles unresolved. The main Pioneer 10, 11 shortcoming was the absence of detectors for plasma turbulence and radio waves. The

observed electron energy spectrum,  $E^{-(1-2)}$  was a surprise to many. However, for many years, astrophysicists knew that cosmic radio sources possessed such energy spectra. If Jupiter's relativistic electron energy spectrum could be understood, the result might be of general astrophysical significance. In addition, Pioneer 10, 11 gave only limited information on low energy (<70 KeV) radiation belt particles. If there are many of these, and if they precipitate, they could be the dominant energy source for Jupiter's upper atmosphere. Finally, the structure of Jupiter's outer magnetosphere, beyond  $L = 20$ , is poorly understood. It is obvious that radiation belt particles do not come directly from the solar wind into a simple dipolar magnetic field, as theory assumes, but must traverse, or be generated in, Jupiter's outer magnetosphere.

### Outer Magnetosphere

Pioneer 10's most interesting result is that Jupiter's outer magnetosphere is spun out into the long extended "magnetodisk" (see Figure 2-1) where the magnetic field is weak and nearly radial. However, on the Pioneer 11 outbound passage at high latitudes, there was little indication of a disk-like configuration in the dayside hemisphere. Near the equator energetic particles are found in the magnetodisk. The low-latitude magnetopause, separating the magnetodisk and magnetosheath, is highly variable in time. This disk-like configuration, so unlike earth's and so reminiscent of pulsar theories, is not well understood.

Theories of Jupiter's magnetosphere have thus far fallen into three classes:

- 1) Radial outflow models. Spurred on by the pulsar analog, various authors have assumed that a magnetodisk would be generated by a miniature Jovian solar wind, driven by particles flowing out from Jupiter's ionosphere or generated in the  $L < 20$  region, and spun up by the planet's rapid rotation. Here the plasma flow in the disk would be radially outward, and the magnetic field would be wrapped into a gardenhose configuration.
- 2) Earth-like convection models. It has also been suggested that reconnection of the solar wind magnetic field with Jupiter's field would drive an internal convection pattern similar to earth's. The extended disk in this model would be due to the fact that the flow has a larger energy density than the magnetic

field. Here, the flow would be, at times, directed in the antisolar direction. Its speed would exceed the local Alfvén speed.

- 3) Quasi-static magnetodisk models. Here it is assumed that particles from Jupiter's atmosphere or inner magnetosphere fill closed field lines and do not flow rapidly outward. Their inertia pulls the field lines out into a disk. Here there are two possibilities for the expected flow speed. If Jupiter communicates its rotation directly to the field lines, a flow velocity at the local corotation speed and direction would be expected. On the other hand, if Jupiter's atmosphere cannot support complete corotation, the flow speed would be less than (perhaps much less than) the solid body corotation speed.

The Pioneer 10, 11 plasma probe was not designed to measure corotation flows, antisolar flows, or magnetospheric distributions. In addition, because of the very great time variability of Jupiter's magnetodisk, it is possible that Pioneer 10, 11 may not have spent enough time in Jupiter's magnetosphere for a distinct pattern to emerge from analysis of the magnetic field data. There remains open the possibility that more than one of the above mechanisms operates, and at different times. Finally, it is worth noting that there may be a remarkable linkage between the dynamics of Jupiter's upper atmosphere and its magnetosphere. It is not beyond the realm of possibility that the upper atmospheric winds of Jupiter are controlled by flows in the magnetosphere (for instance, its polar cap upper atmosphere may not corotate), and that the flow in the magnetosphere is influenced by the state of the upper atmosphere (Kennel and Coroniti, 1974).

#### 2.1.2 Results Anticipated from Mariner-Jupiter-Saturn '77

The Mariner-Jupiter-Saturn '77 (MJS) encounters will provide a wealth of additional information on the dynamics of Jupiter's atmosphere, on planetology of the Galilean satellites, and on some very important magnetospheric processes.

Because of the high data rate, large weight and power capability, spacecraft stabilization and inclusion of a maneuverable scan platform, there will be a huge increase in the science return from the remote sensing instruments (television, IR radiometer, UV spectrometer, and imaging photopolarimeter). It can be expected that MJS will provide complete imaging of the major satellites, complete information on the

dynamics of the Jovian atmosphere, greatly enhanced knowledge of the atmospheric structure and composition, and information on emissions from the region of the satellite orbits. The use of dual frequencies for the radio science investigation may lead to an unambiguous resolution of the present discrepancy between IR and radiometric determinations of the Jupiter temperature-pressure profile.

The magnetospheric information anticipated from MJS should also provide a significant advance in knowledge. The plasma wave investigation is designed to determine the local plasma density profile (by detecting the plasma frequency cutoff), and to identify the wave-particle interaction mechanisms that can precipitate particles from trapped orbits, lead to stochastic acceleration, provide cross-L diffusion, and produce finite electrical resistivity along field lines. It is possible that this investigation will lead to detection of a collisionless shock within the magnetopause, indicating that there is supersonic radial flow outward. The MJS planetary radio astronomy investigation will provide definitive information on the source of the decametric radiation and its modulation by Io, Europa (or other satellites), the possible analog of the earth's intense night side radiation (associated with discrete auroral arcs), and the origin of the very rapid fine structure in Jupiter's radiation. These two experiments may also determine if lightning occurs in Jupiter's atmosphere.

The MJS plasma probe and trapped radiation detector are designed to extend the Pioneer 10, 11 measurements to lower energies, and to observe in different directions. It is possible that MJS will detect corotating flow directly. Moreover, it is anticipated that after the two MJS spacecraft encounter Jupiter, the present relatively small discrepancy between earth-based observations of synchrotron radiation and in situ measurements of energetic particles will have been resolved.

The MJS trajectories have also been selected to provide important information on the dynamical interactions of satellites with Jupiter's magnetosphere. One spacecraft will traverse the Io flux tube and the other will fly through the wake of Ganymede.

## 2.2 SCIENTIFIC OBJECTIVES OF THE PIONEER ORBITER MISSION

### 2.2.1 Magnetospheric Science and the "Flower" Orbit

Although extremely important magnetospheric measurements remain to be made by the two MJS spacecraft, it is already completely clear that the necessary fundamental understanding of Jupiter's magnetosphere will not be attained until a specific magnetospheric orbiter mission is completed. The basic difficulties with any flyby missions are that the spacecraft necessarily traverse only limited portions of the magnetosphere in mid-morning and in the pre-dawn regions (see Figure 2-1; no flyby spacecraft can provide any local information on the magnetospheric tail of Jupiter or on the dusk-afternoon region) and the spacecraft fly past so rapidly that temporal variations cannot be unambiguously understood (the Jovian analog of a substorm may have a time scale of a week or more). Moreover, the Pioneer 10, 11 and MJS payloads were essentially made up on the basis of earlier theoretical ideas on the Jupiter magnetosphere. Thus, there is no magnetospheric plasma probe pointing in a direction to detect radial outflow near noon or dawn, or anti-sunward convective flow near dawn. Finally, certain important measurements that are readily made on an orbiting spinner (e.g., direction of arrival for radio emissions; complete particle pitch angle distributions) are not easily carried out on a stabilized spacecraft. All of these considerations together place several demands on the orbiter trajectory, and this is discussed in more detail.

#### Spatial Coverage

The most basic difficulty with Jupiter orbital missions has recently been resolved. Ordinarily, the local time of the line of apsides of a spacecraft in orbit about Jupiter changes by only 30 degrees a year, as Jupiter slowly traverses its 12-year period about the sun. This means that a spacecraft which initially explores the local dawn sector of Jupiter's magnetosphere will only traverse the local midnight magnetic tail region after 3 years -- the nominal design lifetime of the spacecraft. However, close flybys of the Galilean satellites permit rapid changes in the direction and length of the line of apsides, as well as the inclination of the

orbital plane. This freedom gives the scientific community the opportunity to "design" an orbit according to scientific priorities. The NASA-ESRO PJO working group arrived at the following tentative priorities.

- 1) One large ( $150 R_J$ ) equatorial orbit at local dawn, and one as similar as possible at local evening, to study the asymmetries in the magnetosphere induced by corotation.
- 2) One large ( $150 R_J$ ) equatorial orbit at local midnight, to study the magnetic tail. If convection is important, as it is from earth, most of the particles injected into the magnetosphere will come from the tail.
- 3) The Pioneer Jupiter Orbiter mission should be designed so that the hazard from the radiation belts is acceptable.

Preliminary orbit calculations indicate that objectives 1), 2), 3) can be met within the 3-year design constraint, as shown in Figure 2-2. Several other features of the satellite swingby technique of orbit design are notable. In between the large long orbits, there will be many ( $\approx 38$ ) smaller orbits (typically  $15 \times 30 R_J$ ).

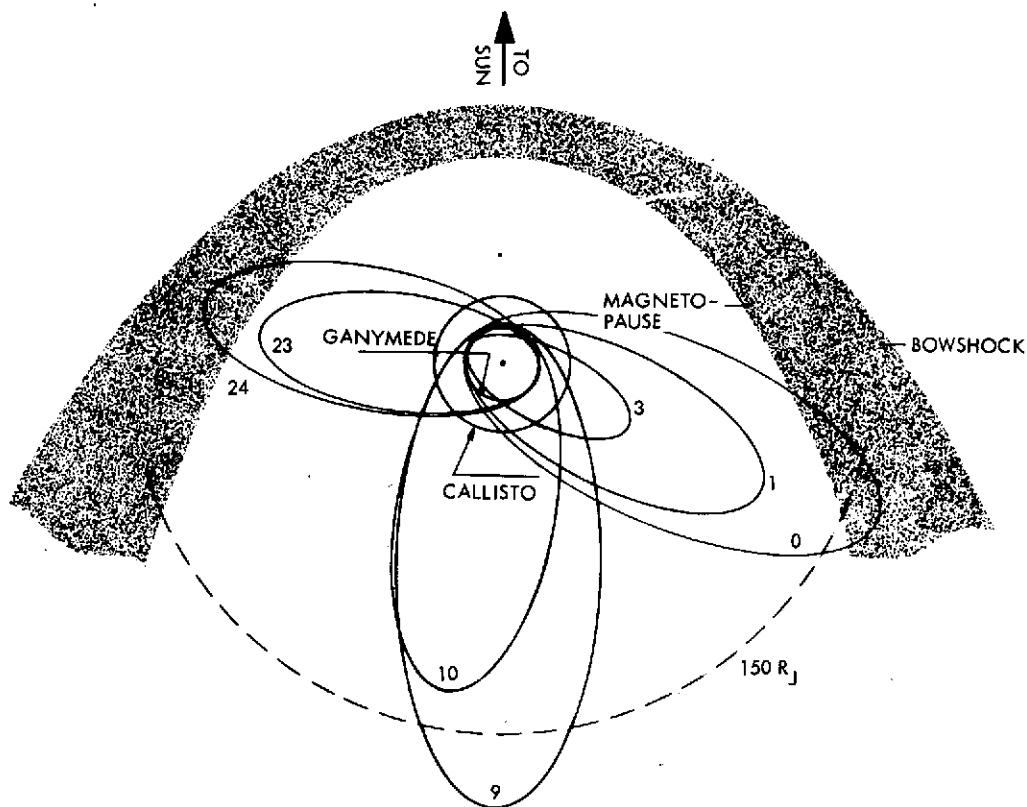


Figure 2-2. Sample "Flower" Orbit (a Jovian Particles-and-Fields Tour)

These orbits will give excellent coverage of Jupiter's outer radiation belts and the transition between dipolar and disk magnetic field regions. The radial diffusion coefficient for energetic particles (and its time variations) should be well determined. Finally, should it be found that as the mission progresses the cumulative radiation dose is mounting too rapidly, the orbits can be redesigned to minimize the radiation damage at the cost of some, but certainly not all, scientific objectives.

In summary, it appears that by using satellite swingbys, one spacecraft will provide as much spatial coverage for Jupiter as many spacecraft for earth's magnetosphere.

#### Temporal Coverage

We already know that Jupiter's magnetodisk is highly time variable. On Pioneer 10's inbound pass, the magnetopause moved over 5 solar radii (from  $100 R_J$  to  $50 R_J$ ) in several days. Multiple magnetopause crossings were encountered on the outbound pass (see Figure 2-1). Moreover, the earth's magnetosphere is rarely, if ever, temporally steady. At earth, the dominant magnetospheric events, in terms of energy, are substorms and magnetic storms, which last hours and days, respectively. If Jupiter has an internal convection pattern (and therefore substorms like earth), its substorms would last, according to theory, about a week. Therefore, Jupiter flybys, even many of them, will probably not give enough time coverage to distinguish the temporal signature of Jovian substorms. For the same reason, we do not know whether Pioneer 10, 11 encountered Jupiter's radiation belts in a "high" or "low" state. (While the synchrotron belts at  $L = 2-3$  are known to have a constant intensity, the radiation belts in the region  $6 < L < 20$  are expected to be much more time variable.) The plasma turbulence which controls the intensity of the earth's outer radiation belt is highly time variable and often spatially localized. Its true significance could never have been evaluated without many passes through the radiation belts.

#### 2.2.2 The Jovian Satellite-Magnetosphere Interactions

As noted above, MJS should provide local information on the interaction of Io and Ganymede with the Jupiter magnetosphere. However, MJS will not investigate the wake of Io or make any local measurements

near Europa or Callisto. There is already some impressive evidence that Amalthea, Europa, and Ganymede do affect the trapped radiation, and there have been reports of a novel Europa modulation on the decametric radiation. It is evident that all of inner satellites have a capability to be significant sources of plasma (by plasma sheath acceleration, production of secondary electrons, sputtering, escape of satellite atmospheres, etc.), and a full understanding of Jupiter requires complete understanding of these satellite interactions.

The "flower" orbit provides at least 42 close swingbys of the Galilean satellites during the nominal 3-year lifetime. There will be many satellite occultations, and data from the radio science experiment should provide information on the atmospheres, ionospheres, and plasma sheaths of these satellites, while the magnetospheric experiments will give detailed information on the local interactions.

### 2.3 PROBE SCIENCE OBJECTIVES

A strong case for Jupiter atmospheric entry missions can be made in terms of the questions that remain unresolved after the Pioneer 10 and 11 flyby missions. On the basis of the Principal Investigators' analyses of Pioneer 10 data on Jupiter, it appears that the infrared photometry and radio occultation experiments fail to provide a precise description of Jupiter's atmosphere. The obstacles to defining Jupiter's atmosphere by means of remote flyby experiments arise from the dense, opaque nature of the atmosphere. In the case of optical spectroscopy, the spectra of the atmosphere has proved to be very difficult to interpret, especially in the infrared.

Since our ground-based and flyby measurements are susceptible to various conflicting interpretations, in situ measurements of local physical properties and chemical composition within the atmosphere are needed to remove dependence on atmospheric modeling and lead to the direct utilization of prior remotely acquired data.

### 2.4 SCIENCE INSTRUMENTS

#### 2.4.1 Orbiter Instruments

The reader is referred to the NASA/ESRO PJO Mission Definition Study [MS(74)33, 30 December 1974] for a detailed discussion of the

scientific objectives and rationale for the selection of a scientific payload for the orbiter. A typical payload, recommended by the Mission Definition Group is shown in Table 2-1.

Table 2-1. PJO Orbiter Model Payload

Instrument	Mass (kg)	Power (W)	Measurement Range	Remarks
Magnetometer	3.0	4.2		
Plasma	8.0	6.5		
- Magnetosheath			{p: 50 eV - 30 keV {e: 50 eV - 30 keV	Angular resolution
- Magnetosphere			{p: 50 eV - 30 keV {e: 1 eV - 30 keV	
- Electron gun	1.0	1.0		To control spacecraft potential
Energetic particles	10.0	6.0	{p: 200 keV - 50 MeV {e: 50 keV - 50 MeV	
Plasma wave/radio emissions	6.0	6.5	10 Hz - 40 MHz	
Radiophysics (X-band beacon)	1.5	11.0		Beacon primarily on for occultation and tracking measurements
Micrometeoroids	2.0	1.8	Mass range $10^{-16}$ - $10^{-8}$ g	
UV photometer IR radiometer Line-scan imager (LSI)	9.0	6.0		
Shielding contingency	6.0			
Total	46.5	43.0		Experiment time sharing needed at end of life

Table 2-1 is similar to the Pioneer 10, 11 payload in that it contains a magnetometer, a plasma probe, an energetic particle detector, a micrometeoroid investigation, a radiophysics investigation, and remote sensing instrumentation to supply simple images and to cover IR and UV emissions. However, a number of explicit and implicit changes from Pioneer 10, 11 were also recommended in the report, and the model PJO payload changes are summarized as follows:

- 1) The recommended PJO mission has less emphasis on the cruise phase than does Pioneer 10, 11 (or MJS), and there is no cosmic ray investigation or plasma probe designed to make high resolution solar wind measurements. The energetic particle instrument is a trapped radiation detector, and the plasma probe is optimized to measure warm plasmas in the Jupiter magnetosphere and magnetosheath. This plasma instrument must be capable of measuring radial outflows and corotating plasma as well as plasma streaming from the solar direction.
- 2) The electron gun is an emissive clamp device, which serves to control the spacecraft potential with respect to the plasma.

- 3) The plasma wave instrument (10 Hz to about 100 kHz) is designed to provide a sheath independent evaluation of the total plasma density and local information on wave-particle interactions all along the orbit. This could be a simple ac electric field detector (as on MJS), but the additional presence of a magnetic antenna would be extremely beneficial. The radio emission investigation, which may cover the range 100 kHz to 40 MHz, is an important remote sensing device that gives information on ionospheric and inner magnetospheric processes when the PJO is far from periapsis.
- 4) A simple micrometeoroid instrument could utilize acoustical sensors and the audio signal processing capabilities of the plasma wave instrument. The basic idea is that the audio signal associated with a micrometeoroid hit will have spectral characteristics that differ from those associated with spacecraft thermal noises.

The ability to change the orbit by frequent satellite encounters greatly improves the value of the science data returned from the above instruments.

The NASA/ESRO Mission Definition Group recommended a modest line-scan imager because of the previous high quality imagery obtained by MJS. Although this recommendation may be appropriate, much higher performance line-scan imagers are possible and could give further data, particularly of temperal changes.

#### Line-Scan Image System

A possible imaging system consists of a linear array of solid-state photodetectors swept in push-broom fashion across the visual scene being observed. The line elements describe concentric circles around the spin axis with radii being determined by the cone angle at which the optical axis of the instrument is pointed. The sweep rate varies with the sine of the cone angle. Viewing objects at cone angles closer than about 10 degrees from the spin axis in the rear hemisphere is to be avoided because the imaging process deteriorates. Cone angles of less than 40 degrees in the forward hemisphere are excluded because the high-gain antenna dish obscures the field of view. Viewing in this direction would also be adversely affected by stray light from the sun.

Table 2-2 gives the characteristics of a JPL-developed Pioneer Line-Scan Image System (PLSI), using charge-coupled devices (CCD) as

Table 2-2. JPL Line-Scan Image System Characteristics

Telescope	Catadioptric, 10-cm aperture, 22.9-cm focal length
IFOV	100 $\mu$ rad square per photodetector
Image width	160 pixels/line at normal sample rate 80 pixels/line at low sample rate
Image length	160 lines/chip (1, 2, or 3 overlapping chips) 320 lines/chip (1 or 2 overlapping chips) 640 lines/chip (single chip only)
Spectral bands	Channel 1 600-1000 nm Channel 2 400-1000 nm Channel 3 400-600 nm
Sensors	Three CCD self-scanned line arrays operated in image motion compensation mode
Cone angle range	2.88 rad range, 175 mrad from antenna axis to 85 mrad from antiantenna axis
Cone angle step	0.5 mrad/step, 3 steps/sec slew rate
Housekeeping data per image frame	16 words, 8 bits/word
Data quantity	Minimum frame size = 102,528 bits (low rate) Maximum frame size = 819,712 bits
Commands	18
Size	20 x 20 x 50 cm
Mass	7 kg
Power	10 W

photodetectors. The detector consists of an array of 160 x (5 to 15) photosensitive elements. The scan direction is along the 5-to-15 dimension; image motion in this direction is compensated by synchronizing the rate of charge transfer. This improves sensitivity by a factor of 5 to 15 over a single-row detector. The last row of the detector is read out one line at a time by sweeping to a corner element of the array.

As optical data for a single frame accumulate in a fraction of one spin cycle, they are buffered and stored. To avoid excessive data storage requirements, image data of each completed frame (a total of 0.820 to 0.103 megabits depending on the frame format selected) must be telemetered to earth before a new frame can be stored.

The system is designed to provide simultaneous and overlapping coverage in three spectral regions between 4000 and 10,000 nm, using three CCD sensors with appropriate light filters. Telemetry bit rates

available at Jupiter distance permit transmission of two to eight multi-spectral image frames per hour, depending on the maximum data content (160 by 160, 160 by 320, and 160 by 640 pixels) per image frame.

An advanced signal processing/data handling system under development by JPL\* can provide image data compression up to a ratio of 8:1. This permits accelerated transmission of image data to earth.

Alternate solid-state line-scan detectors suitable for this application have been developed in recent years. A phototransistor array with 195 image cells per chip and an improved, more sensitive photodetector with 250 cells per chip have been developed by TRW and tested under simulated viewing conditions and image motions representative of planetary and satellite observation.\*\*

#### 2.4.2 Probe Instruments

In situ measurements of local physical properties and chemical composition are needed to fully characterize Jupiter's atmosphere and also to aid in interpreting remotely acquired data. The complement of instruments shown (Figure 2-3) provides this information. Development cost of these instruments is minimized through similarity to those on Pioneer Venus.

##### Near Planetary Radiation Environment

The energetic particle detector provides an integrated measurement of high-energy protons and electrons from  $2 R_J$  to  $1 R_J$ , to aid in completing the mapping of the Jovian radiation environment.

##### Atmospheric Structure

The accelerometer experiment measures the aerodynamically induced deceleration of the entry probe by the planetary atmosphere. The ambient atmospheric density is derived by computation from the aerodynamic deceleration readings. In the lower atmosphere the data on

---

\*"Outer Planet Pioneer Imaging Communications System Study Final Report," Jet Propulsion Laboratory, 760-115, 16 December 1974.

\*\*"Feasibility Test of a Solid-State Spin-Scan Photo-Imaging System," N. P. Laverty, TRW Report 23671-6001-TU-00, 14 December 1973.

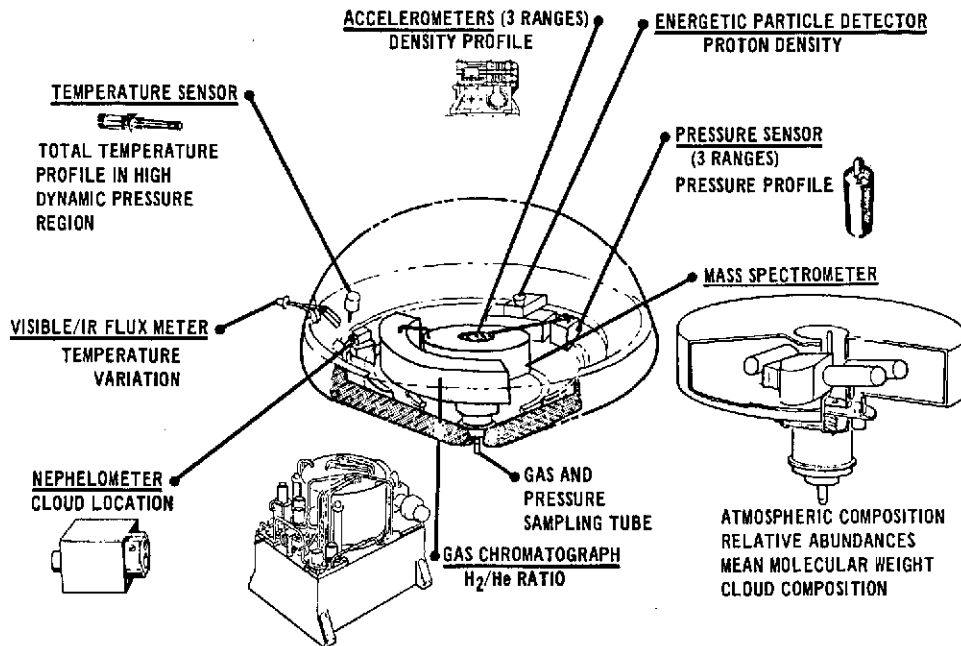


Figure 2-3. Probe Instrument Accommodation

atmospheric structure from the accelerometer are supplemented by direct measurements of atmospheric temperature and pressure.

The location of cloud layers within the atmosphere is to be determined with a backscatter nephelometer. Information on the density of the layers and their optical opacity is obtained by combining a comparison of nephelometer and flux meter data, which is measured in visible and infrared regimes.

#### Atmospheric Composition

The chemical composition of the atmosphere is determined primarily by the mass spectrometer. A supplementary measurement of the hydrogen/helium ratio is provided by an explicitly designed gas chromatograph.

#### Radiation Balance

The thermal energy balance within the atmosphere is measured by the visible-infrared flux meter. These measurements are correlatable with those obtained on the orbiter.

## Data Collection

Figure 2-4 illustrates the data collection sequence. Data is stored until the probe is dropping nearly straight down, assuring that the spacecraft is in the high-gain part of the probe antenna pattern. Previously stored data are interleaved with real time data at a data rate of 44 bps.

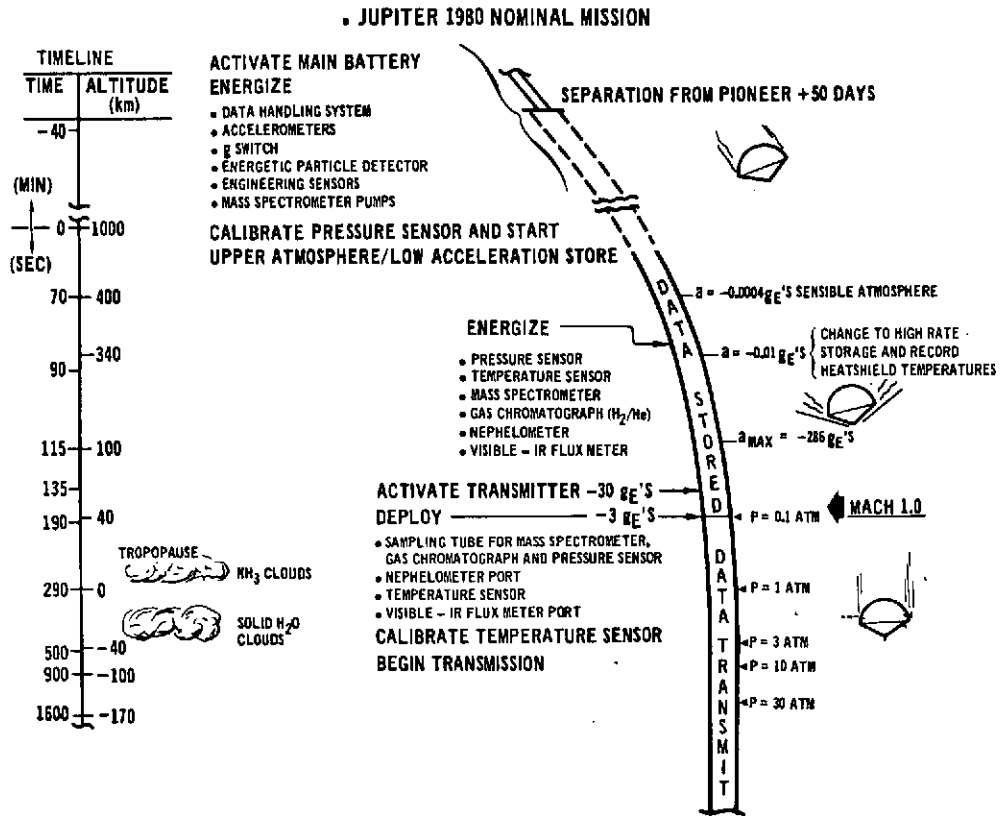


Figure 2-4. Probe Data Collection Sequence



A sample schedule of the major mission events following launch is given in Table 3-1. This table is based on a Type I earth-Jupiter trajectory, which entails the minimum transfer time. (At the end of Section 3 there is a discussion of the mission assuming the use of a Type II trajectory. While the Type II option raises the trip time by some 250 days, it has certain advantages, among which is the location of the entry region on the sunlit side of Jupiter.)

Table 3-1 incorporates several events which are indicative of decisions affecting the conduct of the mission:

- 1) Spacecraft deflection mode. The flight spacecraft is targeted toward the probe impact point on Jupiter until after the probe is released. It is then retargeted. A consequence of this decision is that the probe needn't have any trajectory control capability, nor any ability to change its spin-stabilized orientation from that provided by the spacecraft before it is released.
- 2) Relay-link probe communications. Because typical probe approach trajectory geometry places the entering probe in the vicinity of the sunset terminator (the west limb of Jupiter, as seen from the earth) direct communication from probe to earth is not possible. Instead, a relay link via the spacecraft is used. This reduces probe transmitter requirements because of the comparatively low range and low aspect angle to the bus during the time of probe descent; it takes advantage of the existing, high-performance, spacecraft-to-earth communication link. However, it imposes trajectory constraints on the spacecraft, which must now be at the right place at the right time to serve as the relay station.
- 3) Initial orbit of low periapsis. The low periapsis radius ( $1.8 R_J$ ) of the orbit about Jupiter initially entered by the spacecraft is compatible with minimizing the probe-bus communication range. It also reduces the propellant requirement for the orbit insertion maneuver. However, the spacecraft is exposed to at least one periapsis passage through the more intense regions of the Jovian radiation belts.
- 4) Subsequent orbit of higher periapsis. The propulsive maneuver at the first orbital apoapsis raises orbital periapsis from  $1.8$  to  $14 R_J$ . This establishes the spacecraft in a  $14 \times 150 R_J$  orbit (incidentally requiring less total propellant than a conventional one-impulse maneuver would have). The new orbit avoids further exposure to the most intense radiation regions. It also is compatible with the use of satellite encounters — at first with Ganymede or Callisto; subsequently with Europa also — for additional purposeful changes in the orbit.

Table 3-1. Major PJO<sub>p</sub> Mission Events

Event No.	Date	Event	Remarks
1	6 Dec 1980	Launch	Flight vehicle is put onto earth-Jupiter interplanetary trajectory by launch vehicle
2	14 Dec 1980	First midcourse maneuver	Spacecraft propulsion corrects launch vehicle injection errors
3	26 Dec 1980	Second midcourse maneuver	Residual trajectory errors are corrected
4	?	Further midcourse maneuvers	Trajectory trim maneuvers (as necessary)
5	26 Dec 1982	Probe separation	By earth command, spacecraft releases probe
6	26 Dec 1982	Spacecraft deflection	First use of large thruster; in off-earthline attitude
7	20 Jan 1983	Final approach trajectory correction	
8	29 Jan to 11 Feb 1983	Spacecraft and probe enter Jovian magnetosheath and magnetosphere	
9	E (14 Feb 1983)	First sensing of atmosphere by probe (definition of entry)	Deceleration = 0.0004 g <sub>E</sub>
10	E + 48 sec	Maximum deceleration of probe	(264 g <sub>E</sub> , nominal atmosphere)
11	E + 1.3 min	Start of probe transmission	Deceleration declines to 3 g <sub>E</sub>
12	E + 27 min	Spacecraft is at periapsis	1.8 R <sub>J</sub> from planet center
13	E + 31 min	End of probe transmission	Pressure = 25 to 50 bars (depending on atmospheric model)
14	E + 36 min to E + 63 min	Retropropulsion engine firing	Spacecraft enters 1.8 x 150 R <sub>J</sub> orbit about Jupiter
15	E + 65 min to E + 147 min	Spacecraft is in solar eclipse	
16	E + 82 min to E + 175 min	Spacecraft is occulted from earth	
17	28 Mar 1983	Apoapsis orbit adjustment	Large thruster firing; orbit changed to 14 x 150 R <sub>J</sub>
18	16 May 1983	Second periapsis passage	First opportunity to use satellite encounters (Ganymede, Callisto) to reshape orbit
19	May 1983 to Feb 1986	Additional period of orbital operations (giving total life in orbit of three years). During this time the orbit can be adjusted significantly 30-40 times by satellite encounters to explore different regions of the Jovian environment. In addition, small propulsive adjustments will be made as required for navigational purposes.	

## 3.2 MISSION CHARACTERISTICS

The various aspects of the mission characteristics are investigated to verify the feasibility of the mission and to set forth the requirements to be met by the spacecraft and probe, particularly in areas of propulsion, communications, and guidance accuracy.

### 3.2.1 Launch

The designated launch vehicle for the 1980-81 PJO<sub>p</sub> mission is the Titan 3E/Centaur D-1T/TE-M-364-4. In comparison with the Atlas/Centaur/TE-M-364-4 launch vehicle for Pioneers 10 and 11, this vehicle uses the more powerful Titan for the first stage, permitting the greater mass of the probe-orbiter spacecraft to be sent to Jupiter. While the Centaur stage and the solid-motor third stage are essentially the same as for the Pioneer 10, 11 launch vehicles, these aspects of the interface with the spacecraft are changed:

- 1) The use of the 14-foot diameter Viking fairing (rather than the 10-foot Pioneer 10, 11 fairing) increases the volume available for the spacecraft.
- 2) The heavier spacecraft and its more forward c. g. location requires a larger third stage-spacecraft adapter, which mates with the third stage motor at its 37-inch diameter waist, rather than at an 18-inch diameter ring on its forward dome. It also requires stiffening of the Centaur/third stage interface region by minor changes of the petal hinges, bearing (1, 2)\* retaining clips, and base cone stringers of the spin table.
- 3) A higher level of acoustic environment exists at the spacecraft due to the Titan first stage. However, it is noted that the Pioneer 10 and 11 spacecraft were designed and tested to a mechanical environment enveloping both Atlas and Titan environments. Thus the general level of structural and subsystem designs are appropriate to the Titan environment.

The Titan/Centaur/TE-M-364-4 launch vehicle has a weight-vs-injection energy capability shown in Figure 3-2.<sup>(3)</sup> The lower curve represents the capability if there is continuous thrusting of the Centaur during the coast phase for propellant settling. However, it is felt that propellant acquisition can be assured, even if there is no thrusting during coast; this leads to the improved performance of the upper curve. The

---

\*Numbers in parentheses denote references listed at end of section.

design point for this mission, assuming the upper curve, is  $C_3 = 90 \text{ km}^2/\text{sec}^2$ ; injected weight = 1136 kg.

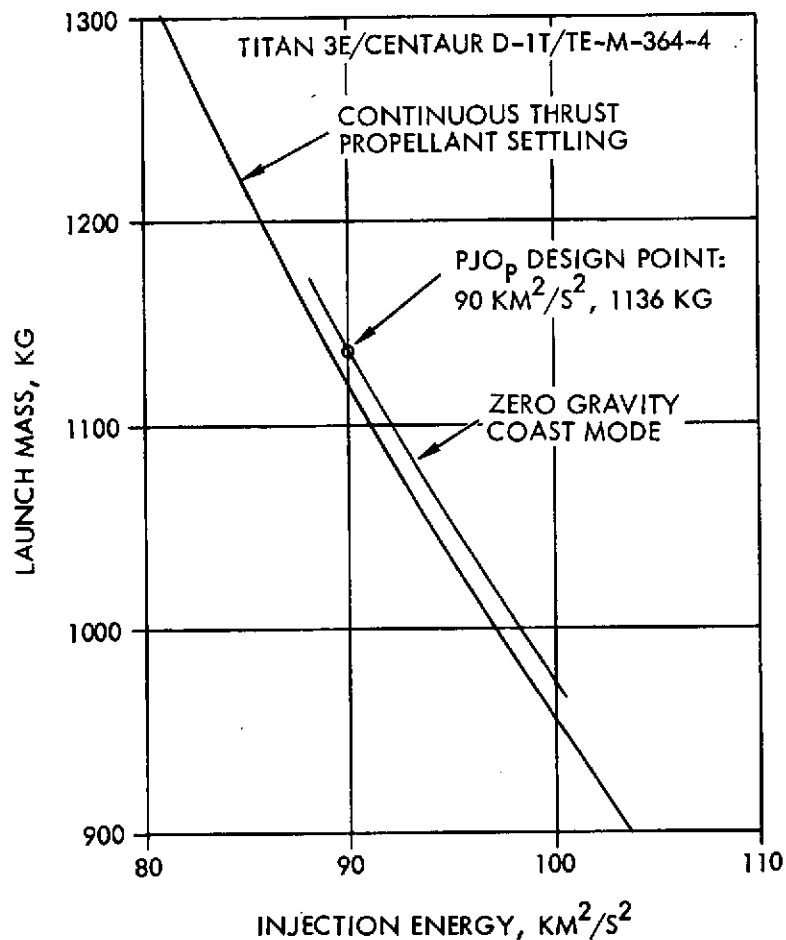


Figure 3-2. Launch Vehicle Capability

Based on trajectory selection discussed in the next section, the sample trajectory defined by the launch and arrival dates of Table 3-1 has a near-earth geometry shown in Figure 3-3. This picture, viewed normal to the orbit plane, shows a parking orbit of 176 degrees (coast duration 41 minutes) between the first and second Centaur burns. This coast phase arises from the northerly declination — about +23 degrees — of the launch asymptote, and causes the second burn and the injection to take place in the vicinity of Australia. Liftoff is from Florida around 9 a.m. The spacecraft is in eclipse from about 12 minutes before injection to 7 minutes after injection.

Figure 3-3 and the data of the above paragraph describe a launch at the opening of the daily launch window, assumed to correspond to a launch azimuth of 90 degrees. Late in the launch window (which has a duration of 2.9 hours if the closing azimuth is 107 degrees, inertial) liftoff is just before noon, the coast angle and duration decrease to about 139 degrees and 32 minutes, and the location of the second burn moves some 43 degrees to the west. (The eclipse has virtually the same timing relative

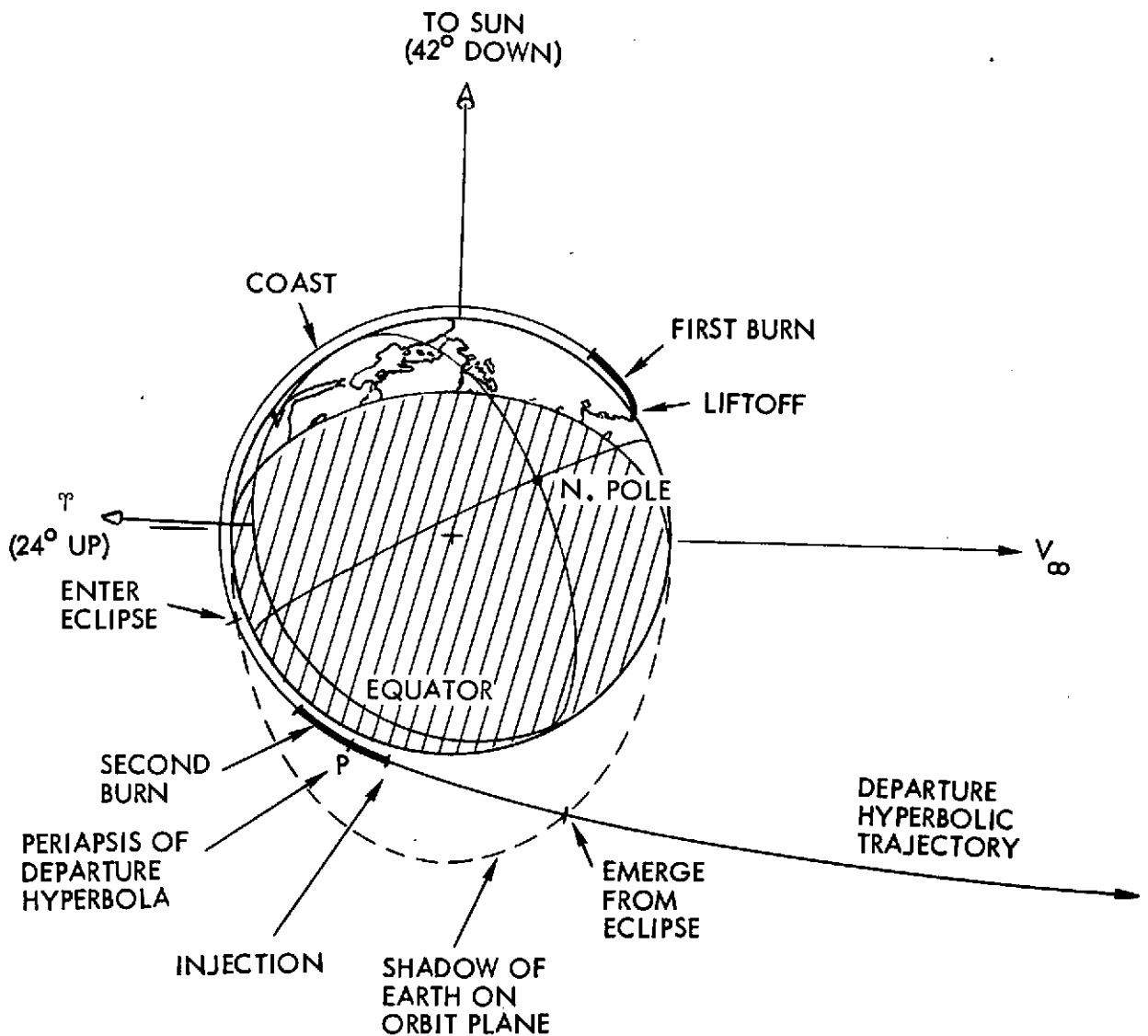


Figure 3-3. Near-Earth Trajectory

to injection.) Of course this excursion of the second burn and injection locations can be curtailed if the launch window is arbitrarily held to a duration less than the 2.9 hours available.

### 3.2.2 Interplanetary

Characteristics of the earth-Jupiter transfer trajectory are shown in Figures 3-4 and 3-5 against departure date and arrival date as coordinates. These parameters are depicted by contours in the two figures:

$C_3$	Launch energy (square of hyperbolic excess departure velocity)
DLA	Declination of the departure asymptote
$V_{\infty}$	Hyperbolic excess velocity of arrival at Jupiter
ZAP	Angle between asymptotic arrival velocity and Jupiter-sun line.

The first two of these parameters pertain to launch vehicle weight capability and near-earth geometry, as discussed in Section 3.2.1, and the last two affect orbiter deboost propulsive requirements and arrival geometry of the orbiter and probe at Jupiter.

Two bands of trajectories are indicated on Figures 3-4 and 3-5, one for sample Type I trajectories (less than 180-degree heliocentric angle between earth and Jupiter) with varying launch date, and one for sample Type II trajectories (more than 180 degrees). The criteria evaluated in selecting the two sample arrival dates are shown in Table 3-2.

Thus the arrival date for Type I trajectories was selected to minimize trip time while recognizing all the above criteria other than the probe entry location. The arrival date for Type II trajectories makes daylight probe entry a primary criterion, at the expense of trip time. The resulting trip times are about 800 and 1050 days, respectively.

In neither case was the arrival date selection influenced to achieve specific early encounters with Jovian satellites. On the first periapsis passage of the orbiter any of the five innermost satellites of Jupiter (Table 3-3) could be encountered, as periapsis is closer to Jupiter than the orbit of any of them. On subsequent periapsis passages Ganymede and Callisto can be encountered, and will be if this mode of orbit shaping

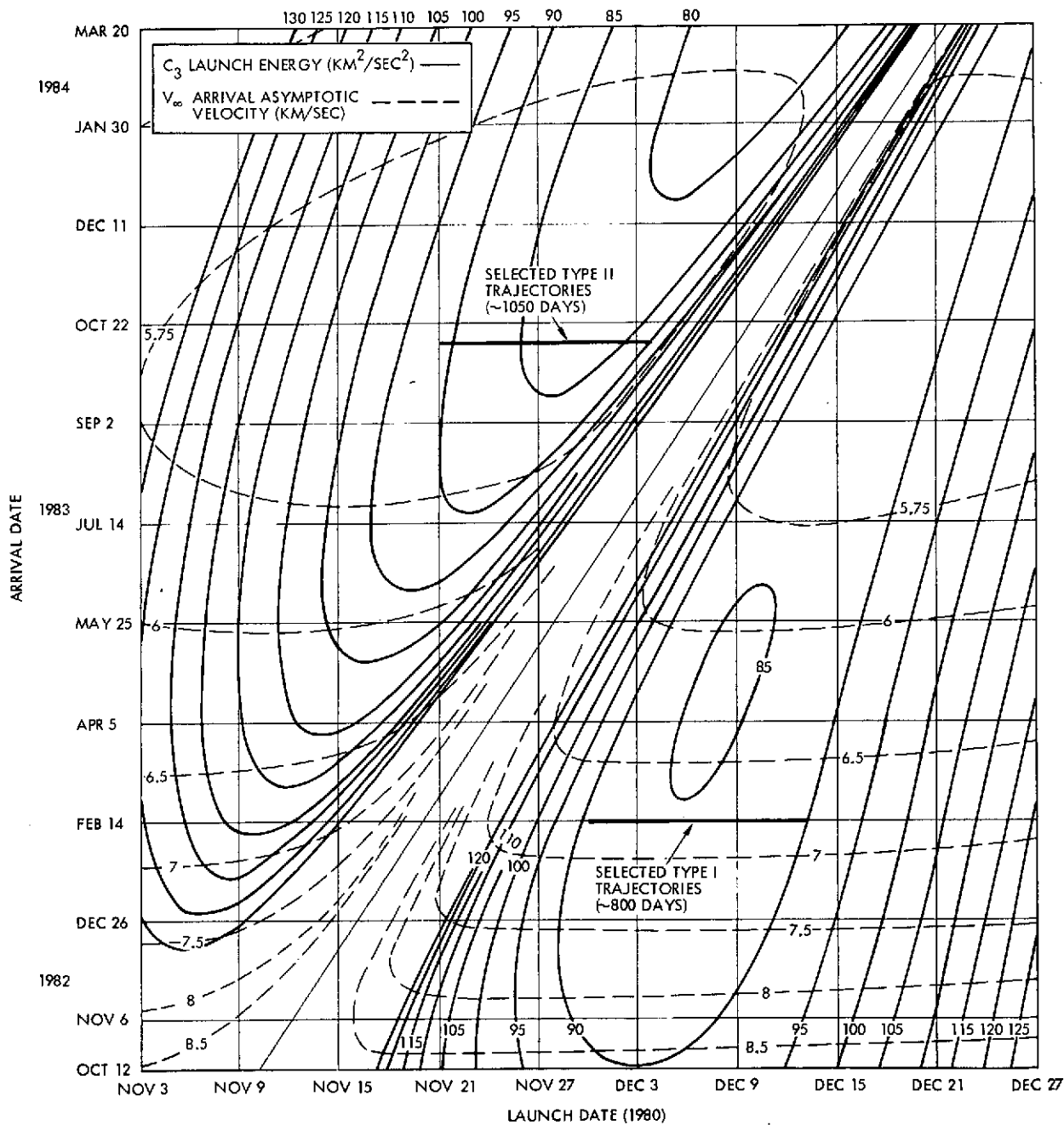


Figure 3-4. Earth-Jupiter Trajectory Characteristics (1980).  $C_3$ ,  $V_{\infty}$ .

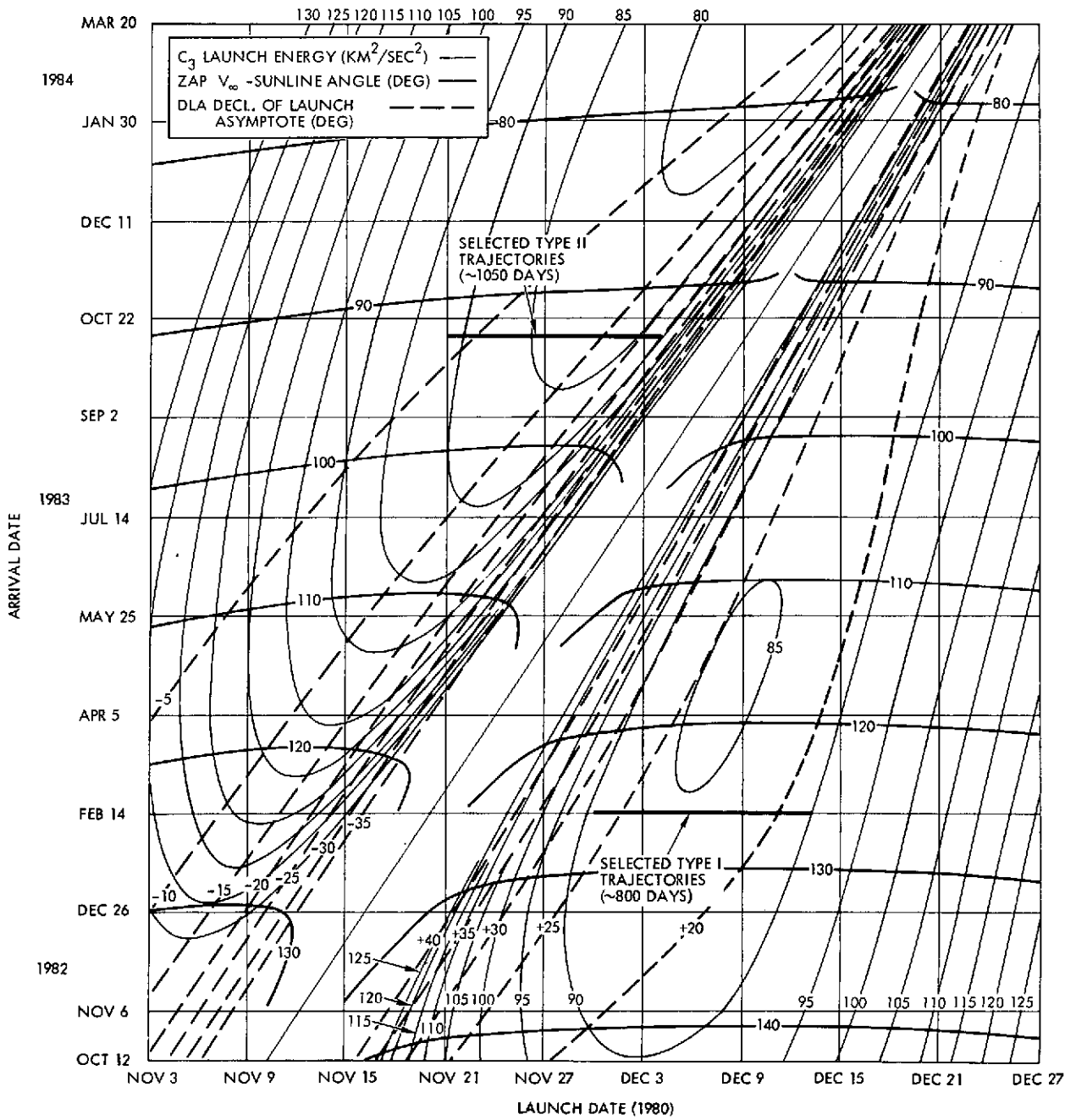


Figure 3-5. Earth-Jupiter Trajectory Characteristics (1980).  
 $C_3$ , DLA, ZAP.

Table 3-2. Criteria in Selection of Sample Trajectories

Criteria	Type I Trajectories	Type II Trajectories	What is Considered Favorable
Launch energy ( $C_3$ )	Yes	Yes	Minimum
Launch asymptote declination (DLA)	Yes	Yes	Avoidance of doglegs or launch azimuth $> 108$ deg. ( $-33$ deg $< DLA < +33$ deg; negative values reduce coast time.)
Orbiter deboost $\Delta V$ magnitude	Yes	Yes	Minimum $V_\infty$
Appropriateness of earth line deboost	Yes	Yes	Angle between Jupiter-earth line and tangent to trajectory at mid-deboost to be minimized.
Earth-Jupiter-sun angle at arrival date	Yes	Yes	$>2$ deg to favor sun sensor as roll position indicator
Trip time	Primary	Secondary	Minimum
Probe entry location (local time)	No	Primary	On daylight side $>10$ deg from terminator throughout 25-minute probe descent

Table 3-3. Inner Five Satellites of Jupiter<sup>(4)</sup>

No.	Name	Mass ( $10^{22}$ kg)	Radius (km)	Orbital Data	
				Radius ( $R_J$ )	Period (days)
V	Amalthea	$10^{-3} \pm 1$	$100 \cdot 2^{\pm 1}$	2.539	0.498
I	Io	$7.2 \pm 0.6$	$1800 \pm 160$	5.905	1.76914
II	Europa	$4.7 \pm 0.1$	$1550 \pm 100$	9.396	3.55118
III	Ganymede	$15.5 \pm 0.2$	$2600 \pm 400$	14.99	7.15455
IV	Callisto	$9.6 \pm 0.8$	$2400 \pm 400$	26.36	16.68902

Note: The orbits of all these satellites are inclined less than  $0.5$  degree to the Jovian equator and have eccentricities less than  $0.008$ .<sup>(5)</sup>

is adopted. The orbiter will not again return as close to Jupiter as Europa until later in the mission, and as close as Io only if desired in the terminal phases of the orbiter mission. Thus the motive of opportunity for a close encounter with a satellite on the first periapsis passage applies primarily to Amalthea and Io, and partially to Europa.

Now a relatively close encounter (close enough for experimental observation of the satellite, but not for significant use of the satellite's gravity) can be obtained by synchronizing the day and time of arrival with the satellite's revolution about Jupiter, but not tailoring the inclination of the orbiter's incoming path to provide a node crossing at the point where right ascension and distance from Jupiter match. This much can be done easily for any of the first three satellites Amalthea to Europa by adjusting the arrival time within a  $\pm 1.77$ -day interval, and, therefore, with no significant alteration of the selected trajectories. However, the following factors may discourage the operational implementation of even this class of encounter:

- 1) The selection of arrival time may also be influenced by considerations of ground station coverage and overlap.
- 2) The selection of arrival time may also be influenced by a desire for the probe entry site to be at a specific Jovian longitude (e. g., the Great Red Spot).
- 3) Attention to the demands of probe communications, spin-up, retropropulsion, occultation from sun and earth, and effects of the radiation belt on the first periapsis passage may preclude other operations, particularly for Amalthea which would have to be encountered close to periapsis.

To get a particularly close encounter with one of these satellites would, in addition to arrival timing, require control of the inclination of the orbiter's approach trajectory. However, this inclination constraint might well conflict with two other bases for the selected inclination:

- 1) The location (in a north-south direction) of the orbiter to best serve as the probe data relay station
- 2) The requirement for an orbit-shaping encounter with Ganymede or Callisto, probably on the second periapsis passage. (Note that the phasing required to achieve this Ganymede or Callisto encounter can be achieved by a small change in the initial apoapsis radius.)

Thus, because operational and targeting considerations may relegate first-passage encounters with inner satellites to a low priority, and because encounters with the outer satellites may well be routine in the subsequent orbiting phase, no attempt was made to recognize satellite encounters as an influence in the choice of earth-Jupiter trajectories.

The sample Type I interplanetary trajectory, in relation to the orbit of Jupiter is shown in Figure 3-6. Subsequent sections (3.2.3 to 3.2.9) detail the mission analyses based on it. The Type II trajectory for the daylight probe entry is discussed in Section 3.2.10.

### 3.2.3 Orbiter Deflection

Shortly after the probe is separated from the spacecraft, the spacecraft is propulsively deflected so as to follow the approach course necessary to reach periapsis at  $1.8 R_J$  from Jupiter's center, and to be in the appropriate position to receive data transmission from the probe during its period of descent after atmospheric entry.

Neglecting the velocity of ejection of the probe, which will be less than 1 m/sec, and ignoring possible out-of-plane components, the geometry of the orbiter's deflection is shown in Figure 3-7. In Jupiter-centered coordinates, the magnitude and direction relative to earth and sun lines of the probe's asymptotic approach velocity is shown. The desired separation  $\Delta V$  is determined by its two components. The cross-track component provides the trajectory separation between the probe (heading to a periapsis at  $0.983 R_J$ ) and the orbiter (heading to a periapsis at  $1.8 R_J$ ). Its magnitude of 52 m/sec achieves the asymptote separation  $\Delta b = 225,000$  km in a time of 50 days (4,320,000 seconds) from separation to arrival. The along-track component attains the desired phasing between the spacecraft and probe arrival times, while compensating for the tendency of the closer-targeted probe to reach its periapsis before the spacecraft does. In the sample trajectory defined earlier, the probe would reach its (projected) periapsis 2.30 hours before the spacecraft reaches its periapsis, if no along-track component were imparted. In the following section it is shown desirable for the spacecraft to be at a position 26 minutes short

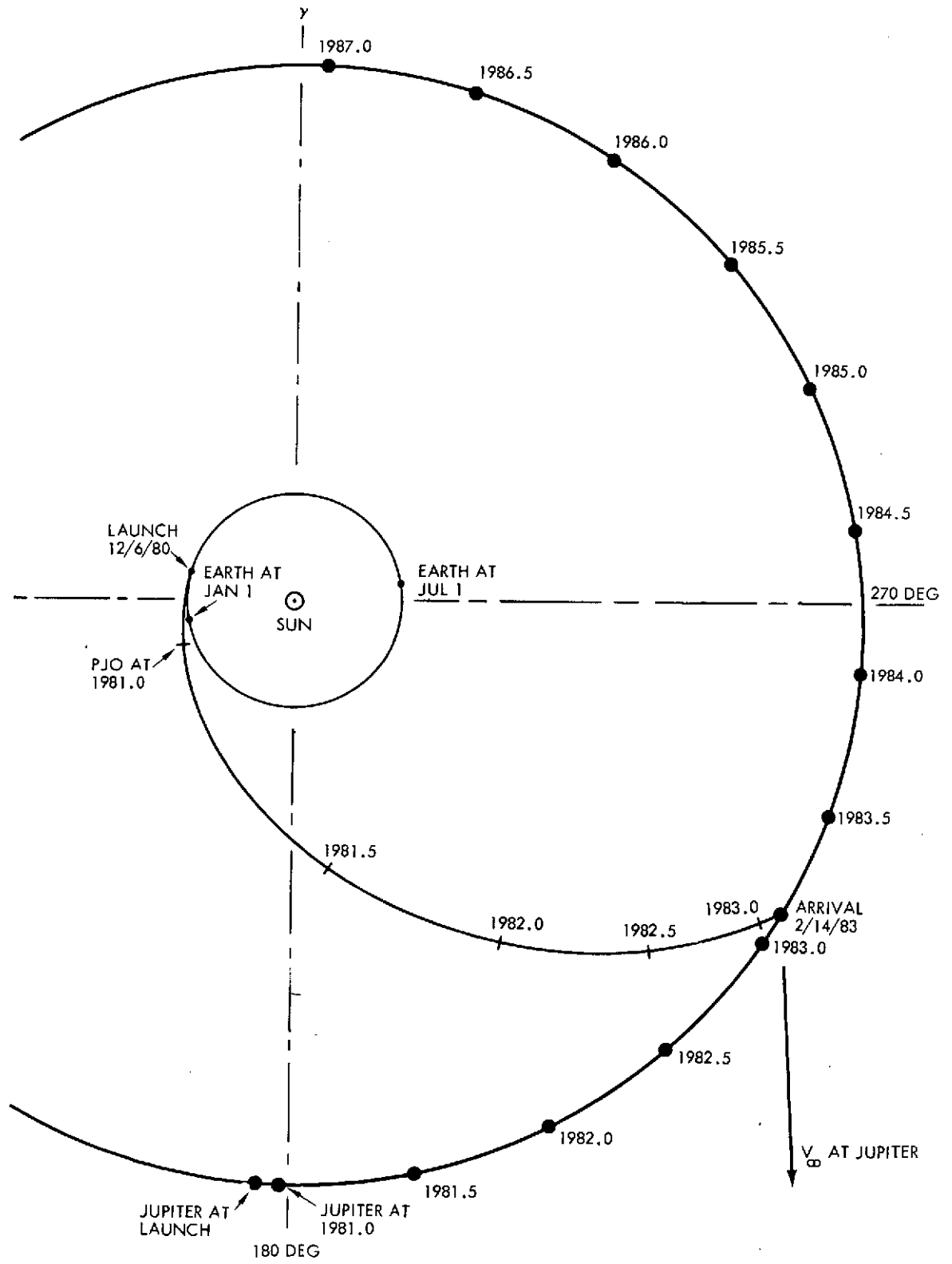


Figure 3-6. Interplanetary Trajectory and Orbital Operations

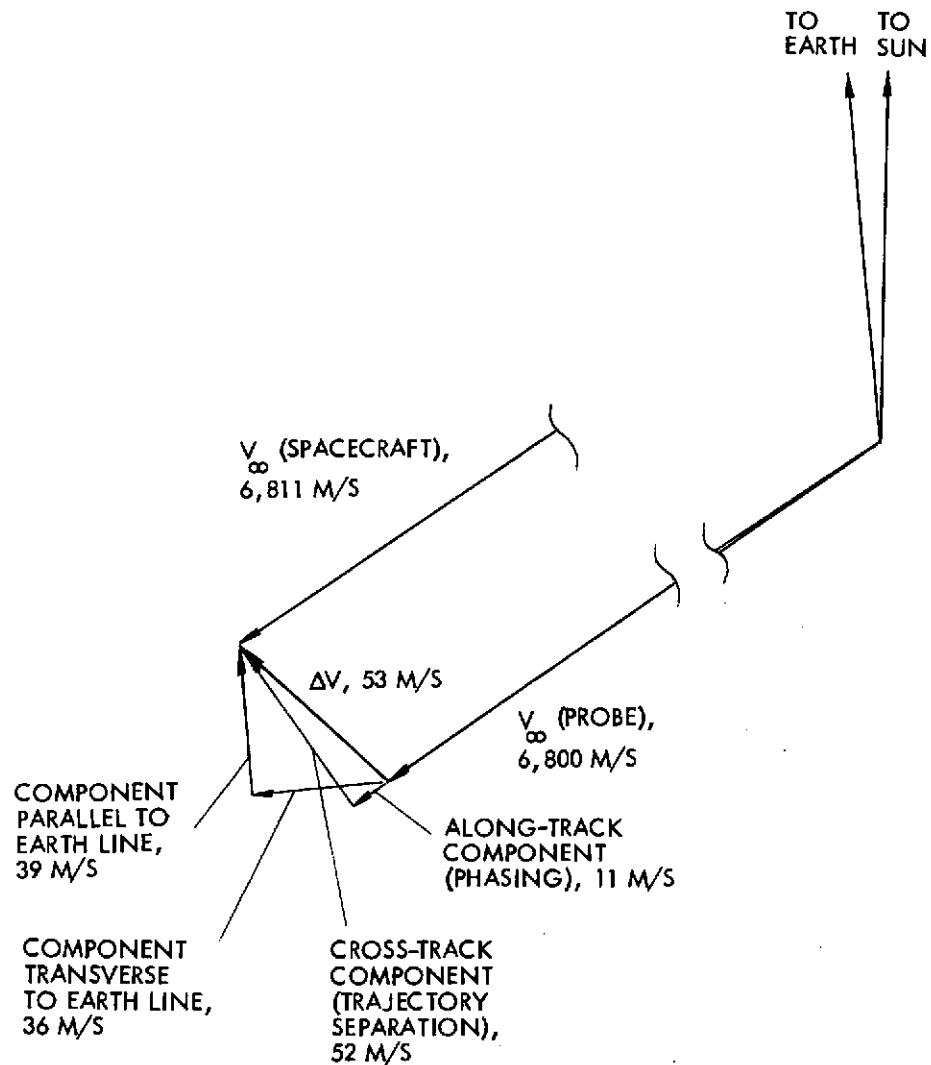


Figure 3-7. Velocity Increment to Separate Spacecraft's Approach Trajectory from Probe's

of its periapsis when the probe enters the atmosphere 5 minutes before it would reach its periapsis if not decelerated by the atmosphere. Thus the spacecraft must be accelerated along the track to reduce the 2.30-hour delay to an 0.35-hour delay. The 11 m/sec along-track component increases the 6800 m/sec  $V_{\infty}$  enough to reduce trip time by the required 1.95 hours in 50 days.

The along- and cross-track components combine to a total  $\Delta V$  of 53 m/sec. With the probe separated, the high-thrust deboost engine is

the most efficient to use, the  $\Delta V$  maneuver being performed in an attitude 43 degrees away from earth pointing. If this off-earth precession were felt undesirable, the separation could be achieved in two components as shown in Figure 3-7:

- 1) A 39-m/sec component toward the earth, using either the high-thrust engine or a pair of aft-pointing 5-lbf engines
- 2) A 36-m/sec component transverse to the earthline, using the two 5-lbf radial thrusters in the pulsed mode.

Returning now to possible out-of-plane  $\Delta V$  components, if the spacecraft is targeted to a greater trajectory inclination about Jupiter than the probe or if both are targeted to the same high inclination, the  $\Delta V$  of separation will no longer lie in the plane of the earthline and the probe  $V_{\infty}$  vector, as assumed in Figure 3-7. The reason for such targeting to fix the inclination of the spacecraft's trajectory could be one of the following:

- 1) (To cater to probe communications)
  - To pass overhead of the descending probe after probe entry, particularly if the entry point is chosen, say, 10 degrees north or south of the equator
- 2) (Independent of the probe)
  - To minimize the inclination of the spacecraft, in contrast with that of the probe
  - To minimize spacecraft exposure to the more intense radiation belts near the magnetic equator
  - To attain a favorable encounter with one of the satellites Amalthea, Io, or Europa, on the first periapsis passage
  - To favor a close encounter with Ganymede or Callisto on the second periapsis passage.

In any event, if an out-of-plane component is to be incorporated into the orbiter deflection maneuver, it will be determined as above, with an along-track component and an out-of-plane cross-track component. And it will be performed as above, with a single thrusting in an off-earthline attitude, or with two components in an earthline attitude – continuous firing parallel to the spin axis and pulsed firing of radial thrusters.

### 3.2.4 Probe Entry

The relation between the probe and spacecraft trajectories approaching Jupiter is shown in Figure 3-8. The probe trajectory approaches Jupiter in a prograde sense. This way the rotational velocity of Jupiter (12.7 km/sec at the equator) subtracts from the inertial entry velocity (60.0 km/sec) to provide the minimum relative entry velocity. The shallow entry angle of -7.5 degrees (inertial) is comfortably within a band defined by a skipout boundary at -4.5 degrees and structural limits (based on  $800 g_E$  peak deceleration) at -11 degrees or greater, depending on which model atmospheric composition from those in Reference (4) is assumed.<sup>(6)</sup> The -7.5 degrees entry angle requires the probe trajectory to have a projected periapsis at  $0.983 R_J$ .

The  $1.8 R_J$  periapsis of the spacecraft trajectory is chosen to optimize communication parameters which are described in the next section. A greater altitude would increase communication range for the probe-spacecraft link, but a lower passage would require broader, lower-gain antenna patterns on both probe and spacecraft to accommodate the greater range of aspect angles.

The  $1.8 R_J$  periapsis is also a compromise between reduced radiation exposure at higher altitudes and greater deboost propulsive efficiency at low altitudes.

Having established the paths of the probe and the spacecraft, the phasing remains to be set. It is desirable to have the spacecraft approximately overhead at some point during the probe's descent, but various factors may tend to adjust the phasing in one sense or the other. The selection of trajectory phasing in Figure 3-8 results in probe communications occurring with the spacecraft not quite as far along in its trajectory as optimum. (The spacecraft doesn't pass the probe's zenith until 34 minutes after entry.) On the other hand, the firing of the retro engine — delayed until after Entry + 30 minutes to avoid operational overlap with the probe data relay — occurs farther along the trajectory than the location which would maximize orbit insertion efficiency. It is also late enough that earth occultation starts only 16 minutes after thruster cutoff. The phasing indicated is therefore a compromise.

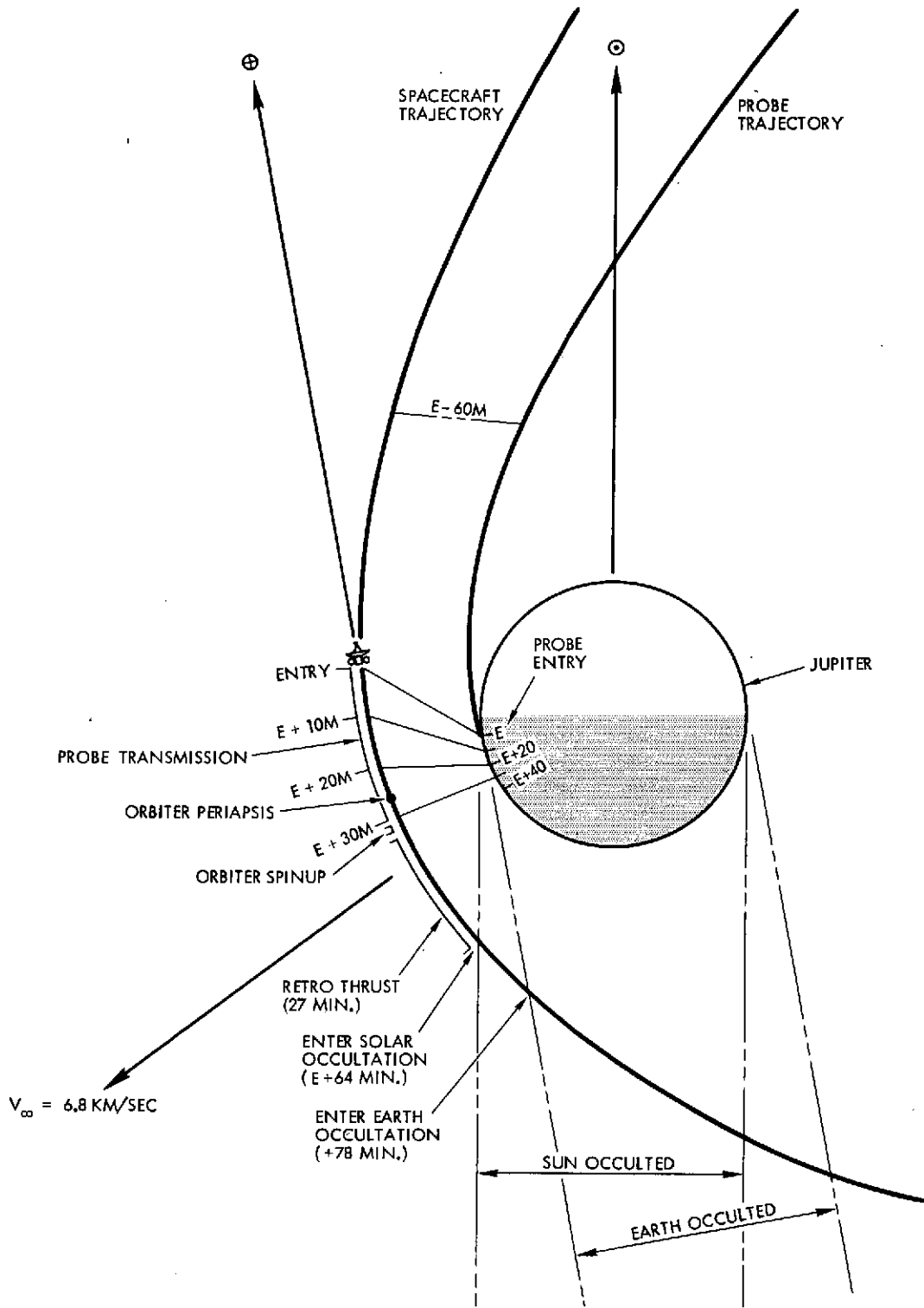


Figure 3-8. Probe and Spacecraft Approach to Jupiter

The major entry transients to which the probe must be designed are the deceleration and heat pulse. These characteristics are dependent on the atmospheric composition and structure at altitudes 100 to 200 km above the 1-bar level, and materially influence the probe design. Figure 3-9 gives an example of the entry transient effects, which are seen to occur within about 2 minutes of the first detectable deceleration. (7)

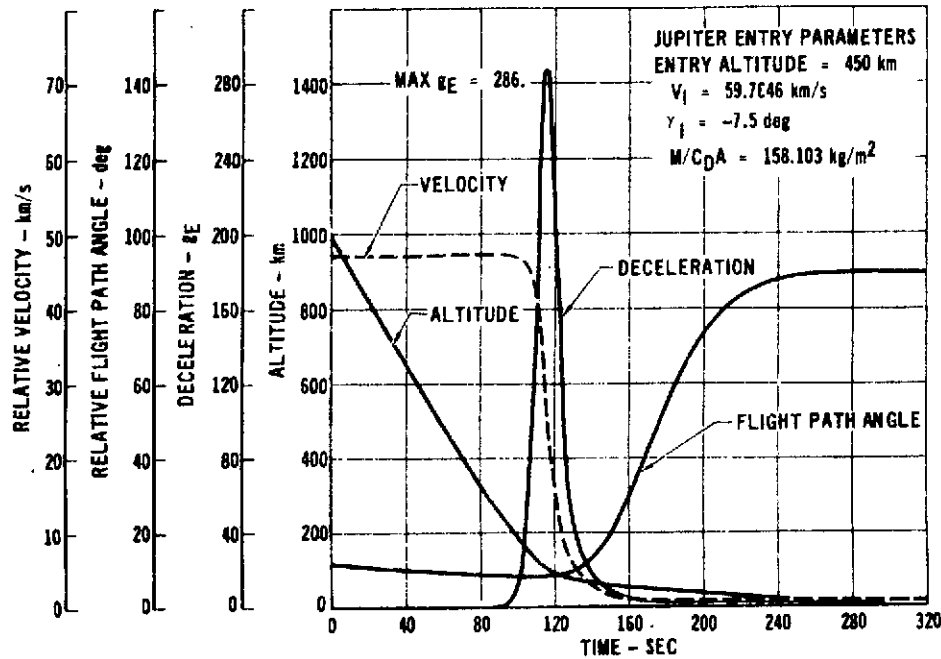


Figure 3-9. Probe Entry Profiles.  
Nominal Atmosphere

The principal model atmospheres examined for probe entry and descent design requirements and performance characteristics are those of Reference (4). Table 3-4 shows the compositions of three models (cool, nominal, and warm), and Figure 3-10 shows pressure-temperature relations. Other characteristics are given in detail in the reference. The result of Pioneer 10's Jupiter encounter tend to favor the nominal and warm models.

The descent profile of the probe after entry transients is also dependent on the atmosphere model, and these characteristics affect the probe design and performance. By affecting the expected termination of

Table 3-4. Compositions of Models of Jupiter's Atmosphere

Parameter		Cool Model	Nominal Model	Warm Model
Fractions by mass (or weight)	H <sub>2</sub>	0.50696	0.75348	0.87674
	He	0.46000	0.23000	0.11500
	CH <sub>4</sub>	0.00857	0.00429	0.00214
	NH <sub>3</sub>	0.00219	0.00109	0.00055
	H <sub>2</sub> O	0.01601	0.00800	0.00400
	Ne	0.00229	0.00115	0.00057
	others	0.00398	0.00199	0.00100
Fractions by number (or volume)	H <sub>2</sub>	0.68454	0.86578	0.93754
	He	0.31057	0.13214	0.06149
	CH <sub>4</sub>	0.00145	0.00062	0.00028
	NH <sub>3</sub>	0.00035	0.00015	0.00007
	H <sub>2</sub> O	0.00240	0.00102	0.00048
	Ne	0.00031	0.00013	0.00006
	others	0.00038	0.00016	0.00008
Mean molecular weight u (grams/mole)		2.70	2.30	2.14

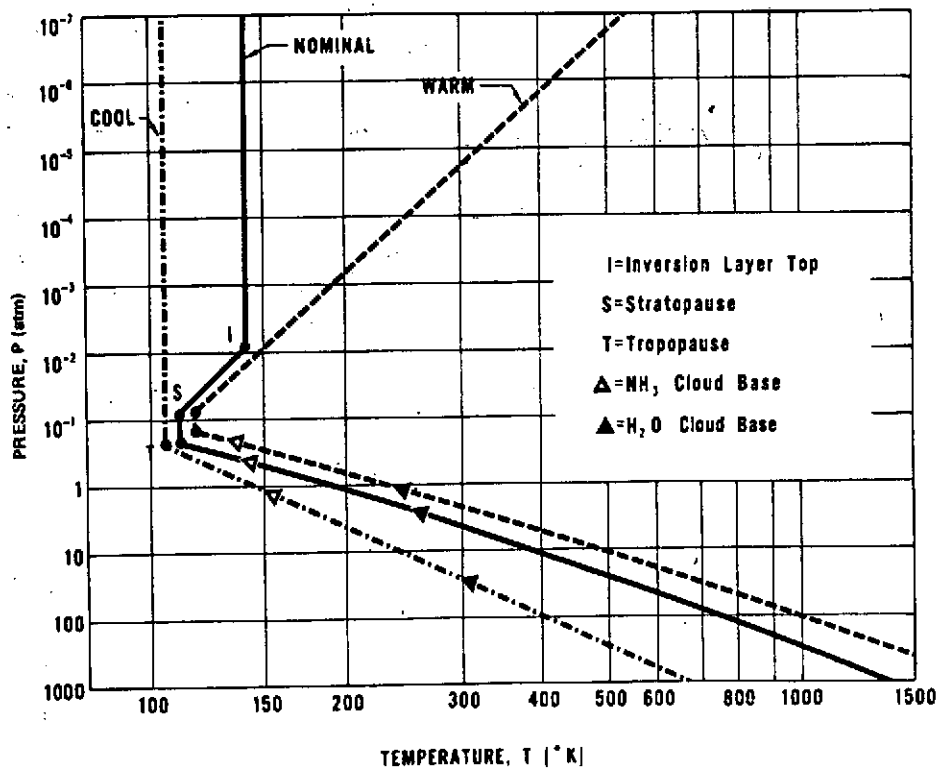


Figure 3-10. Pressure vs Temperature for the Jupiter Model Atmosphere

the probe mission, they also influence the spacecraft mission design.

Figure 3-11 shows descent profiles of the probe in the nominal and warm model atmospheres. Actually, the probe mission can terminate for any one of several reasons:

- 1) Transmission ends at battery depletion (nominally about 30 minutes after entry)
- 2) The probe pressure vessel fails structurally (nominally at a pressure of 30 bars)
- 3) The probe components overheat as descent carries the probe into hotter atmospheric environment.

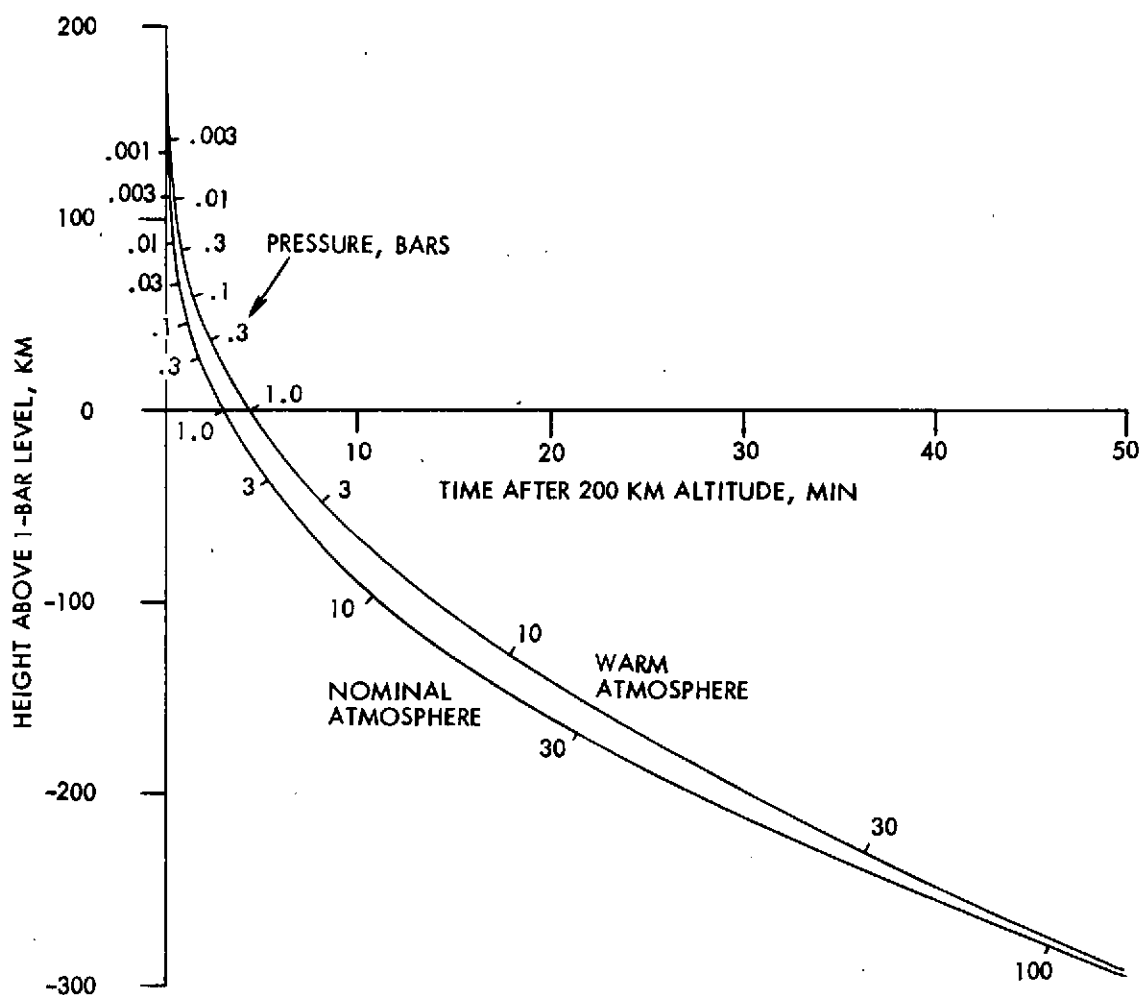


Figure 3-11. Descent Profiles of the Probe

Which of these occurs first depends on the atmospheric model, as is indicated by examination of Figures 3-10 and 3-11. The phasing and operations described herein have been based on the following assumptions:

- 1) The spacecraft is required to receive probe transmission until 30 minutes after expected probe entry
- 2) The major probe results are expected within 25 minutes after entry.

The spin-up and retro thrusting of the orbiter soon after 30 minutes after entry would not preclude receipt of additional probe data, if the probe continued to transmit. It would, however, indicate that first priority was transferred at that time to the orbit insertion maneuver.

### 3.2.5 Probe Communications

Figure 3-12 is the result of abstracting range and angle information from Figure 3-8. It gives probe-spacecraft range and probe and

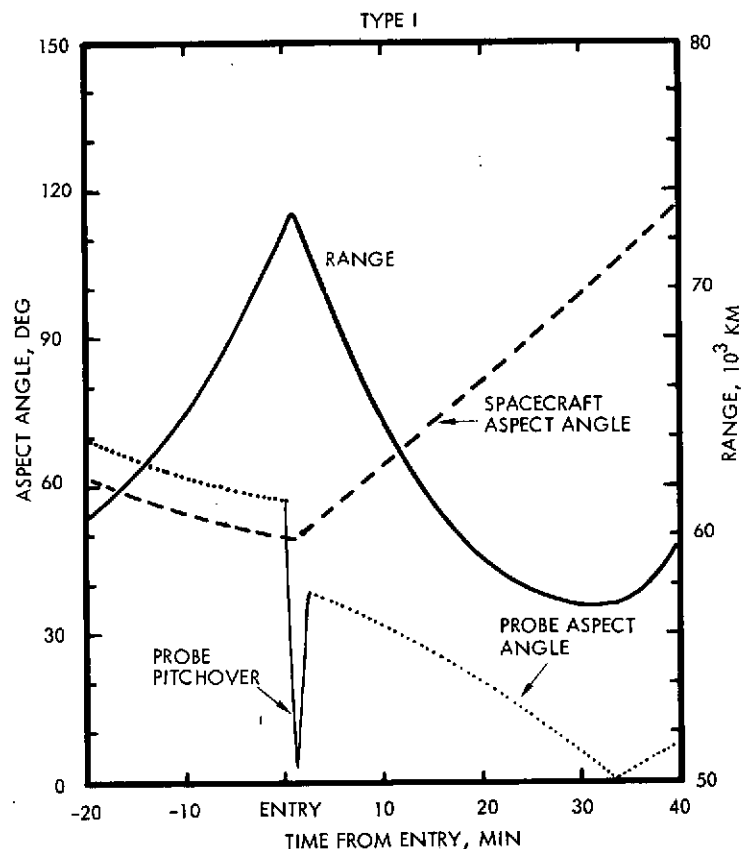


Figure 3-12. Probe Communication Geometry

spacecraft aspect angles vs. time from 20 minutes before entry until 40 minutes after entry. The aspect angles are those between the link direction and axes of spin or symmetry, and are illustrated in Figure 3-13.

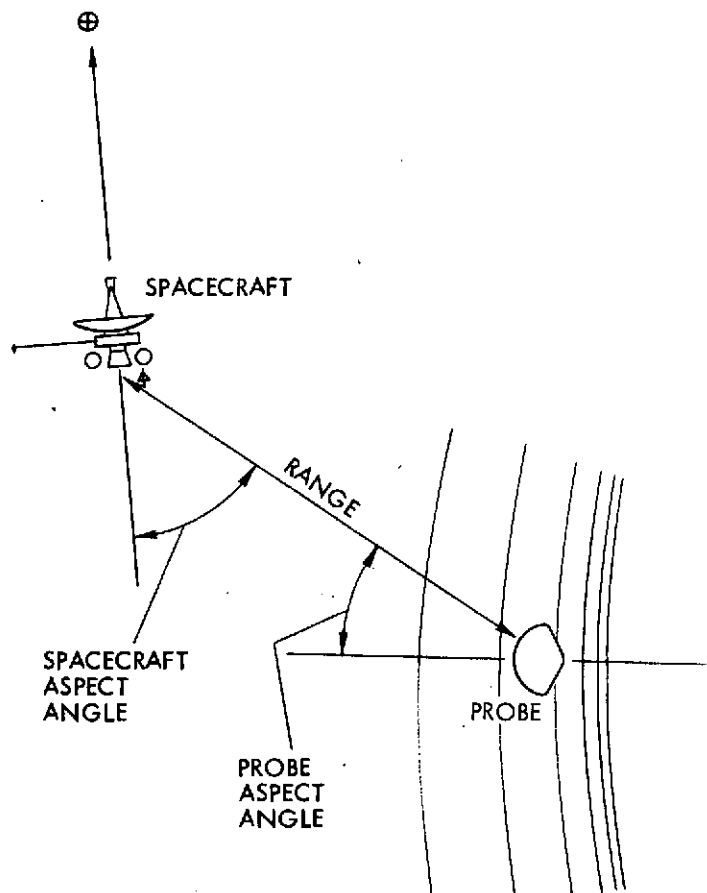


Figure 3-13. Definition of Aspect Angles

The probe aspect angle and the spacecraft aspect angle are almost equal (differing only by the motion of the earth line in the 50 days between probe separation and arrival at Jupiter) until entry. The basic plan of probe operation does not call for transmission during this time; however, if it were to be considered, it would be feasible but would extend the required beamwidth of the probe antenna.

At entry, it takes about 2 minutes for the probe to pitch over to a symmetric, vertical descent (see Figure 3-9), after which the probe aspect angle is that between the zenith and the line to the spacecraft.

It is desirable for antennas on both the spacecraft and probe to have the maximum gain consistent with size and weight limitations, and the requirement to cover the envelope of required aspect angles. However, in each case an axisymmetric antenna is to be employed: on the probe, because the entering probe has no control of its roll position; and on the spacecraft, because it is spinning and a despun antenna, while easing probe transmitter power requirements, would incur penalties in spacecraft cost, weight, and reliability.

For the requirements of axisymmetric antennas, the probe aspect angle remains below 39 degrees, its value just after pitchover. The spacecraft aspect angle lies between 49 degrees (its value at probe entry) and 99 degrees (its value after 30 minutes). The range drops from 73,000 km at entry to 57,000 km 30 minutes later.

### 3.2.6 Orbit Selection

The nominal initial orbit of the spacecraft about Jupiter is shown in Figure 3-14. The hyperbolic approach to a periapsis at  $1.8 R_J$  is seen, as well as half an elliptical orbit from  $1.8 R_J$  to apoapsis at  $150 R_J$ , and half an orbit from  $150 R_J$  to a second periapsis passage at  $14 R_J$ . This figure also shows the relation of the spacecraft orbits to the orbits of the four Galilean satellites.

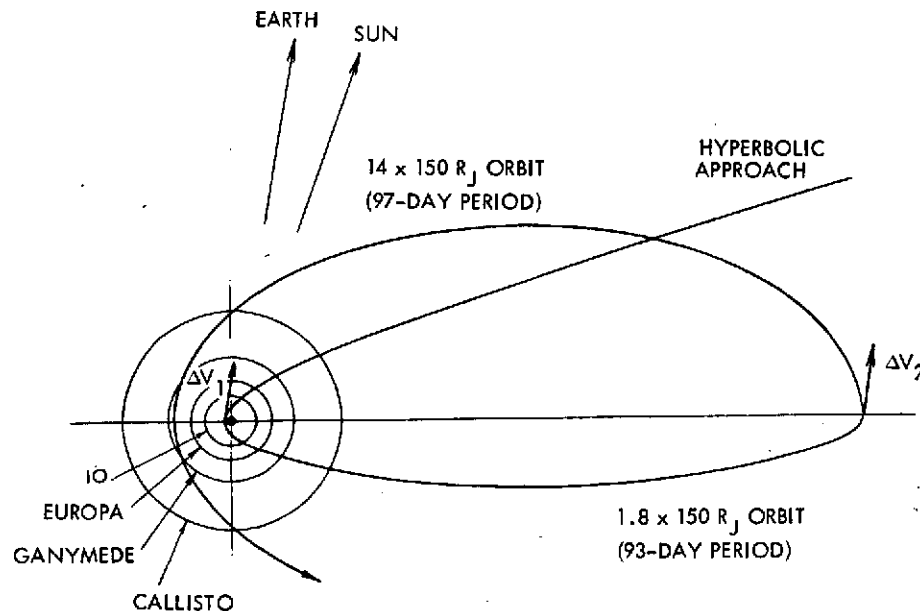


Figure 3-14. Nominal Initial Orbit about Jupiter

### 3.2.7 Orbit Insertion

The ideal transfer (in terms of propulsive efficiency) from the hyperbolic approach trajectory to an elliptic orbit is by impulsive tangential thrusting at the common periapsis point. The actual orbit insertion differs from the ideal in three respects:

- 1) The thrusting is not impulsive, but takes place over a  $\sim 27$ -minute period covering a significant arc of the trajectory
- 2) The thrusting is not tangential because of the desirability of holding to an earthline attitude, and because the trajectory curves during the period of firing
- 3) The thrusting does not take place at periapsis. Because of the precedence of probe data receipt and relay, thrusting does not start until after the hyperbolic periapsis is passed.

Nevertheless, the penalties for these deviations are minor in comparison with the ideal  $\Delta V$  requirements and easily within the capability of the PJO<sub>p</sub> spacecraft.

The ideal transfer requirements are indicated in Figure 3-15, with approach  $V_{\infty}$ , periapsis radius ( $R_p$ ), and apoapsis radius ( $R_a$ ) as parameters. These apsidal radii are measured from the center of Jupiter and are expressed in units of  $R_J$ , the equatorial radius of Jupiter. The total impulsive  $\Delta V$  is found by adding two components. For the example earth-Jupiter trajectory and initial orbit,  $V_{\infty} = 6.8$  km/sec,  $R_p = 1.8 R_J$ , and  $R_a = 150 R_J$ , and the components are:

Hyperbolic to parabolic	518 m/sec
Parabolic to elliptic	<u>264 m/sec</u>
Total $\Delta V$	782 m/sec

The penalties for deviating from the ideal impulsive transfer can be approximated by examining the increase in distance from Jupiter and the angle between the trajectory tangent and the earthline during firing, and are expressed in the following values:

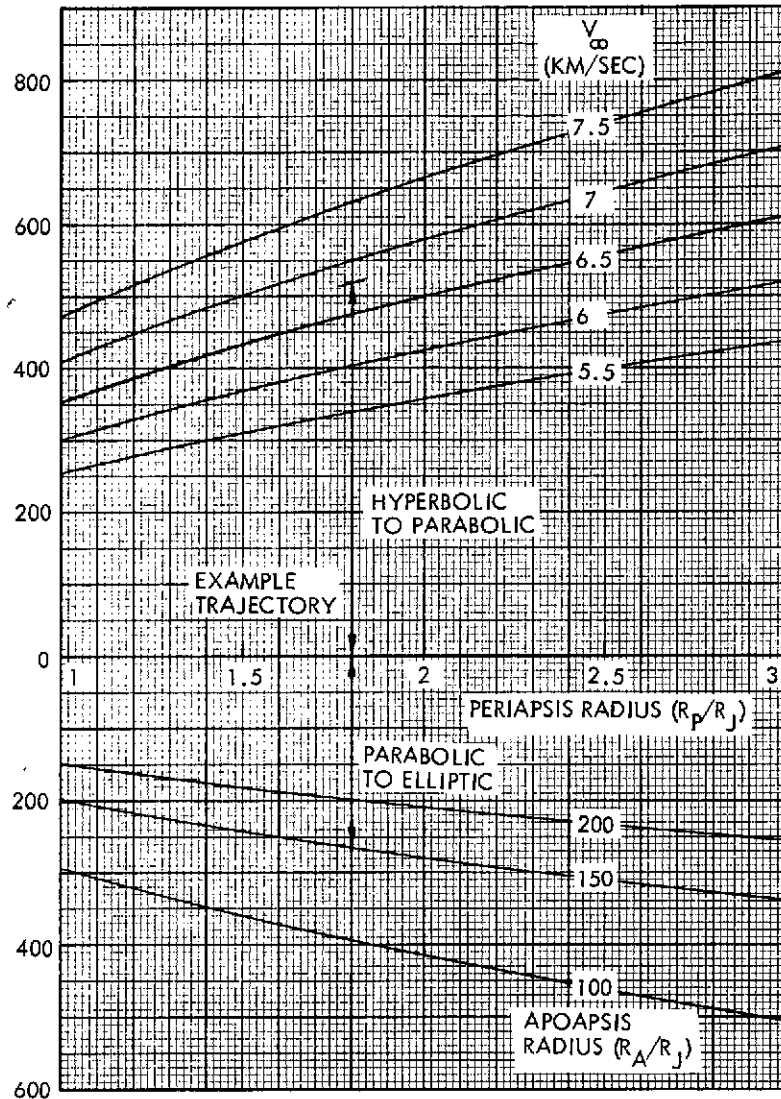


Figure 3-15. Orbit Insertion  $\Delta V$ . Ideal Transfer

	Distance from Planet Center ( $R_J$ )	Tangent- Earthline Angle (deg)
Beginning of firing	1.81	16
Middle of firing	1.87	24
End of firing	1.99	30

Evaluating penalties at the middle of firing, the increased altitude (from Figure 3-15) adds 16 m/sec, and the pointing error (based on sec  $\theta - 1$ ) adds 76 m/sec. Thus the actual orbit insertion maneuver is about 874 m/sec rather than the ideal of 782 m/sec.

### 3.2.8 Raising Periapsis

The maneuver at the first apoapsis, which has the objective of increasing the periapsis radius, can be performed with almost none of the penalties associated with the orbit insertion maneuver. The orbiter moves relatively slowly at apoapsis, so the duration of the maneuver or its deviation from the location of apoapsis impose no significant penalty. Furthermore, since the maneuver can be conducted at leisure without the press of probe communications, an off earthline attitude can be employed if desired to make the thrust tangential to the trajectory.

Thus only the ideal  $\Delta V$  is calculated for this maneuver. It is shown in Figure 3-16 as the difference of two velocities, with parameters of apoapsis radius ( $R_a/R_J$ ) and initial and final periapsis radius ( $R_p/R_J$ ). The two velocities are the apoapsis velocities of the initial and final orbits. In the nominal mission chosen, the velocity increment is shown as follows:

Final velocity ( $14 \times 150 R_J$ )	1421 m/sec
Initial velocity ( $1.8 \times 150 R_J$ )	<u>530 m/sec</u>
Ideal velocity increment	891 m/sec

With the two major propulsive maneuvers of orbit insertion at periapsis and the raising of periapsis by thrusting at apoapsis the orbiter is in a position to vary the orbit size – and the portion of Jupiter's environment to be investigated – by the technique of successive close encounters with the Galilean satellites. Thus the only subsequent propulsive operations are for orbit trim maneuvers, based on the navigational requirements for precise approach to each satellite encounter intended to alter the orbit.

While a detailed analysis of the estimated magnitude of these trim maneuvers has not been made (nor of the algorithms converting earth-based and orbiter-based tracking information into maneuver requirements), a preliminary estimate is that no more than 10 m/sec  $\Delta V$  would be necessary for each such encounter.

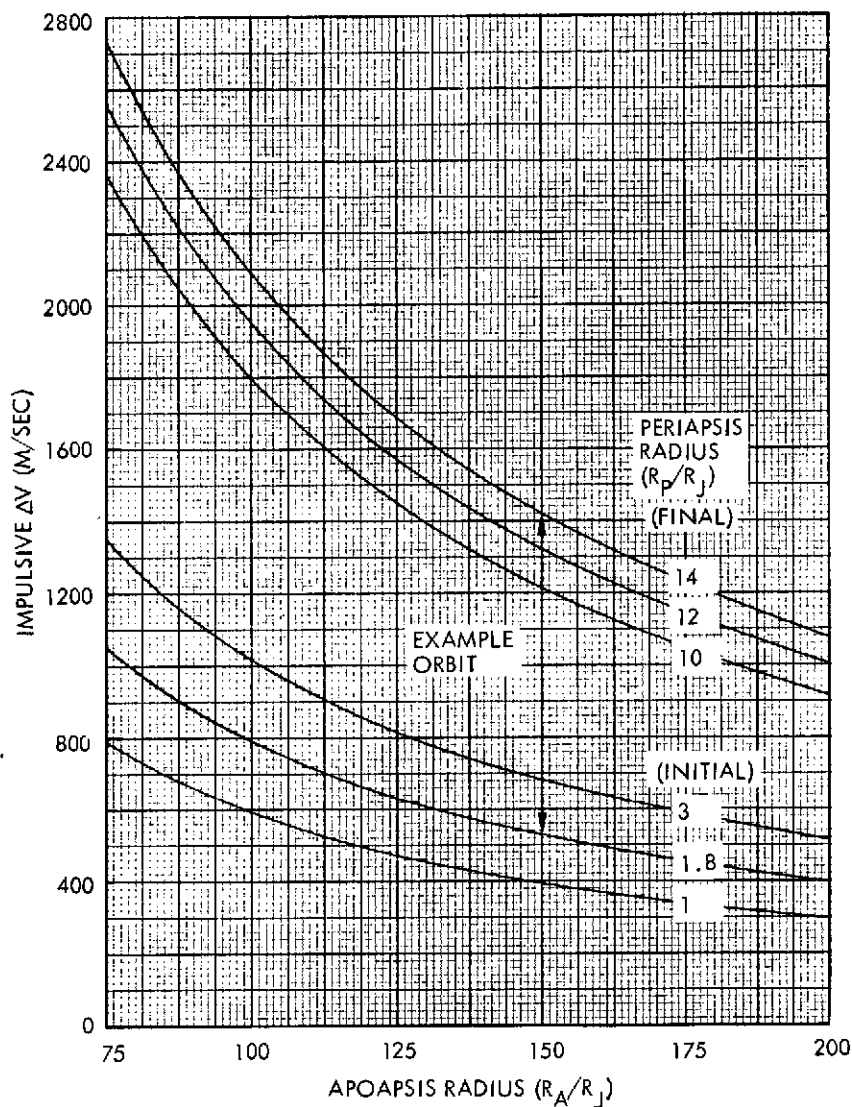


Figure 3-16.  $\Delta V$  at Apoapsis

### 3.2.9 Orbit Shaping by Satellite Encounters

The possibility of shaping and reshaping the orbit about Jupiter by successive encounters with the Galilean satellites has been discovered and published, primarily by JPL personnel. (8, 9, 10) The encounters must be precisely aimed, and be close enough to cause significant gravitational perturbation. By utilizing imaginative computer programs and exercising ingenuity in the selection of alternative encounter opportunities, a wide variety of possibilities may be exploited.

There are several classes of alternatives. In orbit "pumping" the orbital energy is decreased or increased, with corresponding decrease or increase in the periapsis and apoapsis distances and in the orbital period. "Cranking" consists of increasing the inclination of the orbit with each satellite encounter; in the course of several years, it can be increased from zero to perhaps 60 degrees. Either pumping or cranking can be performed by an elegant mode in which the spacecraft repeatedly encounters the same satellite at the same place, each time departing on an orbit whose period is a multiple (or a simple fraction) of the period of the satellite. This mode is called "resonance hopping."

Primarily by orbit pumping, sample PJO missions have been determined leading to a "flower orbit," which is depicted in Section 2. This determination was done for the joint NASA/ESRO consideration of the Pioneer Jupiter Orbiter Mission.<sup>(11)</sup> This mission requires an encounter almost every orbital revolution, with some 30 to 40 necessary in the course of 3 years. It features several orbits of  $\sim 150 R_J$  apoapsis at widely separated directions, to explore the more distant regions of the Jovian magnetosphere, and interim orbits of 20-40  $R_J$  apoapsis which are employed while the apsidal line is being rotated. The orbital plane approximates that of the Jovian equator throughout.

As noted before, work remains to be done with regard to several aspects of the plan of such orbit shaping:

- 1) The adequacy of earth-based radio tracking to determine spacecraft orbits accurately enough for the satellite encounters
- 2) The possible additional requirement for onboard spacecraft measurements to enhance orbit determination
- 3) The algorithm whereby tracking data is converted into instructions for trim maneuvers to remove small errors, and the operational impact of applying it to a succession of satellite encounters throughout the orbiter phase of the mission.

### 3.2.10 Daylight Entry Option (Type II Trajectory)

As discussed in Section 3.2.2, the preceding description of the  $PJO_p$ , based on the use of Type I earth-Jupiter trajectories, satisfies all major mission criteria but one. The defect is that the probe entry point is located on the dark side of Jupiter. By taking a longer trip time to Jupiter (and using Type II trajectories, which become more efficient when trip times exceed 1000 days) the arrival geometry is altered so that the entry point is brought to the daylight side of the sunset terminator.

Figure 3-17 illustrates the variation in several trajectory-related quantities with arrival date:

$C_3$	Injection energy
$V_\infty$	Asymptotic arrival velocity
ZAP	Angle between arrival asymptote and sunline
ZAE	Angle between arrival asymptote and earthline.

$C_3$  is shown for a single launch day (the minimum value) and for the minimum-energy 14-day band (indicating the greatest value in the band). All other quantities are shown for only the launch day corresponding to minimum  $C_3$ . Type I and Type II trajectories are both considered. Of the above quantities, only  $C_3$  differs significantly between Type I and Type II trajectories. The other quantities are effectively functions of arrival date only. Note that ZAP and ZAE angles are equal for trip times of approximately 700, 900 and 1100 days. The criterion, discussed in Section 3.2.2, to avoid arrival with low earth-Jupiter-sun angles excludes arrival dates within  $\pm 12$  days of those coincidences.

The daylight arrival criterion has been stated: the probe shall be no less than 10 degrees on the daylight side of the sunset terminator until 25 minutes after entry. This criterion is largely sensitive to the ZAP angle. Figure 3-18, by plotting sunset and 10 degrees before sunset relative to the probe entry point, shows how the criterion is observed if trajectories longer than 1050 days are used. This is the grounds for the choice of the band of Type II trajectories of approximately 1050 days trip time, outlined in Section 3.2.2.

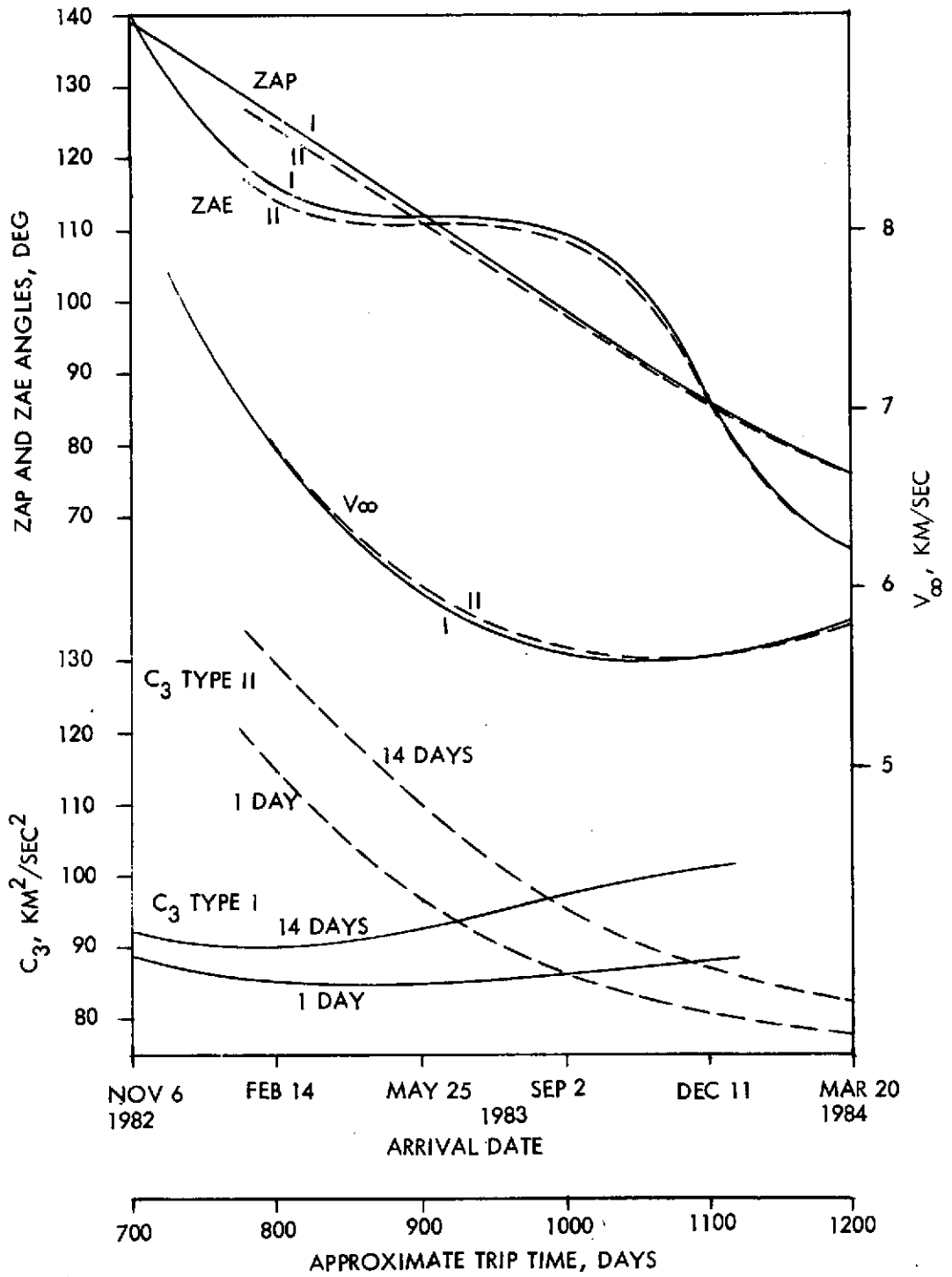


Figure 3-17. Trajectory Quantities vs Arrival Date

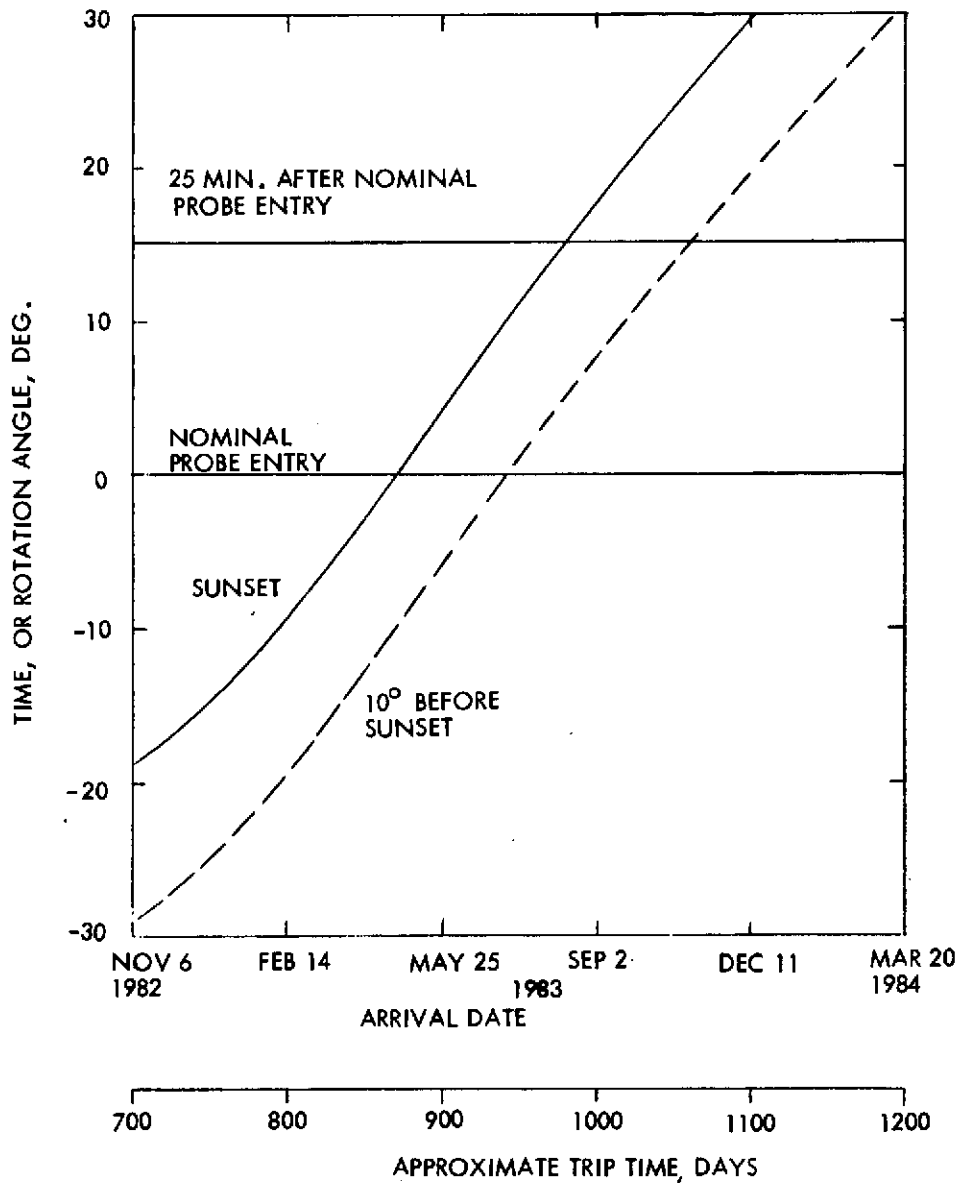


Figure 3-18. Local Time at Probe Entry and Descent

The resulting geometry of the approach of the probe and spacecraft to Jupiter is shown in Figure 3-19. (Compare with Figure 3-8.) This approach geometry translates into revised probe communication geometry which is shown in Figure 3-20. (Compare with Figure 3-12.)

The Type II trajectories selected here do satisfy the daylight entry requirement. Other collateral characteristics which accrue are discussed below, where the comparison is with the Type I trajectories.

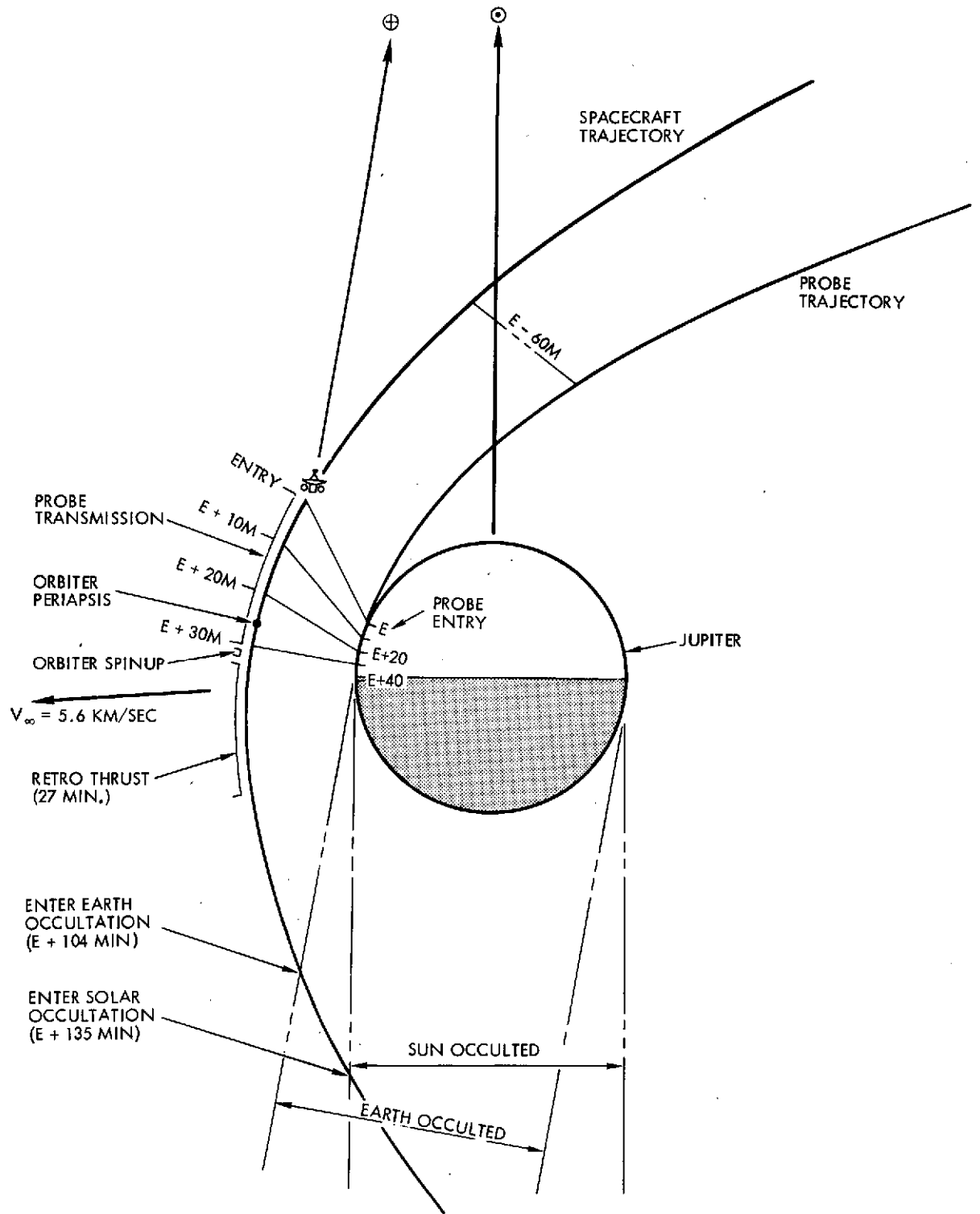


Figure 3-19. Probe and Spacecraft Approach to Jupiter (Type II Trajectory)

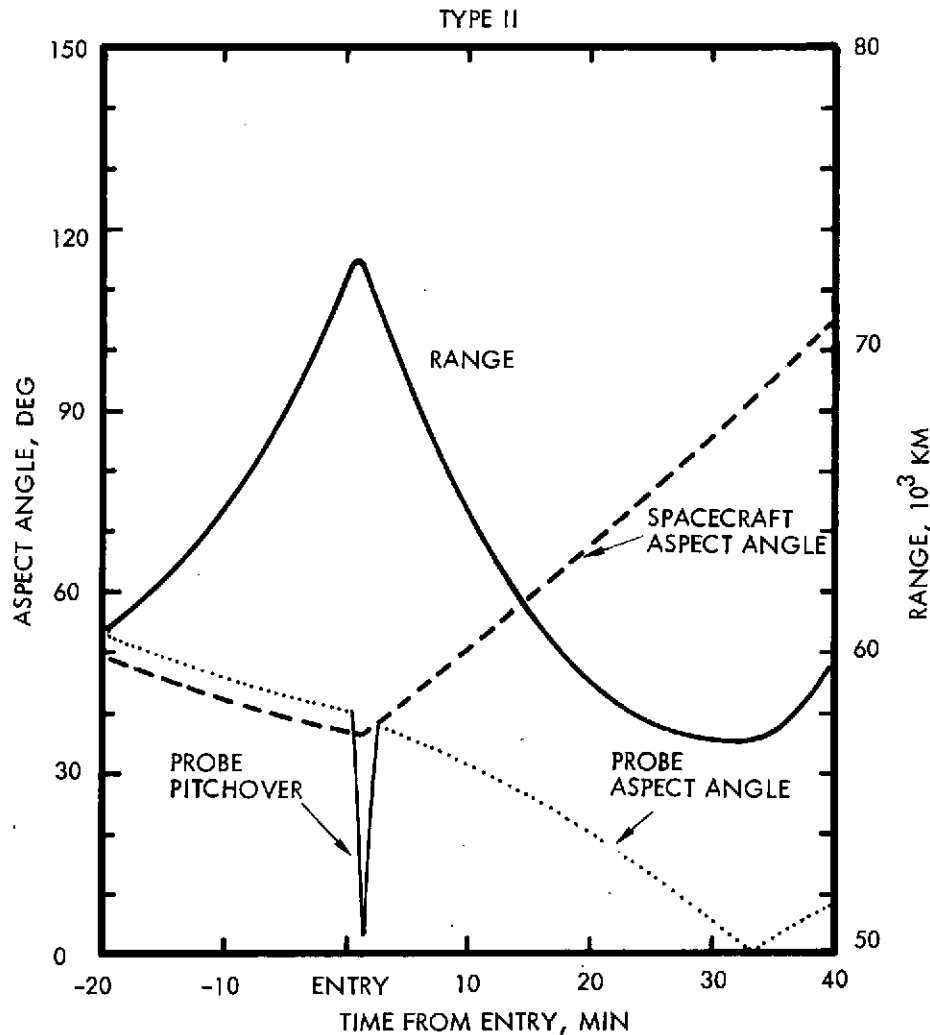


Figure 3-20. Probe Communication Geometry (Type II Trajectory)

The injection energy,  $C_3$ , is slightly higher over the 14-day launch window (91.3 vs. 90.0 km<sup>2</sup>/sec<sup>2</sup>). On the other hand, the  $V_\infty$  of arrival at Jupiter is significantly lower (5.6 vs. 6.8 km/sec). To accommodate the reduced  $C_3$ , 24 kg of propellant would be off-loaded, compared with the weight statement of Section 5. However, the orbit insertion maneuver from the slower approach takes 160 m/sec less  $\Delta V$ , requiring almost 50 kg less propellant, so the weight advantage is with the Type II trajectory.

(In addition to the  $\Delta V$  saving discussed above, there is a reduction of over 60 m/sec in the penalty associated with the pointing error during

firing. Because of the revised geometry, the average pointing error during firing is 9 degrees, compared with 24 degrees for Type I trajectories.)

Another advantage (apparent in Figure 3-19) is that the changed orientation of the sunline relative to the orbit apsidal line postpones the beginning of earth occultation and solar eclipse from several minutes after retro-thruster shutdown to about an hour after. The schedule of events is relaxed somewhat, and, more important, loss of direct communication is deferred until the spacecraft is at a greater distance from Jupiter and therefore farther beyond the peak radiation regions.

The only difference the Type II trajectory causes to the probe-spacecraft communication link parameters after entry is in the spacecraft aspect angle. Because of the different relative direction to the earth, the spacecraft aspect angle range is 36 to 86 degrees, compared with 49 to 99 degrees, for the 30-minute period following entry. This different range is accommodated by shifting the main lobe of the receiving antenna by 13 degrees toward the -Z axis.

The principal disadvantage of the longer trajectory is the influence on spacecraft life in orbit. The total life of the spacecraft is estimated at 6 years in either case. The 1050-day transfer, using 250 more days to reach Jupiter, would decrease estimated life in orbit from 3.8 to 3.1 years. (This assumes that ultimate termination of the mission is due to depletable or degradable components, e. g., the dropoff of RTG power available. If accumulated exposure to Jovian radiation were the dominating factor, then the two options would expect equal life in orbit.)

In summary, the Type II trajectory obtains the scientifically desirable daylight entry feature, the only disadvantage being the influence of the longer trip time on ultimate spacecraft life. On the other hand, it produces an advantage in weight margin and in operations at arrival at Jupiter.

### 3.2.11 Summary Propulsion Requirements and Performance

The propulsion requirements are dominated by the  $\Delta V$  requirements, 10 kg being more than enough for all the anticipated attitude control and spin-up/spin-down maneuvers.

99 percentile requirements are (in m/sec): all midcourse maneuvers 90, orbit deflection 53, orbit insertion 890, apoapsis 891 with orbital maneuver being currently uncertain. Summing, we have  $\Delta V = 1933 + \text{orbital maneuvers}$ .

Available propellant for these maneuvers is 543.5 kg which leads to a capability 2473 m/sec, leaving 440 m/sec for orbital maneuvers. Nominal (50th percentile)  $\Delta V$  requirements are 1867 m/sec giving 606 m/sec as the most probable capability for orbital maneuvers.

Although further study of orbital operation requirements is desirable, it is felt that even the 99th percentile case provides excess capability.

### References, Section 3

1. Letter, A3-910-Delta/JD20-710885, from E. W. Bonnett, Delta Program Manager, McDonnell Douglas Corp., to TRW Systems, August 9, 1971; Subject: DSV-3-17A Spin Table Strength.
2. "Follow-On Pioneer Missions to Jupiter. Volume 2. Pioneer Jupiter Orbiter Mission," TRW Systems Report 20406-6004-RO-00, August 13, 1971, pp 3-20, 3-21.
3. "Pioneer Jupiter Probe Orbiter 1980 Mission," Presentation, November 11, 1974, by NASA Ames Research Center to NASA/ESRO Study Group.
4. "The Planet Jupiter (1970)," NASA SP-8069, December 1971.
5. Russell, Dugan, and Stewart; Astronomy I (1945).
6. "Jupiter Atmospheric Entry Probe," Ames Research Center, September 16-18, 1974, page 5.
7. "Pioneer Jupiter Orbiter Probe Mission - 1980, Probe Description," presentation November 11-13, 1974, by McDonnell Douglas Corporation.
8. Beckman, Smith: "Jupiter Orbiter Satellite Tour Mission," AIAA/AAS Astrodynamics Conf., July 1973.
9. Uphoff, Friedman, Roberts: "Orbit Design Concepts for Jupiter Orbiter Missions," AIAA Paper 74-781, August 1974.
10. Beckman, Hyde, Rasool: "Exploring Jupiter and Its Satellites via an Orbiter," A&A, September 1974.
11. "Pioneer Jupiter Orbiter and Probe," ESRO Report MS(74)33, 30 December 1974.

#### 4. SUMMARY PROBE DESCRIPTION

(Abstracted from studies performed by the McDonnell Douglas Corporation)

The Jupiter probe design emphasizes use of current technology and flight-proven materials, hardware, subsystems, and components. The design stresses development through exploitation of existing testing and research facilities, established fabrication processes, and proven aerospace methods. The probe's size, shape, and internal arrangement are not optimized for minimum weight but for maximum development confidence. The goal is to achieve low technical risk through conservatism and moderate overdesign to increase development confidence with minimum cost and through simplifications that preclude sophisticated validation testing.

Most of the structure, mechanisms, internal support, and other components (see Figure 4-1) have already been fabricated in ARC machine shops. A full-size engineering model, complete with installed ballast equipment, simulated heat loads, wire bundles, and insulation will be

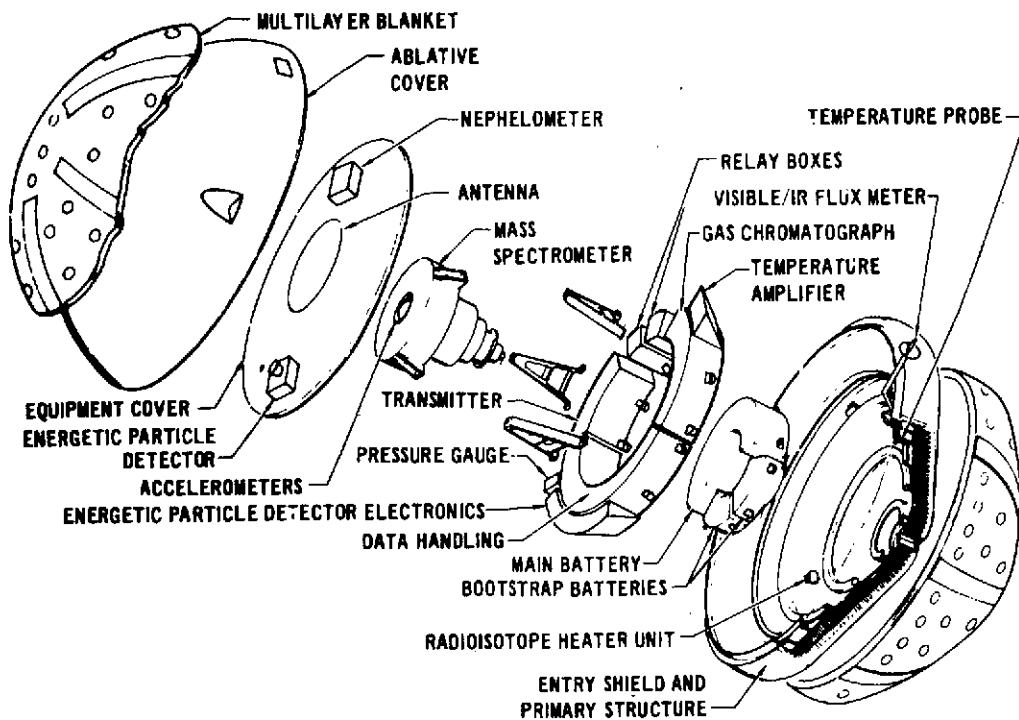


Figure 4-1. Probe Configuration

completed and available for structural, vibrational, and thermal test validation early in 1975. A quarter-size carbon-phenolic forward heat shield has been fabricated, and a full-size heat shield is scheduled for fabrication next year. This heat shield will be used on the engineering model. Many design validations underway include sample inlet and contamination tests, mechanical systems tests, heat shield specimen characterizations, insulation characterizations, structural tests, vibration and shock tests, thermal tests, aerodynamic stability validations, antenna patterns, and communication simulations.

The heat shield is one of the key factors in the probe design. Figure 4-2 shows the sources of ablation and presents weight and mass fraction data for the heat shield. The nominal entry angle is 7.5 degrees.

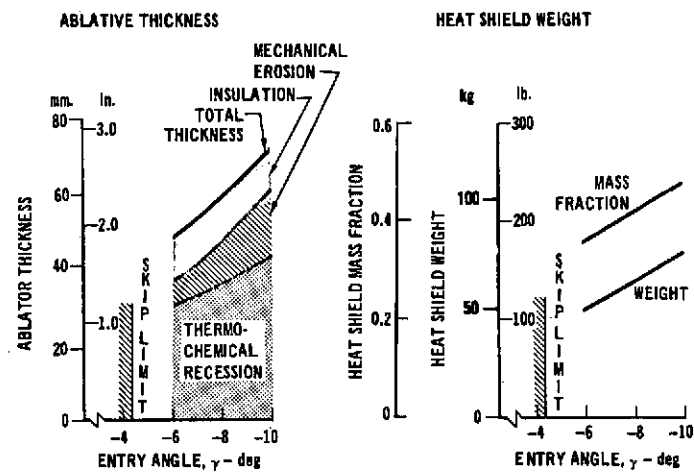


Figure 4-2. Carbon Phenolic Heat Shield Requirements

Another key factor is the need to place the center of gravity as near as possible to the nose (Figure 4-3). Toroidal equipment is used to achieve this factor. The probe-to-spacecraft communications link dominates power requirements (60-watt transmitter), and convolutional coding is used.

SUBSYSTEM	MASS (kg)
STRUCTURE	13.3
HEAT SHIELDS	68.6
HEATERS & INSULATION	6.9
COMMUNICATIONS & DATA HANDLING	10.3
ELECTRICAL POWER	9.3
PYROTECHNICS	3.7
SCIENCE PAYLOAD	20.4
INSTRUMENTATION	0.7
WEIGHT MARGIN (10%)	13.3
PROBE WEIGHT	146.5
LESS:	
INTERFACE WIRING	-1.1
EXTERNAL INSULATION	-2.5
AT ENTRY	142.8
LESS: ABLATION MATERIAL	-42.0
END OF MISSION	100.8
C.G. & INERTIAS AT ENTRY	
X AXIS C.G.* (PERCENT)	0.35
I <sub>x</sub> (ROLL) gm-cm <sup>2</sup> /10,000	11,262
I <sub>y</sub> (PITCH) gm-cm <sup>2</sup> /10,000	6,884
I <sub>z</sub> (YAW) gm-cm <sup>2</sup> /10,000	6,833

\*EXPRESSED AS PERCENT OF DIAMETER AFT OF THE CONICAL FOREBODY AND THE SPHERICAL AFTERBODY.

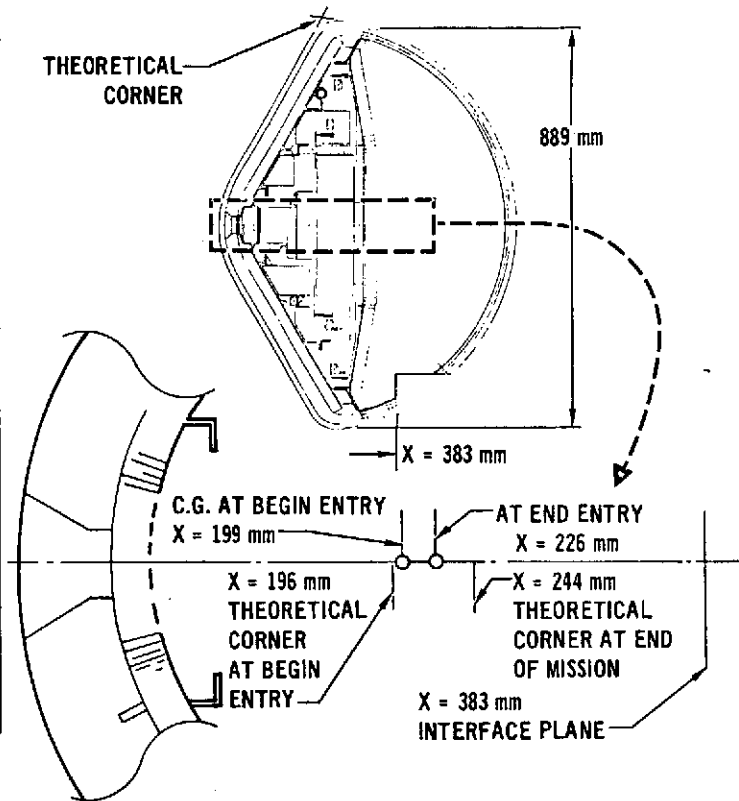


Figure 4-3. Mass Properties

## 5. SPACECRAFT DESCRIPTION

### 5.1 SYSTEM

#### 5.1.1 Configuration and Summary of Requirement Changes from Pioneer 10 and 11

The general philosophy is to use as much of Pioneer hardware as is possible, in the interest of low cost. Residual hardware (flight quality) will be used as-is or as-modified, plus new equipment as necessary for an engineering/prototype unit which will be used for system level qualification tests. The status of residual hardware is given in Appendix A. It is recognized that new boxes or equipment furnished for this unit will have commercial parts, and subsequent qualification of new flight quality boxes and equipment will be required at the box level — to be refurbished as flight spares. Flight hardware will be all newly manufactured.

The major new elements are, of course, the retropropulsion unit and the probe, the latter to be GFE to the spacecraft contractor. The changes necessary to the Pioneer 10 and 11 are primarily related to the accommodation of these new elements and to the probe delivery and data relay, and orbiting mission profiles. Secondly, a revised science payload complement requires revised interface provisions. In particular, the "Pioneer Line Scan Imaging System," under study by JPL, results in a requirement for additional high speed memory.

Figure 5-1 shows the conceptual design of the PJO<sub>p</sub> spacecraft and Table 5-1 summarizes the design drivers which led to this design. The propulsion module tankage, main engine (90 lb<sub>f</sub>) and its valve, pressure regulator, etc., are drawn from the qualified TRW Multi-Mission Bipropellant Propulsion System.

The spacecraft is spin stabilized, obtaining its spin axis pointing information through conically scanning the RF energy from the Deep Space Net. Roll angle is determined from the stellar reference assembly or the fine sun sensor. During occultation, roll angle is deduced from an accurate memory of the roll rate.

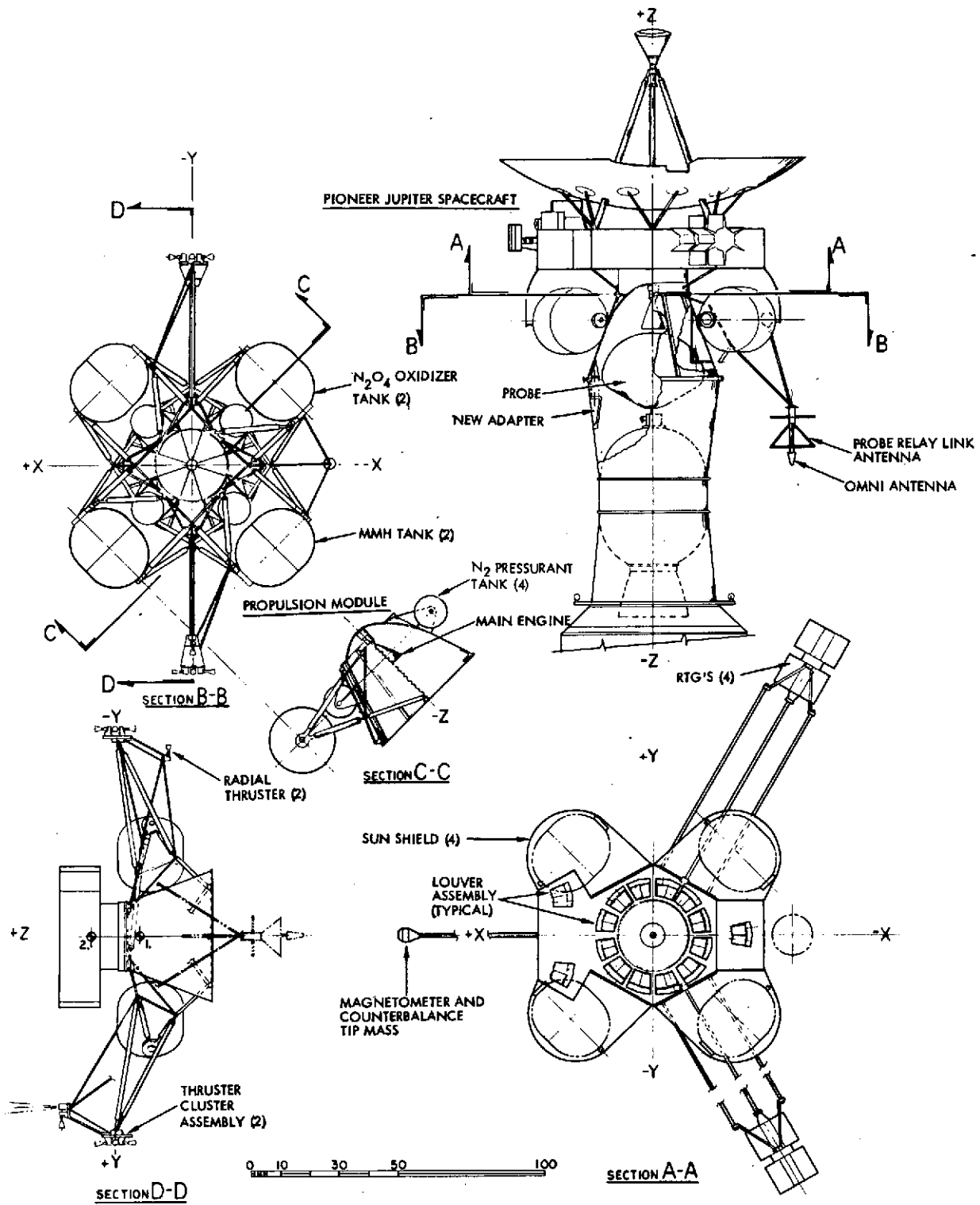


Figure 5-1. Spacecraft Configuration

Table 5-1. Design Drivers Arising from New Mission

- 1) Add retropropulsion unit to provide the propulsion capability required for the new (probe/orbiter) mission profile (to be attached to the Pioneer mounting ring).

Recommended Option. Have retropropulsion unit supply all propulsive functions using one large and several small bipropellant engines in the interest of weight savings and simplified tankage and interfaces. (Functions include attitude control.)

Accommodate probe within the retropropulsion unit and provide for probe release and relay communications and probe data storage and retransmission.

Impact

- Remove propulsion functions from basic spacecraft (Pioneer 10 and 11).
- Design new retropropulsion unit with adaptations to store and release the probe.
- Remove omni antenna from basic spacecraft and add omni and probe relay link antennas to retropropulsion unit. Add probe link receiver/synchronizer and provide for probe data storage.
- Thermal control [see 2) and 3)].
- Dynamics [see 4) and 5)].

- 2) Cope with the effects of louver blockage and solar reflections resulting from the presence of the retropropulsion unit and the probe.

Impact

- Design retropropulsion unit and its probe support structure to minimize louver blockage. This requires the tanks to be supported at a large radius from the centerline. This has the additional benefit of providing inertial stability immediately after separation from the TE 364-4 and before appendages are deployed.
- Provide highly reflective surfaces for structure and tankage seen by the louvers so that, as much as possible, the reflections show outer space.
- Adjust number and placement of louvers as necessary.
- Modify the Pioneer voltage control shunt regulator system to a multiple (sequential) HEAO-type shunt control system to reduce the power, and the variation of the power, that is dissipated in the basic spacecraft (see electrical power subsystem).
- Provide a sun shield over the tanks to isolate them from solar influence and to prevent solar reflections from reaching the louvers. Modify the early mission profile to limit solar cone angle to 45 degrees except for transient periods.

- 3) Provide thermal control for the retropropulsion unit and probe without exceeding the capability of four 50-watt radioisotope thermoelectric generators for total power demand. (These are the currently available model of the Pioneer RTG series and offer improved power/weight ratio.)

Impact

Extensive use is made of radioisotope heater units (RHU's), multilayer insulation for the structure, tanks and probe, and of structural thermal standoffs. Also, the sunshade is used to isolate from variable solar input over the mission profile. Pioneer 10 and 11 used RHU's for the small thrusters. Here we use them additionally for probe heating and for the main part of tank and main engine heating. Electrical line heaters are retained for the propellant lines.

Table 5-1. Design Drivers Arising from New Mission (Continued)

<p>4) Preserve spin axis/body axis alignment before and after appendage deployment and independent of propellant consumption when the plane of deployment (or propellant) no longer passes through the station of the center of gravity (c.g.).</p> <p><u>Impact</u></p> <p>Place a counterweight on the magnetometer boom so there is no lateral translation of the c.g. as a result of RTG and magnetometer boom deployment. In order to avoid transient effects during deployment, use a common-motor driven reel (different diameter for RTG's and magnetometer boom) so that all deployables pay out simultaneously and reach full extension at the same time. This also removes need for matched deployment dampers and reduces testing.</p> <p>Arrange tanks symmetrically and cross-connect tank pressurizing gas and outlets (two oxidizer and two fuel) so spin forces can equalize mass in opposing tanks.</p>
<p>5) Cope with effects of deboost acceleration (90 lb<sub>f</sub> engine) while appendages are deployed.</p> <p><u>Impact</u></p> <p>Involves a balance between increased spin rate during firing to reduce boom sag and to reduce thrust misalignment effects on maneuver accuracy, and structural beef-up resulting from spin rate increase. Preliminary solution involves:</p> <p style="padding-left: 40px;">Spin-up from 5 to 15 rpm</p> <p style="padding-left: 40px;">Possible strengthening of:</p> <p style="padding-left: 80px;">RTG guide rods and guide rod support Magnetometer boom and boom support structure (also to support counterweight)</p> <p style="padding-left: 40px;">Increase magnetometer boom root damper range from ±3 to +3 and -8 degrees and tune the damping constant to match the new inertia properties.</p>
<p>6) Provide roll attitude reference when the sun sensor is inaccurate due to small earth-sun angles (less than 2 degrees for 18-day periods approximately twice per year, taking into account the fact that the stellar reference assembly (Canopus sensor) may be disabled temporarily or permanently due to radiation effects or Canopus may be occulted or interfered with by Jupiter.</p> <p><u>Impact</u></p> <p>Provide a pseudo-period generator which can generate artificial roll pulses at a precommanded rate accurate enough to allow interpolation over an 18-day period with calibration at the start and end of the 18-day period.</p>
<p>7) In the interest of reducing the maneuver time and improving maneuver accuracy, certain large maneuvers are best performed using the main deboost engine in a non-earth pointing attitude. As a result it is recommended that functions be added to make such maneuvers safer than with Pioneer 10 and 11. However, it is also desired to have the capability for combined axial and lateral maneuvers in the earth-pointing mode for most (small) maneuvers.</p> <p><u>Impact</u></p> <ul style="list-style-type: none"> <li>• Provide automatic spin-up, spin-down logic</li> <li>• Provide backup go-to-sun mode</li> <li>• Provide radial thrusters (one above and one below the range of c.g. positions) and use commanded pulsewidth control to provide pulsed lateral thrust effectively through the c.g.</li> </ul> <p>(See attitude control subsystem.)</p>

Table 5-1. Design Drivers Arising from New Mission (Continued)

<p>8) Accommodate additional command (and command storage) capability appropriate to the new mission profile.</p> <p><u>Impact</u></p> <p>Requires an add-on remote command decoder.</p>
<p>9) Accommodate revised science instrument complement including the Pioneer line scan imager.</p> <p><u>Impact</u></p> <p>Revise apertures and mounting for instruments as required.</p> <p>Provide image data storage unit.</p> <p>Possibly provide additional platform area (-X axis compartment of Figure 5-1).</p>
<p>10) Provide capability to maneuver so as to have multiple close encounters with the Jovian satellites for satellite observation but, more important, to allow the orbit to be changed so as to explore different regions around Jupiter.</p> <p><u>Impact</u></p> <p>Requires additional propellant but this is available within the launch vehicle capability.</p>

Attitude control and midcourse maneuvers are provided by low thrust bipropellant thrusters located as shown. The 5-lb<sub>f</sub> bipropellant thruster (N<sub>2</sub>O<sub>4</sub>/MMH) developed by Aerojet Liquid Rocket Company under Air Force Contract No. FO4611-73-C-0061 is a likely candidate. These thrusters use the same propellant combination as the Multi-Mission Bipropellant System. Another possible combination is 392 Newton and 10 Newton (N<sub>2</sub>O<sub>4</sub>/AZ50) engines qualified for Symphonie by Messerschmitt-Bolkow-Blohm GMBH Space Division. Last, the main engine might be a residual Apollo 100-lb<sub>f</sub> engine (N<sub>2</sub>O<sub>4</sub>/AZ50) combined with the MBB 10 N engines.

After probe release, the bus deflection, orbit insertion, periapsis raise and later moderate correction maneuvers are made using the bipropellant engine. For near-equatorial orbits, the orbit insertion maneuver can be made in the earth-pointing attitude with little penalty. The spin rate must be increased from 5 to 15 rpm when the bipropellant engine is fired. The ability to make maneuvers off-earth-pointing is, however, provided. Small corrections can be made without off-earth-pointing by a combination of axial thrusters and pulsed radial thrusters.

Pulse duration control of the radial thrusters (one above the c.g. and one below) allows the average radial thrust to be through the c.g.

Power is supplied by four radioisotope thermoelectric generators (RTG's). These RTG's are the current model of the Pioneer RTG line and offer improved efficiency and power output. The RTG's and magnetometer boom are stowed at launch. They are deployed simultaneously and a counterweight on the magnetometer boom ensures that the spin axis does not shift. Communications provide a dual frequency (X-band carrier only) link and use the MJS-NASA standard dual frequency transponder (without X-band TWT). The S-band link has the capability of 2048 or 1024 bps depending on Jupiter/earth range. A probe relay link is provided and the probe data is transmitted in realtime and also stored in a redundant 160-kbit probe data storage unit for later retransmission. This data storage unit also replaces the Pioneer DSU for normal storage functions. The relay link antenna provides a conical pattern to maximize receive gain on a spinning vehicle. Up to 128 additional pulse commands and 64 commands and delay times can be stored in an add-on remote command decoder. An image data buffer (820 kbits) is also added for line-scan imaging.

The addition of the propulsion module causes partial blockage of the thermal louvers and has been compensated for by using a HEAO-type linear threshold shunt controller that reduces the internal dissipation by 30 watts and its variability from 0 to 40 watts to 0 to 10 watts. This, combined with heaters to replace nonoperating equipment, allows the louver system to be sized for a virtually constant power dissipation within the thermally controlled compartment. Also, the tanks are held far out to minimize blockage, and sun shields are added to isolate tanks and louvers from any solar heating effects.

### 5.1.2 Mass Properties

Table 5-2 summarizes the weight (mass) of the flight vehicle. Rather than show a weight margin, we show a propellant loading well above mission requirements. The adapter weight includes a telemetry package and reflects the new adapter structure. Table 5-3 provides a history of center of gravity and moment of inertia values and principal

axis direction. The K values relate to spin stability and to nutation amplitude buildup during precession as a function of the number of spin revolutions between precession pulses. Pioneer 10, 11 had a value of 0.86 which is more stable than our operating range of 0.59 to 0.75. However, Pioneers 6-9 operated well with a K value as low as 0.1. Calculations show that this range can still live with the Pioneer 10, 11 logic of one pulse pair/revolution for open loop precession and one pulse pair/three revolutions for conscan precession. In addition, the counterweight on the magnetometer boom significantly improves the performance of the boom damper. Note that  $(1+K)\omega$  is the coning rate of the Z axis in inertial space while  $K\omega$  is the rate seen by the boom damper in body coordinates.

Table 5-2. Pioneer Jupiter Orbiter Plus Probe Launch Weight

	Weight	
	(lb)	(kg)
Basic spacecraft - launch	579.0	262.6
Retropropulsion unit - dry	252.5	114.5
Probe	<u>323.0</u>	<u>146.5</u>
Spacecraft - dry	1154.5	523.6
Residuals		
Pressurant	33.1	15.0
Fuel	6.8	3.1
Oxidizer	11.0	5.0
Expendables		
Fuel - MMH	469.6	212.9
Oxidizer - N <sub>2</sub> O <sub>4</sub>	<u>751.0</u>	<u>340.6</u>
Spacecraft at launch	2426.0	1100.2
Adapter - spacecraft/TE364	<u>78.9</u>	<u>35.8</u>
Payload at launch*	2504.9	1136.0

\*NASA/Ames revised mission launch vehicle capability for: 800 days,  $C_3 = 90$  (km/sec<sup>2</sup>), 14-day launch window and zero gravity Centaur coast.

Table 5-3. PJO<sub>p</sub> Mass Properties – Pioneer Jupiter Orbiter with Probe

Spacecraft Condition	Weight (kg)	Centroid $\bar{z}$ (cm)	Principal Moments of Inertia			Principal Axis Location ( $\theta$ , * deg)	** K
			$I_{\bar{x}}$	$I_{\bar{y}}$	$I_{\bar{z}}$		
Spacecraft at BOL (appendages stowed)	1100	61.7	697	557	855	37.48	0.35
Spacecraft at BOL (fully deployed)	1100	61.7	904	1060	1566	30.15	0.59
Spacecraft - probe jettisoned (BOL less probe)	953	72.3	820	976	1554	30.15	0.73
Spacecraft at EOL (fully deployed, less probe and propellant)	399	98.3	507	584	957	~0	0.75

Notes: BOL = beginning of life  
 EOL = end of life  
 No lateral (x, y) centroid travel  
 $\bar{z}$  measured from separation plane

\* Principal axes  $\bar{x}$  and  $\bar{y}$  are in the x-y plane.  $\theta$  measured counterclockwise about +z axis from +x axis.

$$** K = \left( \frac{I_{\bar{z}} - I_{\bar{x}}}{I_{\bar{x}}} \frac{I_{\bar{z}} - I_{\bar{y}}}{I_{\bar{y}}} \right)^{1/2}, \quad \frac{\Omega}{\omega} = 1 + K = \text{ratio of nutation to spin speed}$$

$K^2 \leq 0$  is unstable.  $K \rightarrow 1$  is very stable.

Table 5-4 summarizes the weight of the basic spacecraft (flight vehicle less probe and retropropulsion unit) in a way that allows easy comparison with measured Pioneer 11 weights. Table 5-5 provides a detailed breakdown of these same weights, again in comparison to Pioneer 11.

Table 5-6 gives retropropulsion unit weights (masses). These reflect the use of TRW and Aerojet hardware (see Section 5.2.5) which is somewhat heavier than corresponding ESRO hardware presented in the 11 November meeting at NASA/Ames.

Table 5-4. Basic Spacecraft Subsystem Weight Summary

Subsystem	Weight		Pioneer 11 <sup>*</sup> Weight
	(kg)	(lb)	(lb)
Electrical power	72.1	159.0	159.4
Electrical distribution	19.0	42.0	38.0
Communications	12.1	26.7	22.5
Antenna	19.7	43.5	45.5
Data handling	8.6	19.0	11.8
Attitude control	6.8	15.0	12.6
Thermal control	10.4	22.9	16.3
Structure	58.6	129.2	104.5
Balance mass	8.8	19.5	5.9
Scientific instruments	46.5	102.5	67.0
Propulsion - wet	0	0	85.2
Name plaque and actual weight correction	0	0	0.8
Basic spacecraft - launch	262.6	579.0	569.5

\*Pioneer 11 mass properties based on final measurements prior to shipment.

Table 5-5. Basic Spacecraft Subsystem Details

Subsystem	Weight		Pioneer 11 (Reference) (lb)
	(kg)	(lb)	
Electrical Power	<u>72.1</u>	<u>159.0</u>	<u>159.4</u>
RTG 50-watt HPG design (4)	54.4	120.0	120.4
Power control unit	4.9	10.9	10.9
Battery (including cell protection)	2.4	5.3	5.3
Inverters (2)	4.6	10.2	10.2
Central TRF assembly	5.4	11.8	11.8
Strip heat assembly	0.4	0.8	0.8
Electrical Distribution	<u>19.0</u>	<u>42.0</u>	<u>38.0</u>
Command distribution unit	4.0	8.8	8.8
Cable and connectors (as required)	15.0	33.2	29.2
Communications	<u>12.1</u>	<u>26.7</u>	<u>22.5</u>
Spacecraft ↔ earth	(10.2)	(22.5)	
Conscan signal processor	0.36	0.8	0.8
Receivers, AGC's and preamps (2)	4.6	10.2	10.2
TWTA (2)	3.6	8.0	8.0
Transmitter drivers (2)	1.2	2.6	2.6
Attenuators (2)	0.02	0.05	0.05
RF cabling and connectors (as required)	0.4	0.9	0.9
Spacecraft ↔ probe	(1.9)	(4.2)	0
Transponder	1.9	4.2	0
Antennas	<u>19.7</u>	<u>43.5</u>	<u>45.5</u>
High-gain antenna assembly	14.5	32.1	33.4
Parabolic reflector	(11.5)	(25.5)	(25.5)
Reflector mount subassembly	(1.7)	(3.7)	(3.7)
Feed support assembly	(1.3)	(2.9)	(2.9)
Feed movement mechanism	0	0	(1.3)
Low-gain antenna	0	0	0.7
Medium-gain antenna	1.7	3.7	3.7
Diplexers and coupler (2/1)	1.9	4.3	4.3
Switches (2)	0.6	1.3	1.3
RF cabling and connectors (as required)	1.0	2.1	2.1
Data Handling	<u>8.6</u>	<u>19.0</u>	<u>11.8</u>
Digital telemetry unit	3.0	6.8	6.8
Data storage unit	1.5	3.3	3.3
Digital decoder unit (2)	0.8	1.7	1.7
Image data buffer	0.7	1.5	0
Probe data buffer	0.7	1.5	0
Remote command decoder	1.9	4.2	0

Table 5-5. Basic Spacecraft Subsystem Details (Continued)

Subsystem	Weight		Pioneer 11 (Reference) (lb)
	(kg)	(lb)	
Attitude Control Subsystem	<u>6.8</u>	<u>15.0</u>	<u>12.6</u>
Control electronics assembly	2.9	6.5	5.1
Stellar reference assembly	1.2	2.6	2.6
SRA light shade	1.5	3.4	3.4
Sun sensor assembly	0.5	1.1	1.1
Spin/despin sensor assembly (2)	0.7	1.4	0.4
Thermal Control	<u>10.4</u>	<u>22.9</u>	<u>16.3</u>
Insulation	5.1	11.3	11.3
Thermal louvers	2.6	5.8	4.3
Sun shade - propellant tanks (4)	2.4	5.2	0
RHU and support (sun sensor)	0.3	0.6	0.6
Gehrels' cover	0	0	0.1
Structure	<u>58.6</u>	<u>129.2</u>	<u>104.5</u>
Science compartment (-X)	6.8	15.0	0
Platform assembly	8.4	18.5	18.5
Side panels and interior bulkhead (11)	5.5	12.1	12.1
Cover panels (4)	3.2	7.1	7.1
Frame assembly	3.9	8.6	8.6
Separation assembly	6.3	13.9	13.9
Thruster support assemblies (2)	0	0	5.8
Magnetometer support assembly	7.7	17.0	7.6
RTG support assemblies (2)	12.7	28.0	22.4
Wobble damper	0.8	1.7	1.2
Miscellaneous and attach hardware (as required)	3.3	7.3	7.3
Actual weight correction	0	0	0.5
Balance Mass	<u>8.8</u>	<u>19.5</u>	<u>5.9</u>
Static and dynamic balance provisions	3.6	8.0	5.9
Counter mass - magnetometer boom	5.2	11.5	0
Propulsion - Wet			<u>85.2</u>
Thruster cluster assemblies	0	0	9.0
Propellant supply assembly	0	0	13.9
Line/heater assemblies	0	0	1.3
Propellant and pressurant	0	0	61.0

Table 5-6. Retropropulsion Unit Subsystem Weight

	Weight	
	(lb)	(kg)
Structure	<u>77.8</u>	<u>35.3</u>
Truncated cone assembly	48.4	22.0
Support truss - propellant tanks (as required)	11.6	5.3
Support assembly - N <sub>2</sub> spheres (4)	3.3	1.5
Support and release - probe (3)	1.2	0.5
Engine support - main	1.8	0.8
Thruster support - low level (2)	6.0	2.7
Fittings (8)	2.0	0.9
Support - antenna	1.2	0.5
Attach hardware (as required)	2.3	1.1
Electrical Distribution	<u>3.5</u>	<u>1.6</u>
Cable and connectors (as required)	3.5	1.6
Thermal Control	<u>14.6</u>	<u>6.6</u>
Heat shield - main engine	3.4	1.6
Insulation (as required)	9.8	4.2
Heaters - lines (as required)	1.4	0.4
Communications	<u>2.2</u>	<u>1.0</u>
Link antenna	1.3	0.6
Omni antenna	0.9	0.4
Propulsion System - Hardware	<u>154.4</u>	<u>70.0</u>
Main engine	10.4	4.7
Low thrust engines (10)	13.0	5.9
Tank assembly - propellant (4)	62.4	28.3
Pressurization spheres (4)	44.1	20.0
Pressurization control	10.4	4.7
Plumbing and valves	<u>14.1</u>	<u>6.4</u>
Retropropulsion Unit - Dry	252.5	114.5
Propulsion system - fluids	<u>1271.5</u>	<u>576.6</u>
Residual fuel - MMH	6.8	3.1
Residual oxidizer - N <sub>2</sub> O <sub>4</sub>	11.0	5.0
Pressurant - nitrogen	33.1	15.0
Fuel expendable - MMH	469.6	212.9
Oxidizer expendable - N <sub>2</sub> O <sub>4</sub>	<u>751.0</u>	<u>340.6</u>
Retropropulsion Unit - Launch	1524.0	691.1

### 5.1.3 Electrical Power Requirements

Table 5-7 shows  $PJO_p$  power requirements in comparison to measured values for Pioneer 10, 11. The dominant differences are associated with propulsion heaters and increased experiment power. The conversion to the NASA standard S-X transponder also causes a slight increase in power.

These requirements can be supported out to a 6.8-year life using four of the Teledyne Isotopes High Performance Generators (50 watts at 30 pounds). These generators are the currently available version of the Pioneer 10, 11 generators and offer improved efficiency.

## 5.2 SUBSYSTEMS

### 5.2.1 Structure

The structure of the basic Pioneer spacecraft is virtually unchanged except for the possible addition of a compartment for additional equipment stowage located on the -X axis as shown in Figure 5-1. Some minor beef-up of the RTG mounting fixtures and the magnetometer boom and boom support will be required as well as the increase in the boom damper operating angle. The removal of the tankage and thrusters from the basic spacecraft provides additional platform area in the center of the spacecraft, but this area is probably of little use since it must be insulated against the main engine heat soakback and therefore will be useful only for equipment that dissipates little power. The sunshade is an additional structural item which will probably be attached to the basic spacecraft. It is probably a lightweight fiberglass structure.

The retropropulsion structure consists of a central cone which supports the probe and interfaces with the launch vehicle adapter. The probe is supported by three bathtub fittings in the cone and is released by ball-lock pins, and separated by matched springs. Truss members from this center cone are used to support the tanks and small thrusters. These truss members dump their loads tangentially to the cone surface. Preliminary analyses indicate that the truss support structure for the tanks is quite efficient in spite of the distance to which the tanks are extended in order to minimize louver blockage. The main engine is

Table 5-7. PJO<sub>P</sub> Power Requirements

	Pioneer 10, 11 (W)	PJO <sub>P</sub> (W)
<b>Secondary DC Power</b>		
Communications		
Receivers (2)	3.4	-
Driver	1.3	-
Conscan processor	1.2	1.2
Attitude Control		
Control electronics assembly	2.7	3.5
Sun sensor assembly	0.2	0.2
Stellar reference assembly	0.3	0.3
Command		
Digital decoder unit	1.3	1.3
Command distribution unit	3.1	3.1
Remote command decoder	-	1.0
Data Handling		
Digital telemetry unit	3.7	3.7
Data storage unit	0.6	-
Probe/DTU storage unit	-	0.2
Image data storage unit	-	0.6
Subtotal (CTRF output)	17.8	15.1
CTRF input from inverter for above (63% efficiency)	28.4	24.1
<b>Primary DC Power</b>		
Communications		
Receivers (2)	-	5.0
Driver	-	3.0
TWTA, S-band (8 watts)	27.8	27.8
Attitude Control		
Control electronics assembly	0.4	0.4
Command		
Command distribution unit	0.2	0.2
Propulsion		
Transducer	0.2	0.3
Propulsion heaters	2.4	15.0
	+ RHU's	+ RHU's

Table 5-7. PJO<sub>p</sub> Power Requirements (Continued)

	Pioneer 10/11 (W)	PJO <sub>p</sub> (W)
Probe		
Heaters	-	0.0
Data link	-	+ RHU's 10.0*
Experiments (except PLSI and X-band)	24.0	30.0
Pioneer line scan imager	-	10.0**
X-Band beacon (250 mW)	-	12.5***
Power		
Battery electronics	0.1	-
Cable losses	<u>0.6</u>	<u>1.4</u>
Subtotal (28V dc loads)	55.7	83.1
Power control unit losses	7.7	11.5
CTRF input (from above)	<u>28.4</u>	<u>24.1</u>
Inverter output	91.8	118.7
Inverter input (4.2V dc) at 88% efficiency to supply above	104.4	135.0
RTG cable losses	<u>4.2</u>	<u>7.0</u>
Required RTG power	108.6	142.0
RTG power at 5.2 years	118.6	153.1
Time for RTG's to degrade to above level	6.7 yr	6.8 yr

\* Used once at 800 days so not counted in end-of-life budget

\*\* Operates for 0.1 sec every half hour - time share with other experiments near end of life

\*\*\* Used primarily during onset and emergence from occultation (time share with other experiments near end of life)



supported inside the cone and above the probe from a dome-shaped member attached to the cone. A Marman clamp, identical to that used on Pioneer 10, 11 is used to mate the retropropulsion system to the basic spacecraft. A new conical adapter is required, but the separation features of the existing adapter are retained. The N<sub>2</sub> pressurant tanks are supported directly off the cone, as shown. The truss structure supporting the thrusters (and one sun sensor) are designed so that thermal deflections result in minimum misalignment of paired thrusters (spin, despin, up, down and radial pairs). This truss arrangement appears superior, from a thermal insulation point of view, to the 11 November 1974 concept of supporting the engines off of the tanks. It does result in tanks mounted at 45 degrees to the principal axes.

### 5.2.2 Thermal Control

Major considerations in thermal control are to provide adequate louver and other radiating areas to manage the internal power dissipation in the presence of blockage by the retropropulsion unit, to provide thermal control for the retropropulsion unit and probe, and to isolate from solar effects.

Changes have been instituted in the shunt regulator to minimize the power and the variation of the power which is dissipated inside the spacecraft, as discussed in Section 5.2.3. This, combined with infrared reflective surfaces on the retropropulsion tankage and the structure, allows the louvers to largely see space, even if by reflection. Figure 5-2 shows the allowable internal dissipation for the Pioneer 10, 11 louver complement as a function of effective louver blockage. The power normally dissipated in the spacecraft varies from 112 to 123 watts. This indicates that only a small amount of blockage can be tolerated unless further changes are made in the thermal control subsystem. Changes contemplated include increased louver area, some areas of direct radiation surfaces, and control of the average power level dissipated inside the spacecraft. For example, the power available is such that if an experiment is turned off, a heater can be turned on to replace its dissipation. The combination of the sun shield shown in Figure 5-1 plus good insulation and a pointing profile which limits the sun to cone angles less than 45 degrees, except for the transient conditions, isolates the thermal control system from solar effects.

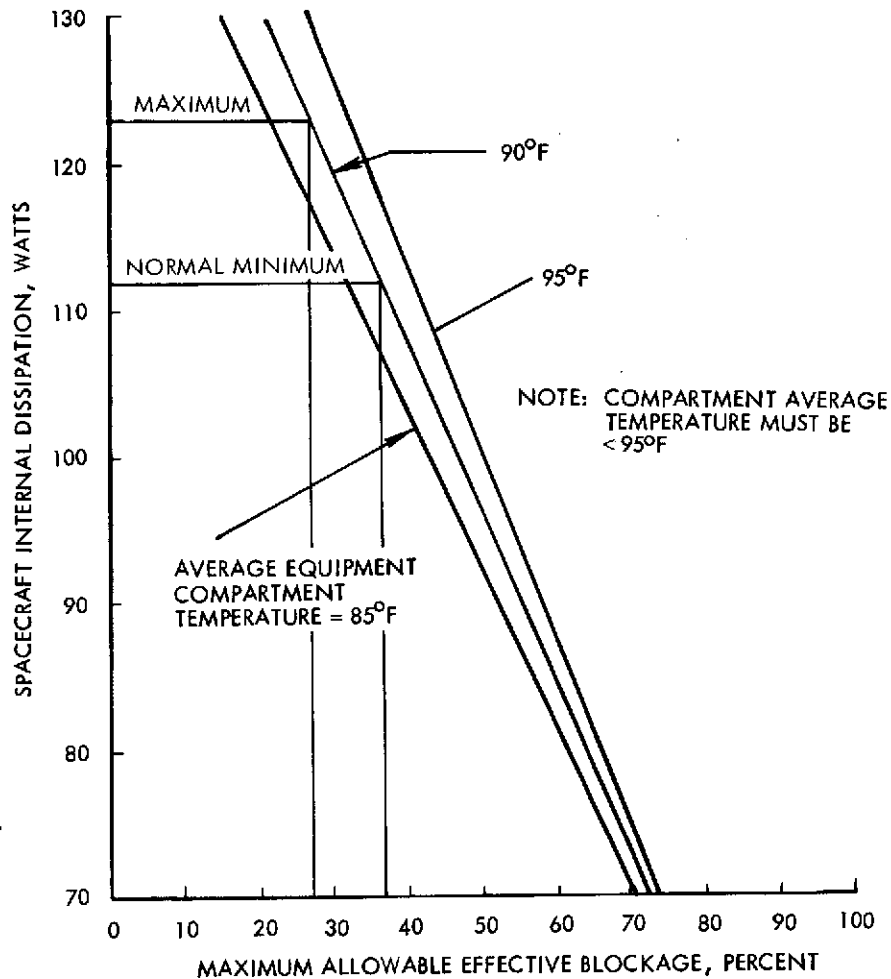


Figure 5-2. Allowable Effective Blockage of the Pioneer 10, 11 Louver System vs Internal Spacecraft Dissipation

Thermal control of the tankage and propellant lines is achieved through the use of multilayer insulation and heaters. Electrical heaters are used for the propellant lines and to supplement, for control purposes, radioisotope heater units (RHU's) for the tanks. The heater power required represents one of the major causes of increased power demand for this mission, which is allowed for by the improved RTG's available today. It is anticipated that only RHU's will be required for thruster thermal control. Probe thermal control can also be by RHU's if the back of the probe is well insulated, since this would give similar thermal control conditions whether the probe is attached or in free flight. The sun shade also isolates the tanks and probe from solar effects.

### 5.2.3 Electrical Power

Louver blockage and higher (200-watt) RTG capability makes it desirable to provide for a smaller range of power dissipation inside the basic spacecraft. One main cause of variable power in Pioneer 10, 11 was the shunt control element which could dissipate from 0 to 38 watts, depending on the state of the RTG's and the power demand. The use of a HEAO sequential shunt allows this power to be reduced to a range of 0 to 10.5 watts. It utilizes two of three majority voting reference and error amplifiers, as did Pioneer 10, 11 to generate an error signal which controls the shunt elements. It would have six identical linear elements with separate thresholds such that only one of the linear elements is in the maximum power dissipating region for any given shunt requirement. Five elements could handle the maximum current with the sixth included to provide for an open failure in any one of the five. Short failures are removed by relay and ground command. This design can be implemented with changes which are restricted to the A slice of the power control unit, Figure 5-3.

The shunt control power dissipated in the spacecraft is calculated as follows and is illustrated in Figure 5-4. The total power available from the new RTG's is 200 watts ( $4 \times 50$ ). Assuming that the under-voltage is now 73 watts and RTG cable losses are 7 watts, the total power for the shunt to control is  $193 - 73 = 120$  watts.

Assuming the same nominal bus voltage, 28 volts, the shunt current requirement is  $120/28 = 4.29$  amperes. With five segments, the current to each segment is  $4.29/5 = 0.86$  ampere.

The maximum power in each shunt segment occurs at the point where the voltage across the transistor and the voltage across the shunt radiator resistors are equal, which is at one-half the bus voltage and one-half the maximum current. Maximum power for each segment is therefore  $(1/2 \times 28) \times 1/2 \times 0.86 = 14 \times 0.43 = 6.02$  watts.

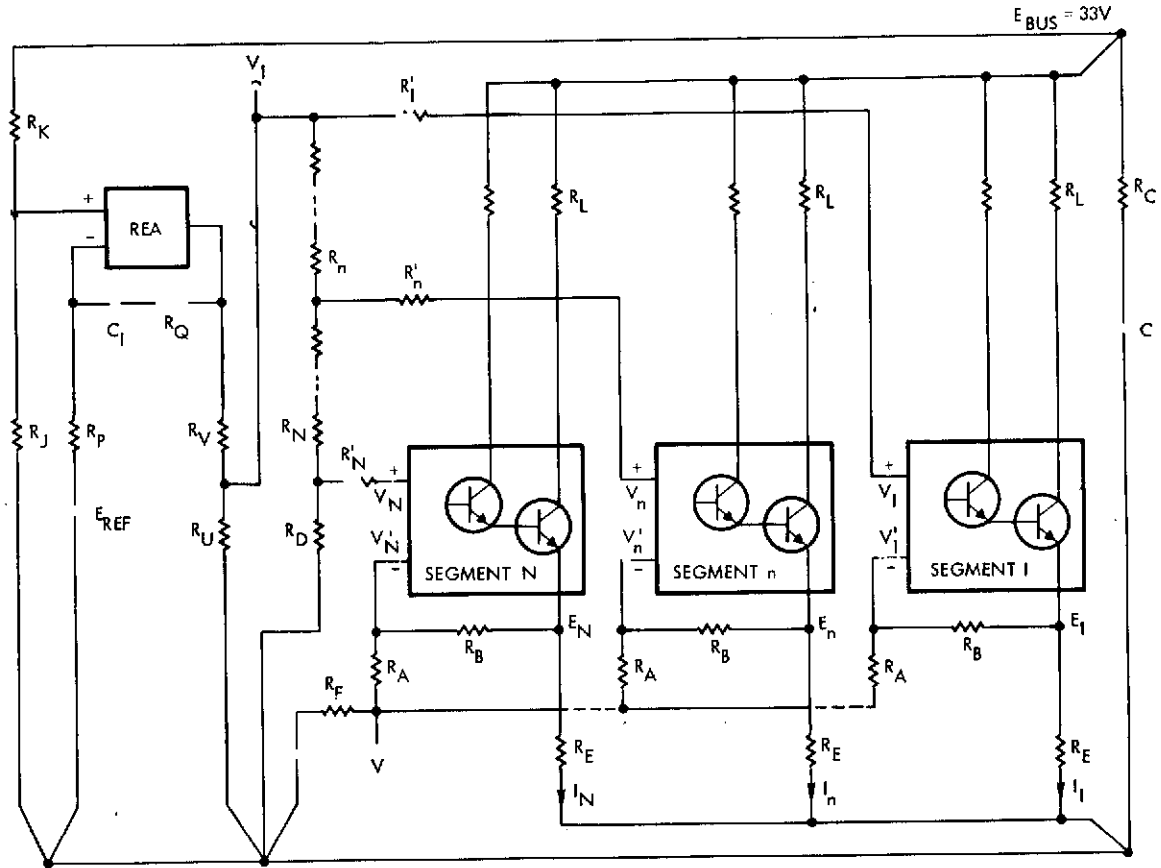


Figure 5-3. PJO<sub>p</sub> Shunt Regulator Diagram

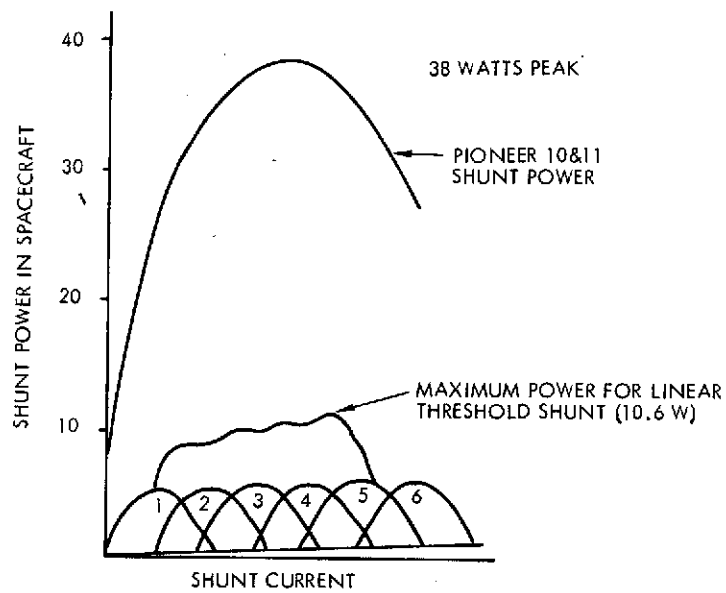


Figure 5-4. Comparison of Total Shunt Power Dissipation

The power dissipation for a saturated segment is the sum of the dissipation in the saturated output transistor and the drive power. The output transistor presently used in the shunt is conservatively derated (ECH) to have less than 0.1-volt drop for currents less than 1 ampere with a gain of 20. The collector dissipation is then  $0.86 \times 0.1 = 0.086 = 86 \text{ mW}$  when fully saturated. Assuming a gain of 20 and a drive voltage of 2 volts, the base drive losses are  $(0.86/20) \times 2 = 0.086 \text{ watt}$ . Assuming a worst case gain of 10 in the driven transistor and a drive voltage of 15 volts, the predriver current is 4.3 mA and the power =  $4.3 \times 15 \times 10^{-3} = 65 \text{ mW}$ . Assuming twice this amount for the remainder of the circuit, the total power for the saturated shunt segment is as follows:

$$P_{\text{SAT}} = (3 \times 65 \text{ mW}) + (2 \times 86 \text{ mW}) = 0.37 \text{ watt.}$$

#### Total Shunt Power

The total shunt power is greater than the sum of one of the individual peaks and the accumulated saturation powers because of the current HEAO requirement to overlap the individual shunt range to allow for the failure of a single element. Based on HEAO breadboard tests, the peak power in the output devices sums to 1.57 times the individual peaks. Assuming that the PJO shunt would be overlapped in the same manner, the peak power in the total shunt would be as the fourth element was going off and the fifth was coming on. At this point, we would have  $1.57 (6.02 + 3 (0.37)) = 10.56 \text{ watts maximum}$ . The figure shows maximum power dissipated as a function of shunt current in comparison to Pioneer F and G. The minimum (end of life for RTG's) would be zero. The PCU swing is reduced from Pioneer 10, 11's 38 watts to 10.56, allowing thermal louver blockage to be accommodated.

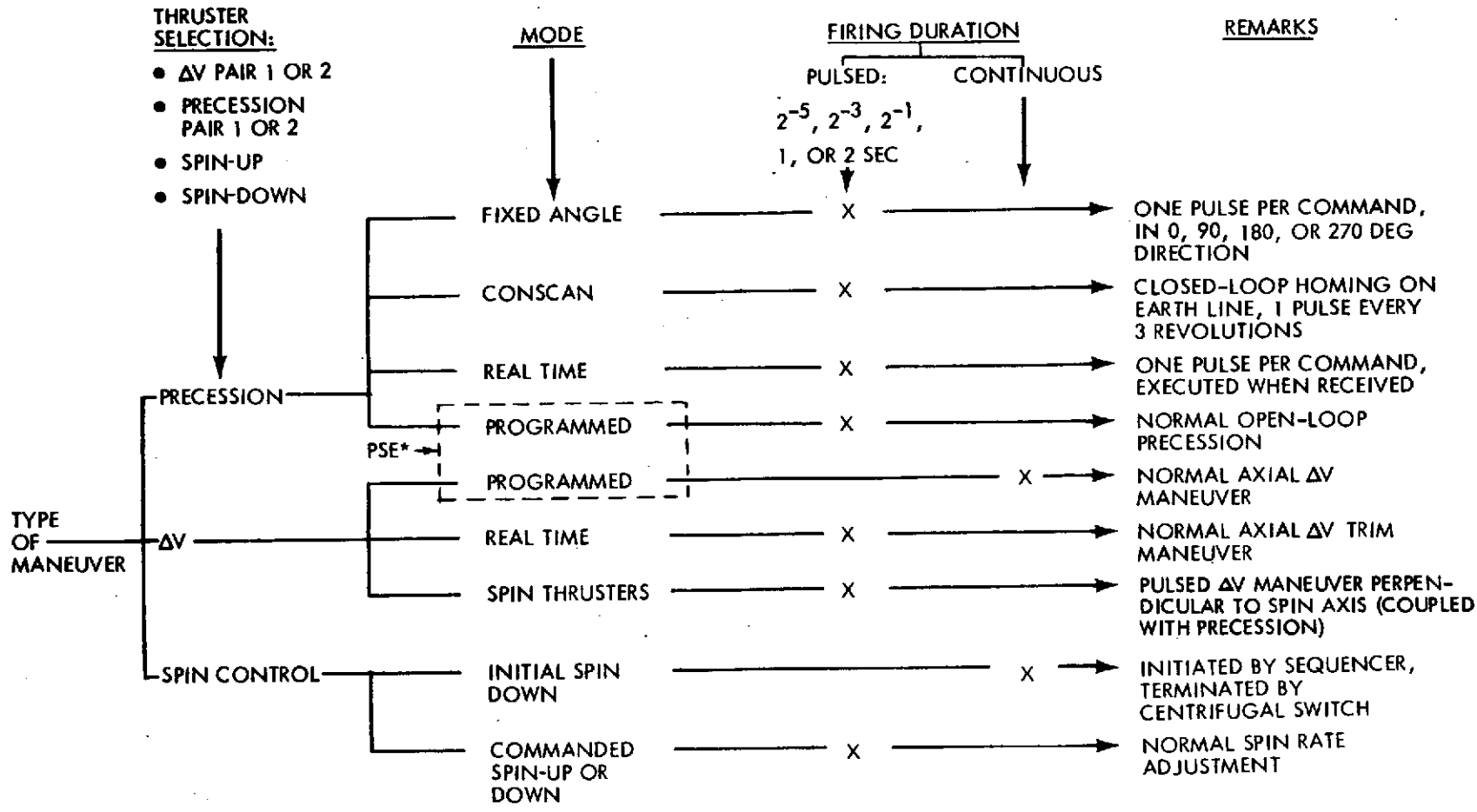
Tests of a six-segment shunt with only No. 1 and No. 6 being used show that the shunts operate properly without overlap, promising further reductions if necessary, at the expense of a slightly greater controlled voltage range.

#### 5.2.4 Attitude Control

Figure 5-5 shows the existing Pioneer 10, 11 maneuver control modes. Additional attitude control capabilities are desired for this mission. In particular, the separation maneuver following probe release is best done using the high thrust engine in an off-earth pointing mode. Similarly, large maneuvers in orbit about Jupiter required in order to encounter Jupiter's satellites should be performed using this main engine. However, for small maneuvers it is desired to have the capability to perform lateral maneuvers while earth pointing. This desire to off-earth point leads to the need for a backup mode to the already existing maneuver capability which will guarantee that the spacecraft can reacquire the earth. This backup mode, indicated in Table 5-8, provides for automatic return to a sun pointing attitude in the event of any failure of the existing capability to maneuver away from and back to the earth. Commands can be received on the medium-gain antenna from this sun pointing attitude and a normal conscan earth acquisition can be initiated. The use of the large engine requires that the spacecraft be spun up to a higher speed, tentatively 15 rpm. This reduces magnetometer boom sag and improves the accuracy of the maneuver. Since this spin-up/spin-down will be done several times it was felt desirable to have an automatic spin-up/spin-down capability.

Table 5-8. Backup Sun Seeking Mode

- Initiated automatically on non-receipt of communications for several hours
- Causes automatic precession toward sun
- Turns off automatically at about  $1 \pm 0.2$  degrees from sun line
- Enables uplink communications to be reestablished with spacecraft
- Provides backup for failures of or during off-earth pointing maneuvers
- Requires addition of a small amount of logic and a turn-off sun sensor. Also uses existing sun sensor assembly.



\* PSE: PROGRAM STORAGE AND EXECUTION CIRCUIT STORES ALL PARAMETERS (PRIMARY AND REDUNDANT) FOR PRECESSION-ΔV-PRECESSION SEQUENCE

Figure 5-5. Pioneer 10 Maneuver Control Modes

This capability is described in Table 5-9 and the circuitry to implement both the backup sun-seeking mode and the automatic spin-up/spin-down are shown in Figure 5-6. The implementation for lateral maneuvers in the earth-pointing mode is shown in Figure 5-7 and the circuitry in Figure 5-8. The basic concept is to control the net lateral thrust so that it goes through the c. g. and does not cause precession.

Table 5-9. Automatic Spin-Up/Spin-Down

- Needed to provide stiffness and stability during 88-lb<sub>f</sub> engine firings
- Spin-up to 15 rpm done automatically just prior to engine firing
- Spin-down to 4.8 rpm done automatically just after engine firing
- Spin speed determined onboard by comparing spin period (as determined by the sun sensor pulses) to fixed periods
- Spin-down also triggered prior to entry into backup sun-seeking mode
- Initiation of spin-up/spin-down controlled by existing stored program logic
- All precessions continue to be made at 4.8 rpm
- Spin thrusters should be in couples to reduce wobble due to the displacement of c. g. out of thruster plane

The Canopus sensor can be interfered with by a bright Jupiter and may not survive for the many orbits expected in a 3-year orbit lifetime. Further, there are periods twice a year in which the sun sensor does not provide good roll reference information because the sun is less than 2 degrees from the earth. A backup roll phase reference can be provided by a pseudoperiod generator shown in Figure 5-9. The roll period is determined on the ground by looking at either the conscan modulation or, better, polarization modulation of the X-band beacon which has only a small Faraday rotation and can be determined to an accumulated error of a fraction of a degree in an 8-hour tracking pass. This corresponds to an error in the spin period of one part per million or better. This period is transmitted to the spacecraft and loaded into the 22-bit shift register shown. The contents of the shift register are transferred to the 22-bit parallel-in, up counter which is counted down by a 262 kHz

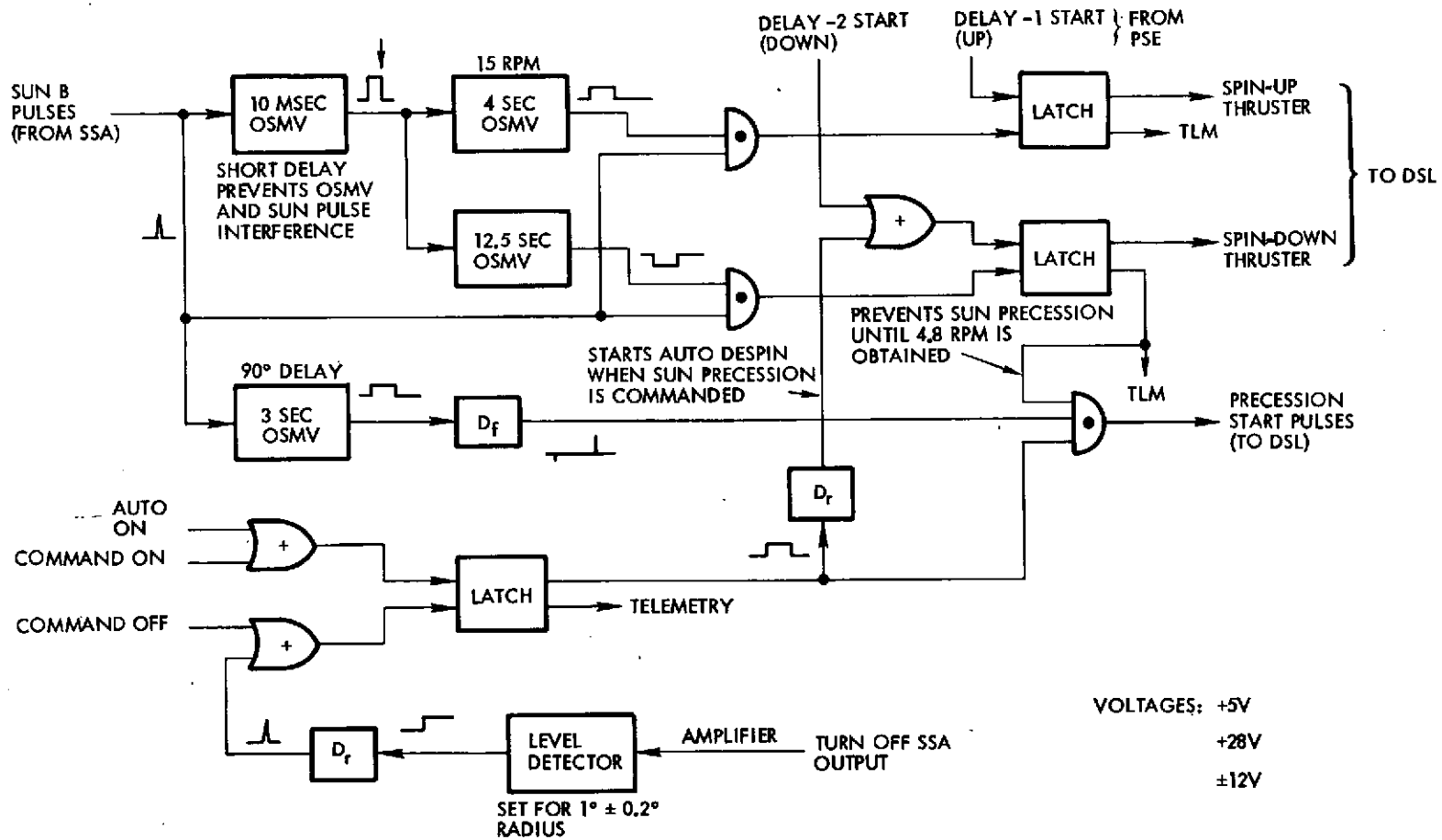


Figure 5-6. Sun Precession and Auto-Spin Logic Block Diagram

- PULSED FIRING OF 5-LB<sub>f</sub> RADIAL THRUSTERS CAN PROVIDE  $\Delta V$  WHILE REMAINING EARTH-POINTING
- THRUSTERS PLACED ABOVE AND BELOW THE C.G. RANGE CAN BE VARIED IN LENGTH OF PULSE FIRING TO COMPENSATE FOR ACTUAL C.G. LOCATION TO
  - MINIMIZE UNDESIRE PRECESSION
  - REDUCE INEFFICIENCIES (DUE TO COSINE LOSS)
- FIRING ANGLES ARE PRE-COMMANDED TO PROVIDE EQUAL MOMENTS ABOUT ACTUAL C.G.
- TWO REGISTERS AND A COUNTER MUST BE ADDED TO CONTROL THE FIRING ANGLES. EXISTING REGISTERS CONTAIN
  - INITIAL FIRING ANGLE
  - FIRING DURATION

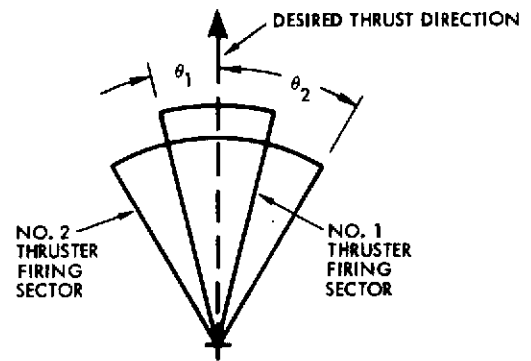
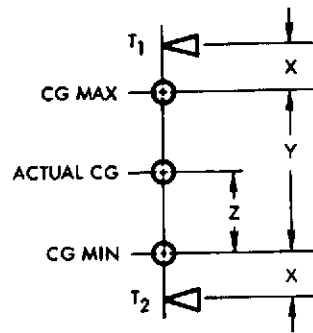


Figure 5-7. Radial Thruster Control (PJO<sub>p</sub>)

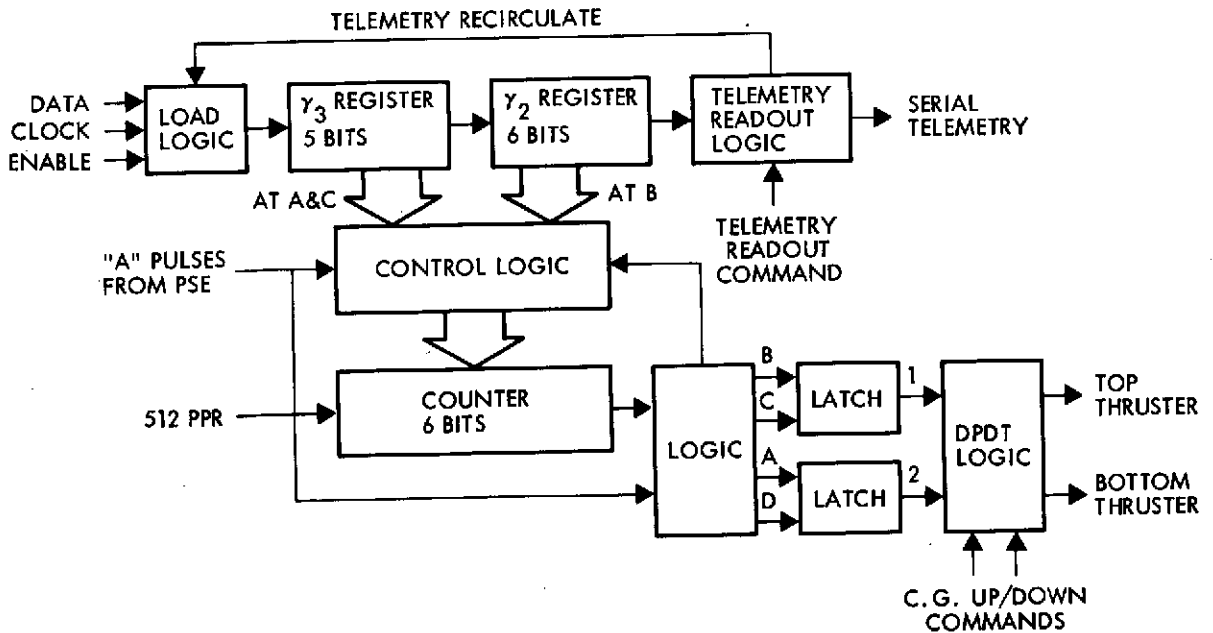


Figure 5-8. Radial Thruster Program Logic

signal derived from the 4.19 MHz clock. A pulse is transferred out at the end of a revolution and the 22-bit in-parallel out shift register contents are again transferred in for the next revolution. This allows accuracy adequate for science requirements over an 18-day period when calibrated by a good roll reference at the end of the period. If an earth pointing maneuver is made during the period, the spin period should be re-determined and the counter updated.

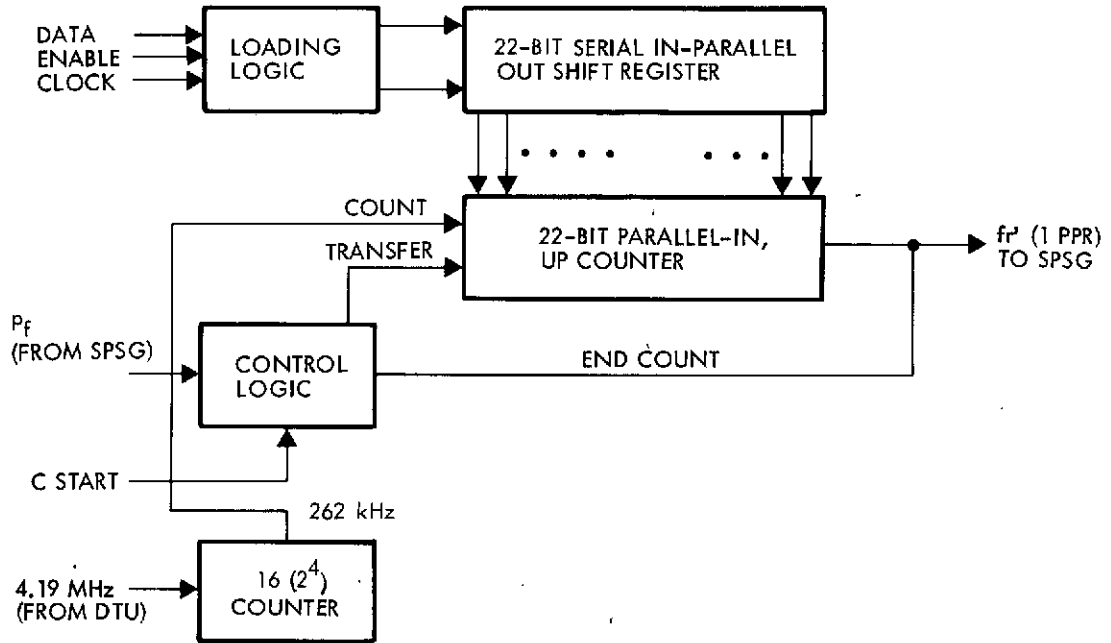


Figure 5-9. Pseudoperiod Logic Block Diagram

### 5.2.5 Propulsion

Adequate control and midcourse maneuvers are provided by low thrust propellant thrusters located as shown in Figure 5-1. The 5-lb<sub>f</sub> bipropellant thruster (N<sub>2</sub>O<sub>4</sub>/MMH) developed by Aerojet Liquid Rocket Company under Air Force Contract No. FO4611-73-C-0061 is a likely candidate.\* These thrusters use the same propellant combination as the

\* R. C. Schindler and L. Schoenman, Aerojet Liquid Rocket Company, Sacramento, California, "Development of a Five-Pound Thrust Bipropellant Engine," AIAA Paper No. 74-1179, presented at AIAA/SAE 10th Propulsion Conference, San Diego, California, October 21-23, 1974.

J. I. Ito, Aerojet Liquid Rocket Company, Sacramento, California, "Design Analysis for Performance and Exhaust Contamination of a Five-Pound Bipropellant Engine," AIAA Paper No. 74-1180, presented at AIAA/SAE 10th Propulsion Conference, San Diego, California, October 21-23, 1974.

Multi-Mission Bipropellant System. Another possible combination is 392-Newton and 10-Newton ( $N_2O_4/AZ50$ ) engines qualified for Symphonie by Messerschmitt-Bolkow-Blohm GMBH Space Division. Last, the main engine might be a residual Apollo 100-lb<sub>f</sub> engine ( $N_2O_4/AZ50$ ) combined with the MBB 10-N engines.

Some data on the Aerojet engine is shown in Figures 5-10, 5-11, 5-12, 5-13, and 5-14, and Table 5-10. This is data supplied to us by Aerojet, who extracted it from Report AFRPL-TR-54-51, the final report on the Five-Pound Thrust Bipropellant Program funded by RPL. They also said that \$500K to \$750K would be required to complete qualification and the recurring cost would be \$35K. They also recommended using  $I_{sp}$ 's of 290 seconds for continuous thrust and 255 seconds for pulsed operation for calculation purposes.

The main engine, propellant tanks, pressurant control assembly, fill and vent assembly, and propellant supply assembly are drawn from the qualified TRW Multi-Mission Bipropellant Propulsion System. The pressurant tanks were used on the Saturn IVB. In this application, the engine gimbals would be removed. Appendix B provides a recent data package describing this system.

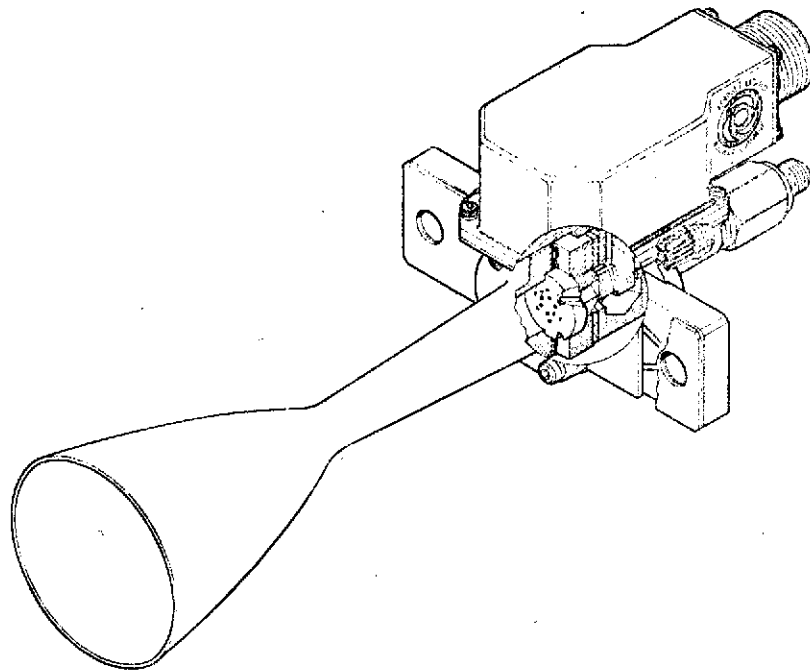


Figure 5-10. Five-Pound Thrust Biopropellant Engine

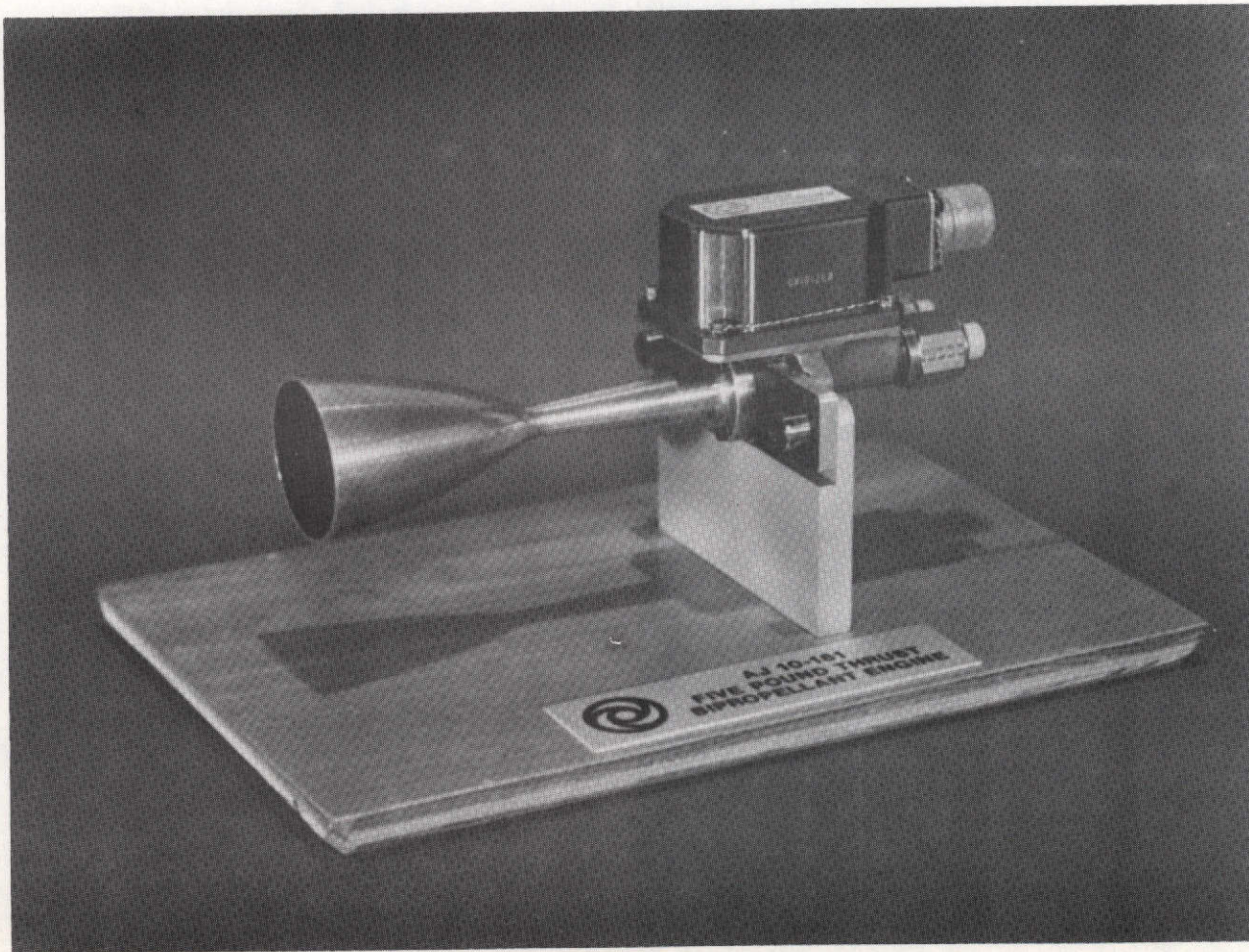
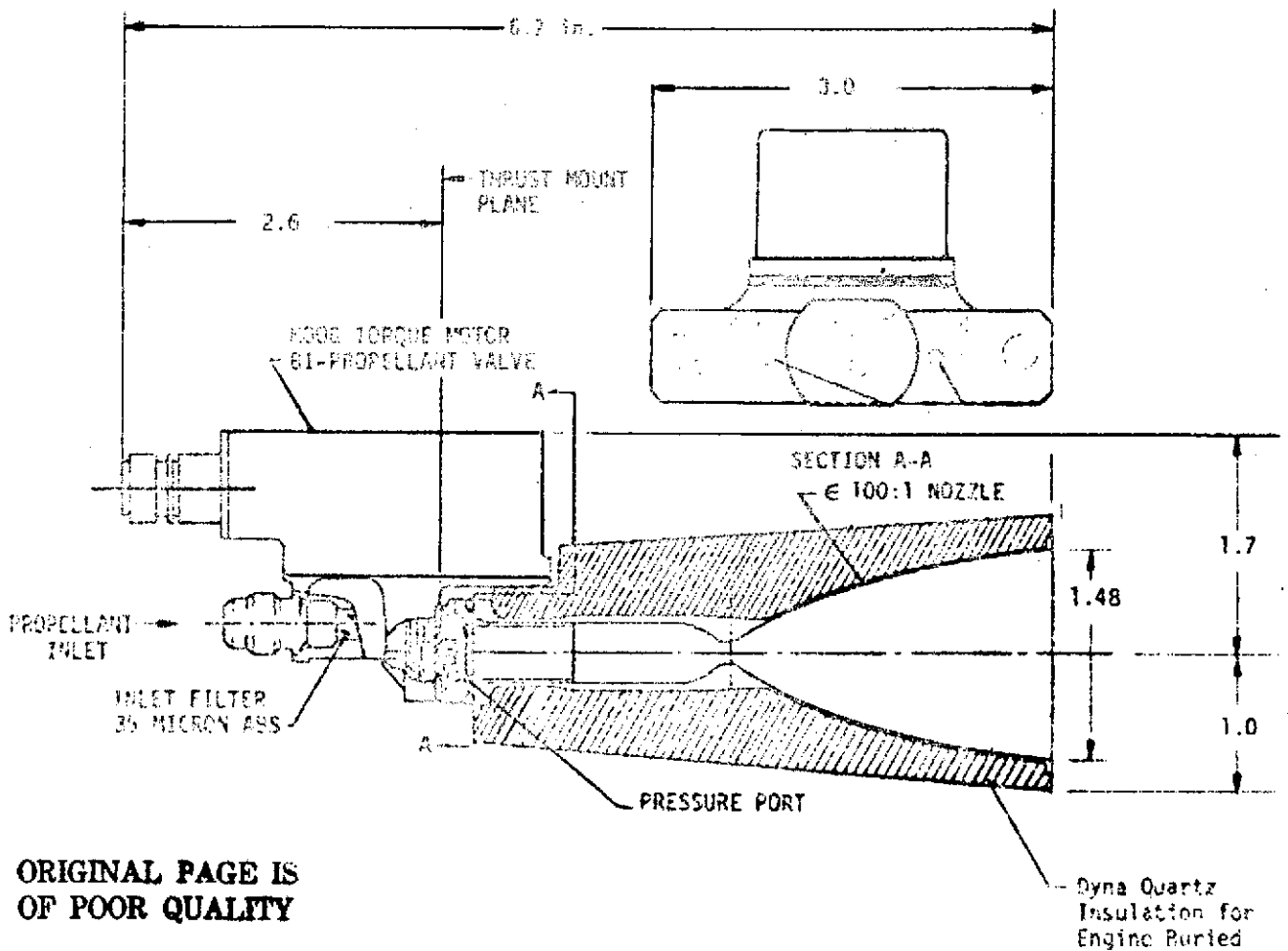


Figure 5-11. Five-Pound Thrust Propellant Engine



ORIGINAL PAGE IS  
OF POOR QUALITY

Operating Characteristics

	Full Thrust	Min. Thrust
Thrust, lbf	4.5	2.2
Chamber Pressure, psia	150	75
Feed Pressure, psia	300	125
$I_{sp}$ Steady State, sec	283*	255*
$I_{sp}$ for 0.050 lb-sec Impulse Bit	228	200
Min. Impulse Bit, lb-sec	0.025	0.012
Min. EPW, sec	0.005	0.005
Valve Response Time to Full Open, sec	0.003	0.003
Valve Response Time to Full Shut, sec	0.003	0.003
Sec to 90% of $P_c$	0.005	0.006
Propellant	$N_2O_4/MMH$	
Mixture Ratio	1.6	
Engine Weight, lb	1.3	

\* $A_e/A_t = 100$ ; Add 2.5 sec for  $A_e/A_t = 150$

Figure 5-12. AJ10-181-1 Engine

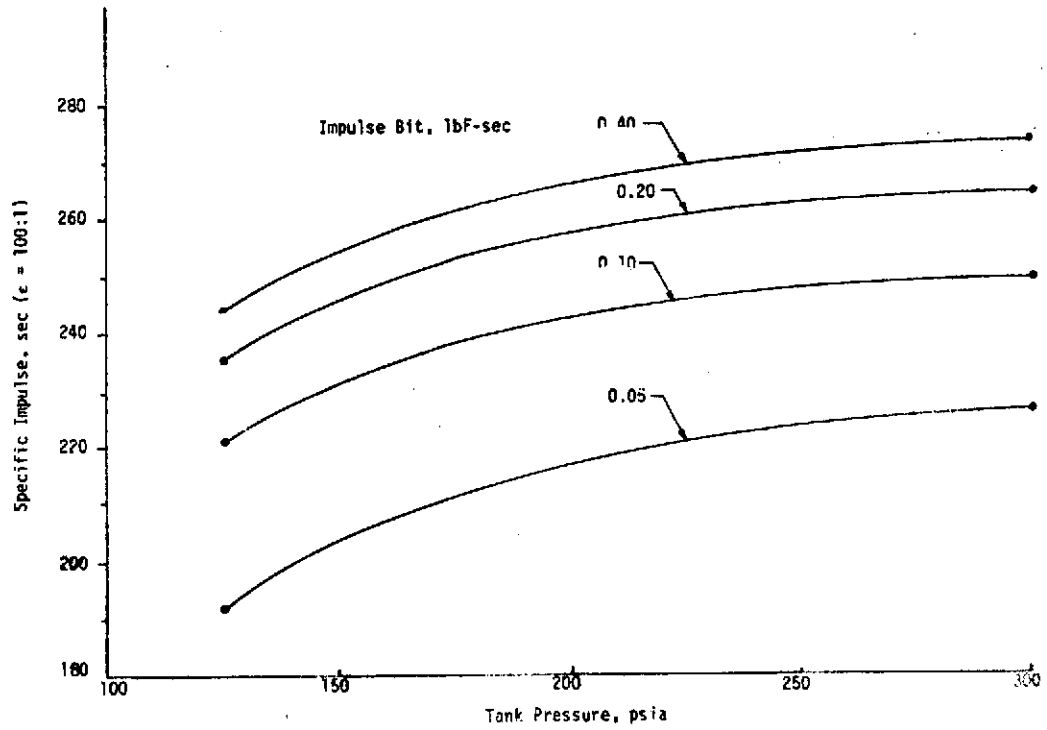


Figure 5-13. Pulse Mode Performance—AJ10-181-1

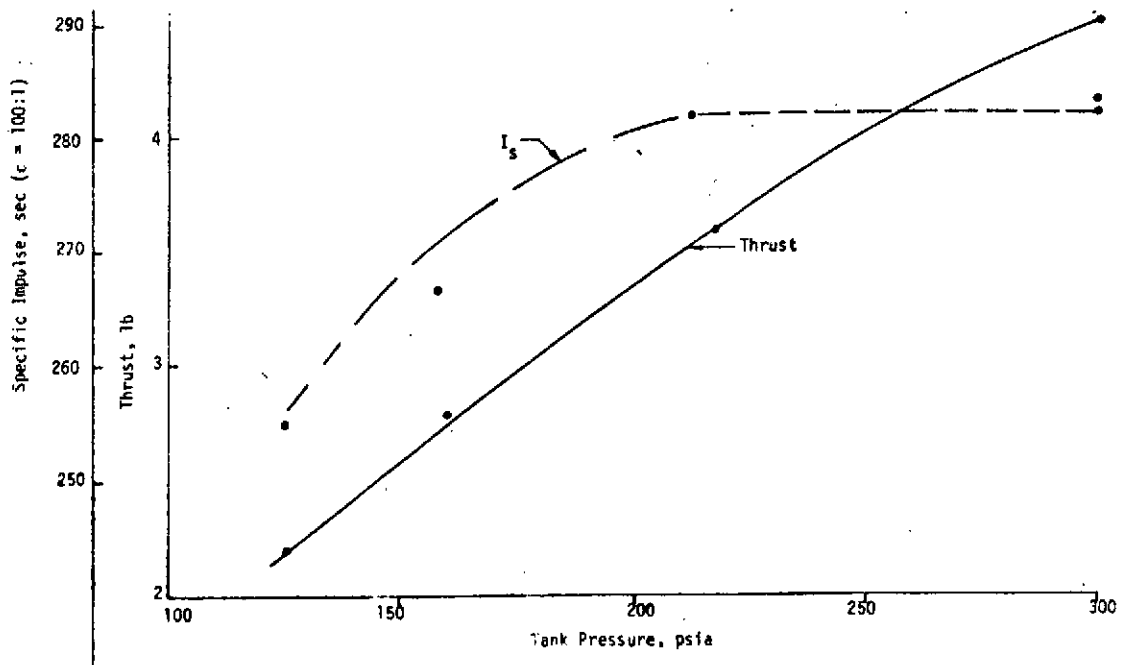


Figure 5-14. Steady-State Performance—AJ10-181-1

ORIGINAL PAGE IS  
OF POOR QUALITY

Table 5-10. RCS Propulsion - Engine SN 2 MIB Repeatability

Demonstrated Minimum Impulse Performance (lbf-sec)

Contract Defined Goal 0.050 ± 0.005 lbf-sec

<u>Pulse No.</u>	<u>Bit Impulse</u>									
1	0.0174	11	0.0172	21	0.0177	91	0.0188	101	0.0189	
2	0.0184	12	0.0177	22	0.0171	92	0.0186	102	0.0184	
3	0.0211	13	0.0186	23	0.0177	93	0.0189	103	0.0194	
4	0.0159	14	0.0171	24	0.0177	94	0.0189	104	0.0185	
5	0.0180	15	0.0177	25	0.0178	95	0.0187	105	0.0193	
6	0.0155	16	0.0179	26	0.0180	96	0.0186	106	0.0192	
7	0.0203	17	0.0178	27	0.0175	97	0.0187	107	0.0191	
8	0.0179	18	0.0174	28	0.0180	98	0.0186	108	0.0195	
9	0.0169	19	0.0172	29	0.0176	99	0.0191	109	0.0178	
10	0.0190	20	0.0180	30	0.0181	100	0.0190	110	0.0186	
Mean	0.01804		0.01766		0.01772		0.01879		0.01887	

Mean of 50 Pulses 0.0182 lbf-sec ± 0.0006 lbf-sec (+ 3%)

Operating Condition: Tank Pressure 100 psia  
 MR 1.6  
 Electrical Pulse Width 0.010 sec  
 Duty Cycle .3

5-32

### 5.2.6 Communications

The science requirement for a coherent X-band beacon requires new communications equipment. The NASA standard S/X transponder, without the X-band TWT, is an appropriate candidate. This type of equipment has already been flown on the Mariner Mars Orbiter and will be flown on Viking.

One concept of a new S/X feed, which will be required, is shown in Figure 5-15. The X-band feed is on-axis and the S-band is off-axis to provide conical scan (-1 db point). The S/X feed movement mechanism would be removed. This feed would require development but allows use of a fixed low-loss waveguide for the X-band signal.

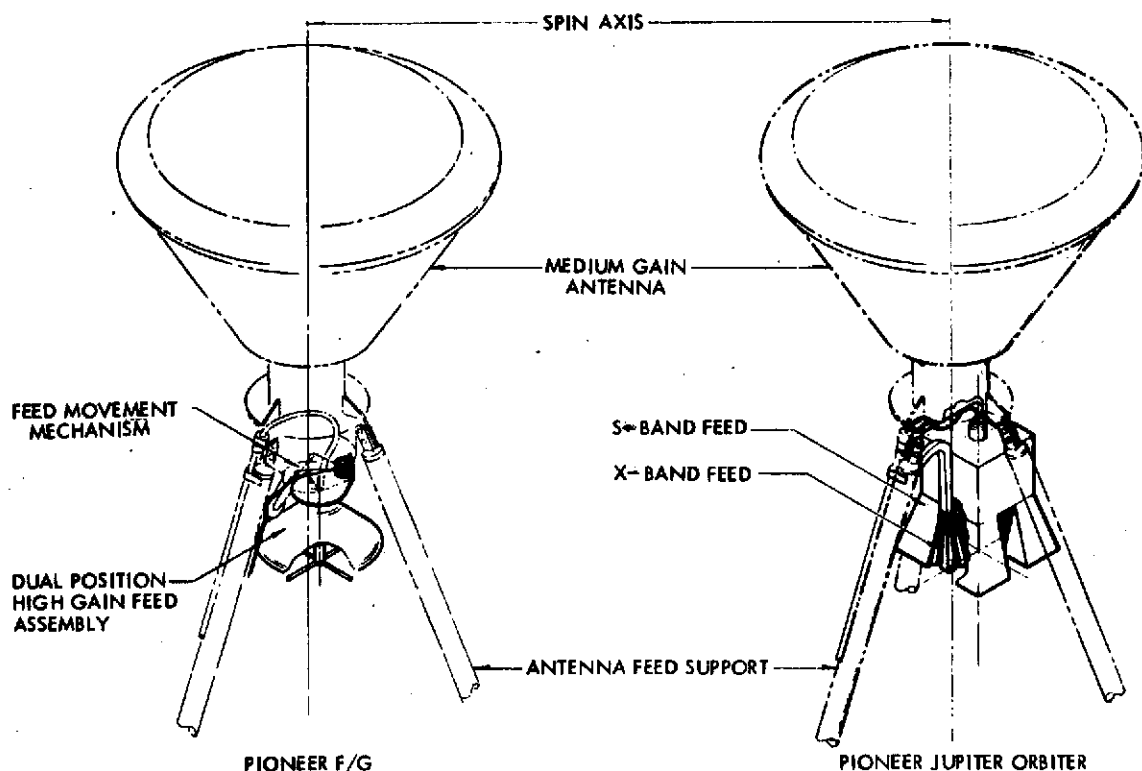


Figure 5-15. New S/X Feed System

Another concept involves the use of a dichroic subreflector. This is a unique double layer frequency selective surface (FSS) design. It was developed by Harris for the UK-60 Skynet Telemetry and Command Station and was recently used to modify ALTAIR for dualband operation.

The subreflector permits simultaneous Cassegrain and prime focus antenna operation. Such subreflectors have an array of crossed dipole elements on each of two surfaces. (See Figure 5-16.) The front or convex surface is shaped and performs the reflecting function in a conventional Cassegrainian feed.

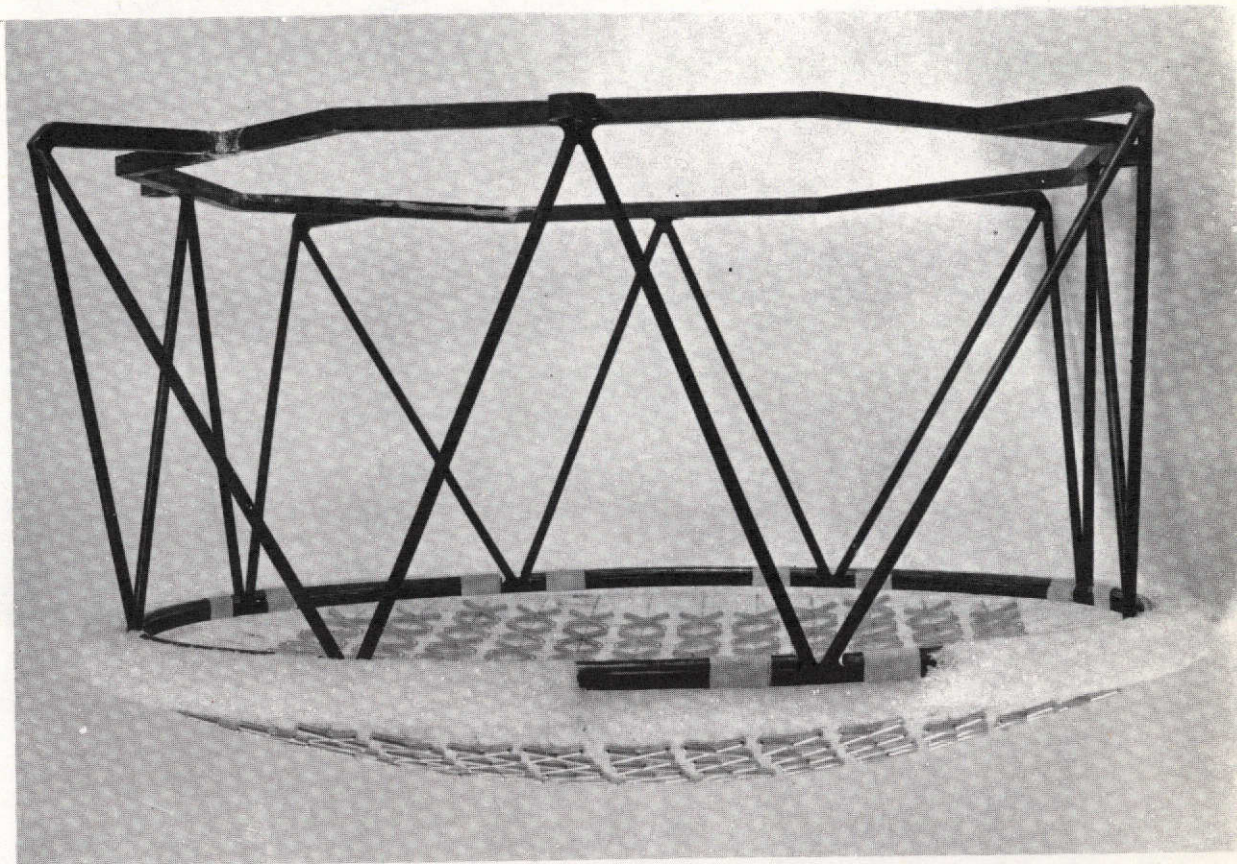


Figure 5-16. ALTAIR Scale-Model FSS Subreflector

The dipoles are sized, formed, and spaced so that the surface is highly reflective. Reflection coefficient is constant with respect to the incident angle over the entire frequency band of the Cassegrain feed. At the frequencies of the prime focus feed, the dipoles are small with respect to the wavelength and permit energy to pass through the surface with only minor degrading effects, which are due to the reactance of the surface. These effects are minimized by adding a second surface slightly less than  $\lambda/4$  behind, with a reactance identical to that of the front surface. Thus, the two surfaces appear as a perfect match to the prime-focus feed energy.

The subreflector has been demonstrated by test to have less than 0.25 dB loss in the K-band and less than 0.1 dB loss in S-band. The subreflector can readily be shaped to increase aperture efficiency.

This concept is also being developed in S/X band for the Mariner Jupiter Saturn Mission. The use of this concept simplifies the X-band waveguide routing and does not require feed development. The existing Pioneer S-band feed, and an X-band corrugated horn feed, which was used for the TRW DSCS-2 spot beam antenna (see Figure 5-17), can be used. Further study of these options, perhaps leading to an engineering model, appears to be a desirable task.

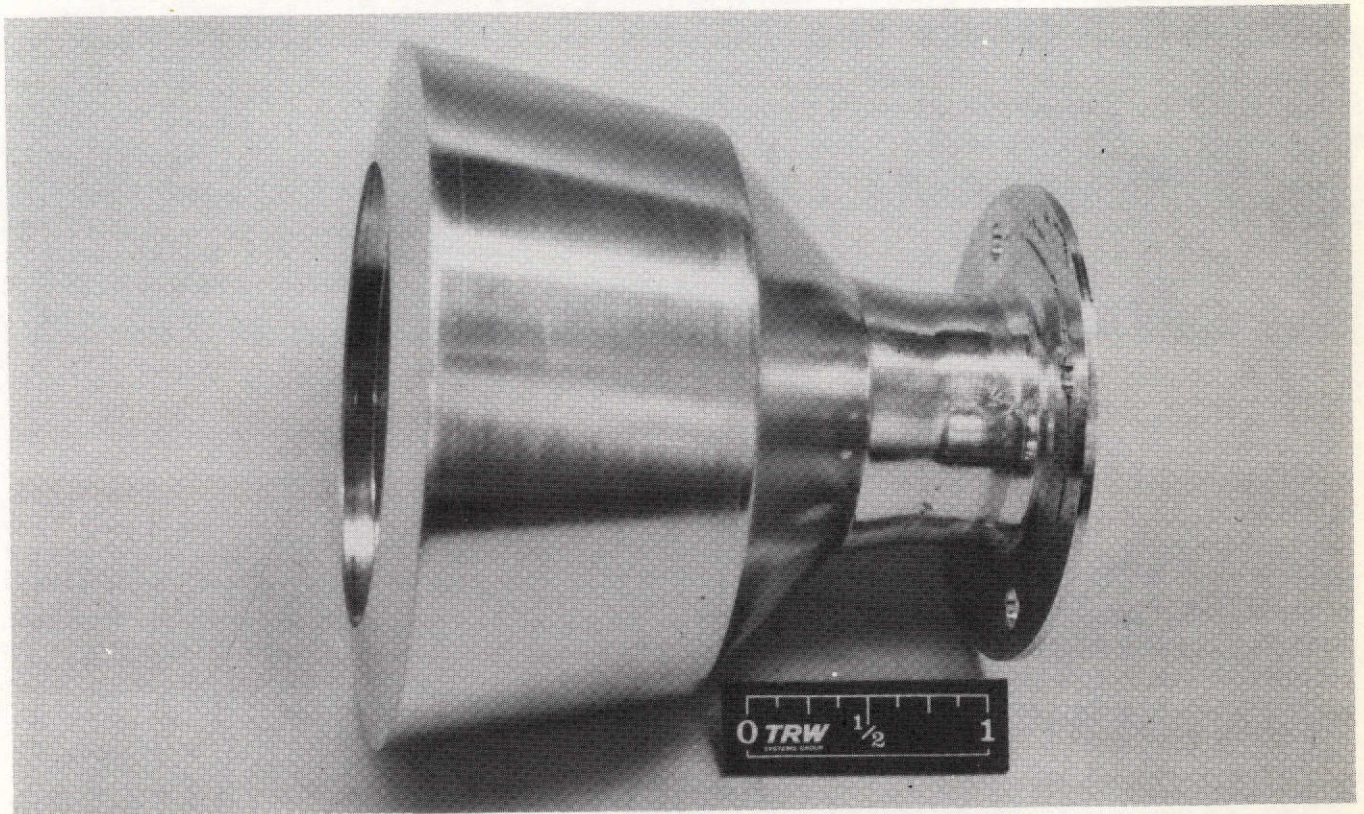


Figure 5-17. Corrugated Horn Feed Used for DSCS-II Spot Beam Antenna

Figure 5-18 shows the command capability for various versions of the Deep Space Net. Figure 5-19 shows the downlink communications capability.

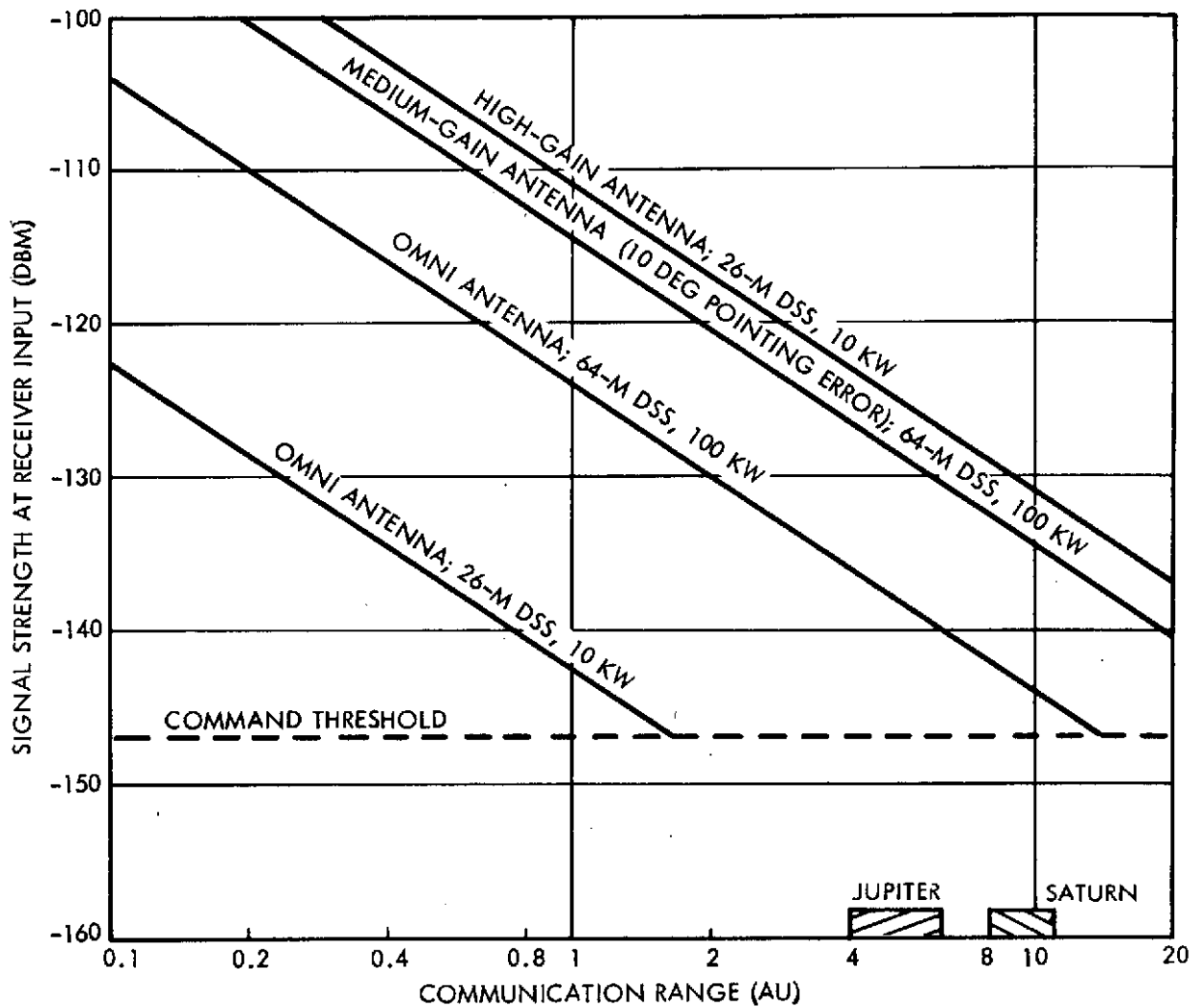


Figure 5-18. Uplink Communications Performance

Table 5-11 shows the X-band beacon link budget and Figure 5-20 shows the beacon link margin as a function of range and also the range as a function of time in Jupiter orbit. The 250-mW transmitter provides adequate margin to account for defocusing losses during fairly deep occultation. The S-band carrier has even greater margin.

The probe-to-spacecraft link design has been the responsibility of the probe study contractor and the reader is referred to item 8) of Section 1.3 and to their final report, to be published, for link budgets, etc. The link geometry is covered in Section 3.2.5. If a higher gain

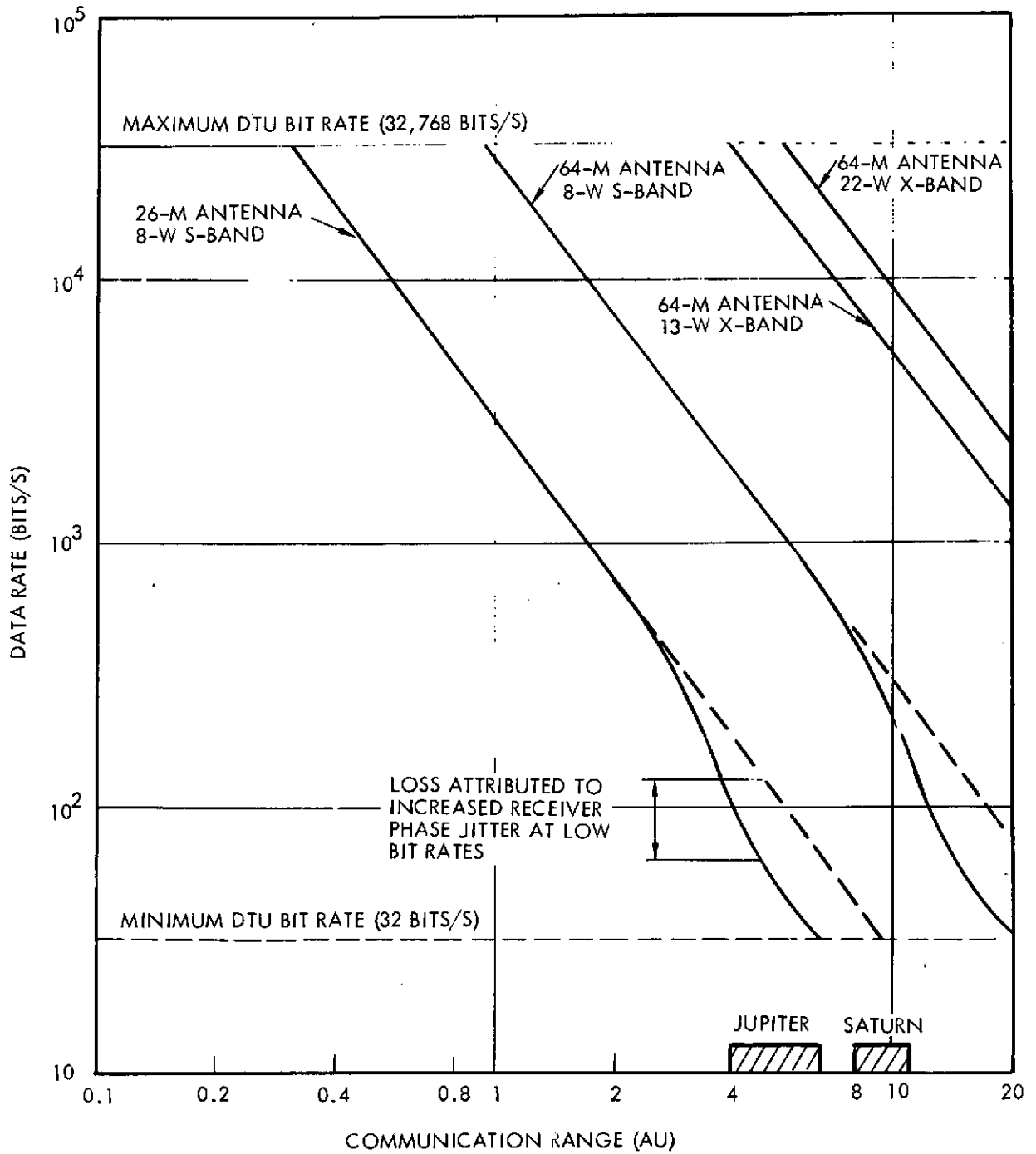


Figure 5-19. Downlink Communications Performance

Table 5-11. X-Band Beacon Link Budget

Frequency (MHz)	8400.0
Spacecraft transmitter power (dBm) (250 mW)	24
Spacecraft coupling loss (dB)	-1.8
Spacecraft antenna gain (dBi)	44.1
Antenna point loss (dB)	-0.9
Polarization loss (dB)	-0.2
Space loss (dB) (6.5 AU)	-290.6
Atmospheric attenuation (dB)	-0.2
Ground station antenna gain (dB)	71.5
Total received power (dBm)	-154.1
Ground station system noise temperature ( $^{\circ}$ K)	27
Relative increase in system noise temperature losses ( $^{\circ}$ K)	6
Ground station noise spectral density (dBm/Hz)	-183.4
Total received power to noise spectral density ratio (dB-Hz)	29.3
Carrier loop threshold loop bandwidth (dB) ( $2B_L = 3$ Hz)	4.8
Carrier loop SNR threshold (dB)	10.0
Carrier performance margin (dB)	14.5

spacecraft antenna were ever desired, an adaptation of the electrically despun antenna studied by Texas Instruments on contract to NASA/Ames\* for Pioneer Venus is a possibility. A 2 x 32 element array located on the periphery of the 9-foot spacecraft dish, operating at 590 MHz could supply 19 db gain. The phasing design circuitry, except for frequency, would be identical to that studied for the Pioneer Venus application.

\*"An Electronically Phased Modular Array Antenna for Pioneer/Venus Communications," U1-991840-F, Texas Instruments Incorporated, 22 November 1972.

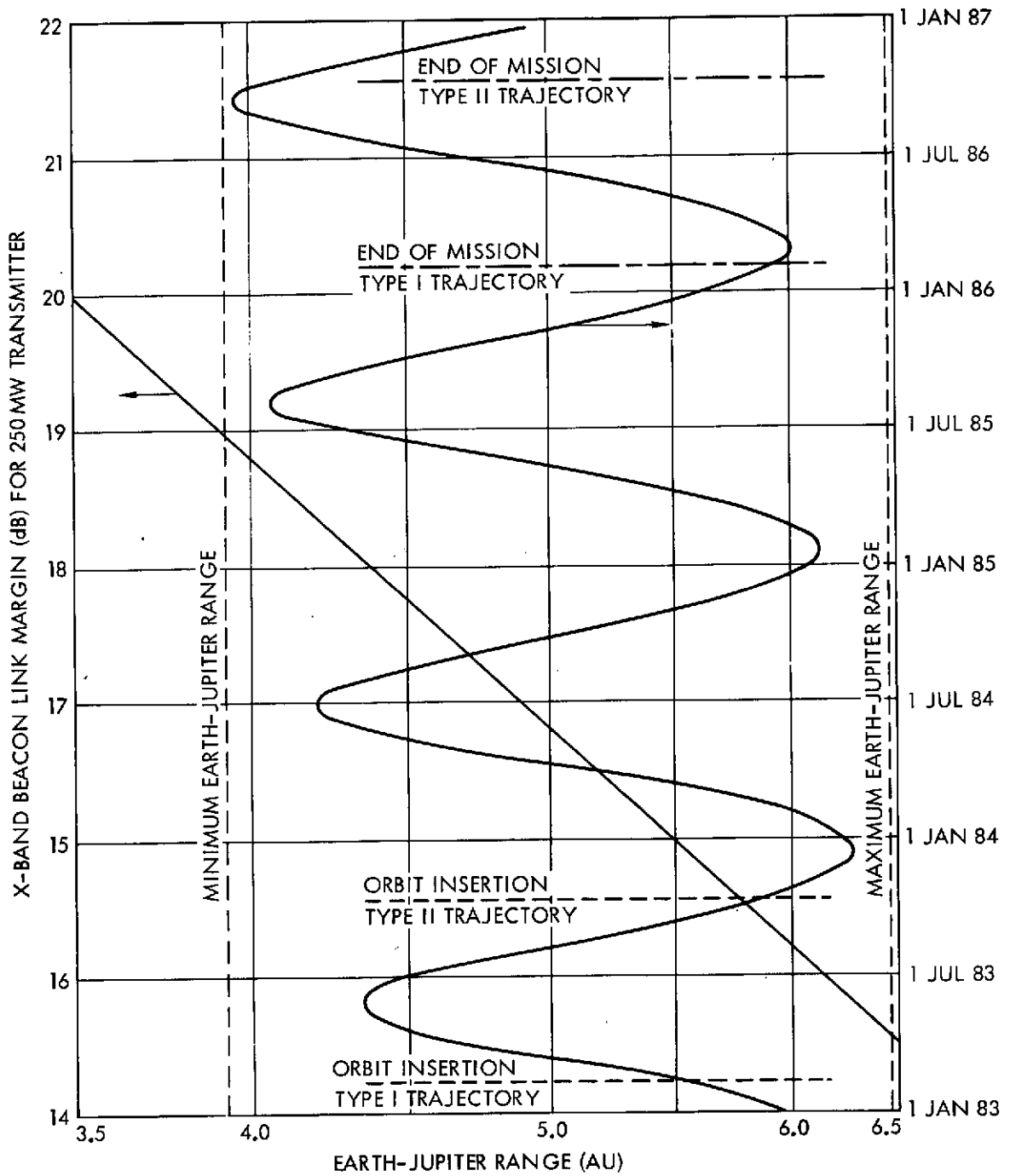


Figure 5-20. X-Band Beacon Link Margin Versus Range and Range Versus Time in Orbit

### 5.2.7 Command and Data Handling

The command and data handling subsystems incorporate additional units that provide enhanced capability. In the command area additional serial digital commands (undecoded before) are routed to a new remote command decoder which decodes up to 128 new pulse commands and secondary power switches. It also stores up to 64 commands and delay times. This unit is a simple addition to the previous command system shown in Figure 5-21.

In the data handling area the Pioneer digital storage unit is replaced by redundant 160-kbit data storage systems which provide increased data storage for normal operations plus storage for the probe telemetry during the probe descent. There is also a new image data storage unit for use with the Pioneer line-scan imager. As seen in Figure 5-21, these, again, are add-on units and do not change the remainder of the data handling equipment. The changes are summarized in Table 5-12, and Table 5-13 gives the source of these changes.

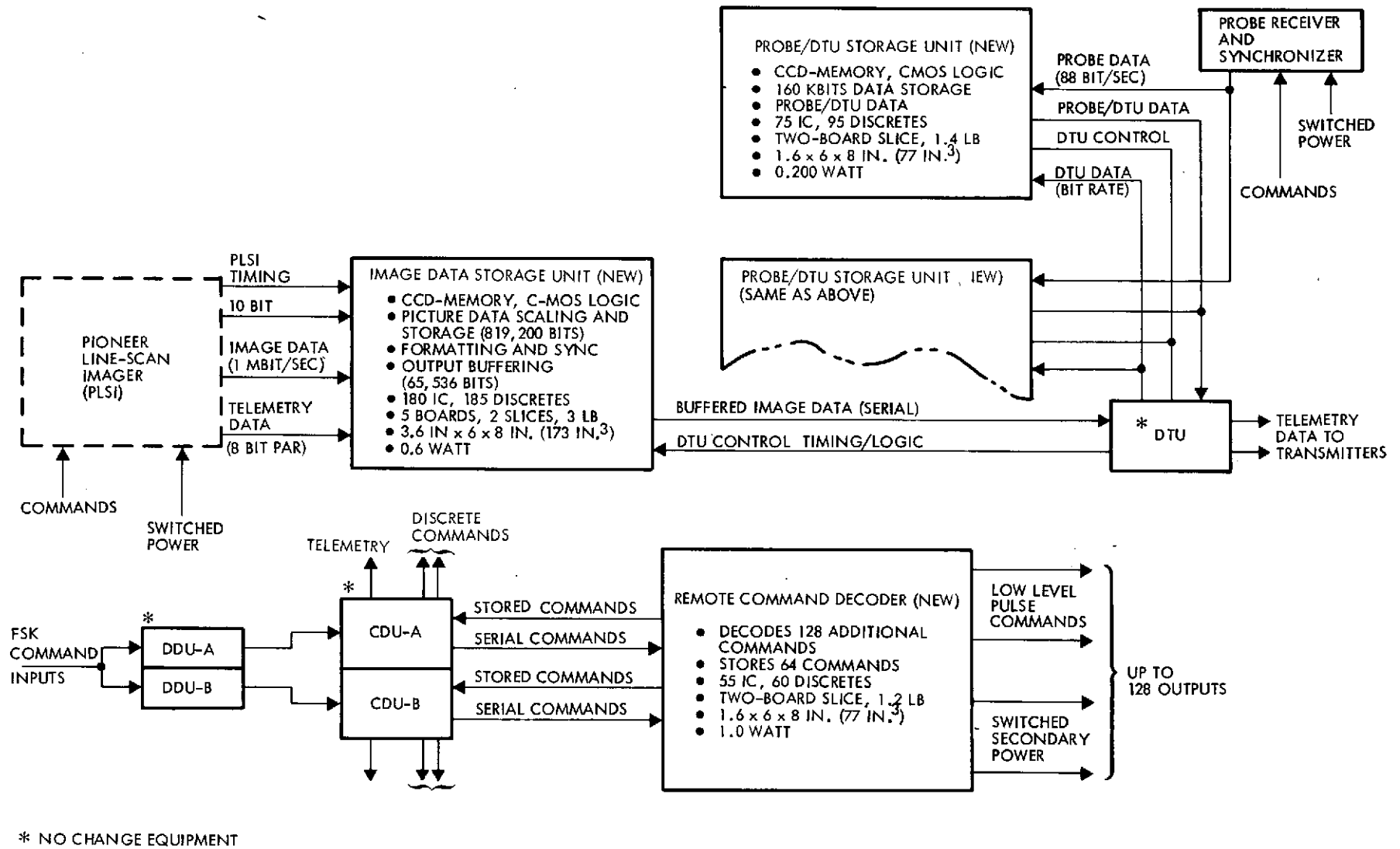
Figure 5-21. PJO<sub>p</sub> Command and Data Handling Equipment

Table 5-12. PJO<sub>p</sub> Command and Data Handling Unit

Subsystem	Requirement (Change from Pioneer 10 and 11)	Expanded Capability	Equipment Changes
Command	77 additional commands (43 more than available spares) Up to 40 stored commands	Up to 128 additional commands 64 stored commands	Remote command decoder 115 parts
Data Handling			
DTU	Probe data telemetry	Existing D format	No change
DSU	820-kbit image data storage unit 160-kbit probe/DTU data storage unit DTU data buffer no longer required	820-kbit image data Redundant 160-kbit memories for probe and DTU data	Image data storage unit CCD memory 365 parts Probe/DTU buffers (A/B) CCD memory 170 parts (each)

ORIGINAL PAGE IS  
OF POOR QUALITY

Table 5-13. Source of New Requirements

1. Command Subsystem	2. Data Handling Subsystem																																										
<p>a) Command Requirements (additions to Pioneer 10/11)</p> <p>Pioneer line scan image (PLSI)</p> <table border="0"> <tr> <td>New equipment</td> <td></td> <td></td> </tr> <tr> <td>  PLSI</td> <td>36</td> <td></td> </tr> <tr> <td>  Additional equipment</td> <td><u>18</u></td> <td>44</td> </tr> <tr> <td>Deleted equipment</td> <td></td> <td></td> </tr> <tr> <td>  IPP</td> <td><u>15</u></td> <td>15</td> </tr> <tr> <td>Net new commands (PLSI)</td> <td></td> <td><u>29</u></td> </tr> <tr> <td>ACS</td> <td></td> <td>11</td> </tr> <tr> <td>Magnetometer boom</td> <td></td> <td></td> </tr> <tr> <td>Propulsion</td> <td></td> <td>6</td> </tr> <tr> <td>EPDS</td> <td></td> <td>6</td> </tr> <tr> <td>Probe</td> <td></td> <td><u>24</u></td> </tr> <tr> <td>Required additional pulse commands</td> <td></td> <td>77</td> </tr> <tr> <td>Available spares</td> <td></td> <td><u>34</u></td> </tr> <tr> <td>Total additional capacity required</td> <td></td> <td>43</td> </tr> </table> <p>b) Command storage of up to 40 stored commands</p> <p>c) Remote command decoder - new C-MOS slice which decodes an unused CDU serial command routing address to give 128 additional outputs (low level pulse commands and switched secondary power) and storage for 64 serial digital commands.</p>	New equipment			PLSI	36		Additional equipment	<u>18</u>	44	Deleted equipment			IPP	<u>15</u>	15	Net new commands (PLSI)		<u>29</u>	ACS		11	Magnetometer boom			Propulsion		6	EPDS		6	Probe		<u>24</u>	Required additional pulse commands		77	Available spares		<u>34</u>	Total additional capacity required		43	<p>a) DTU can handle probe and image data downlink transmission in D formats with no changes to DTU.</p> <p>b) DSU</p> <p>Requirements</p> <ul style="list-style-type: none"> <li>Image data storage - data available at 1 MWPS. 640 pixels x 160 lines x 10 bits/pixel = 1.024 Mbit (102.4 K words). 10-bit words scaled to 8 bits, memory = 819,200 bits.</li> <li>Probe storage - 44 bps for 30 minutes, convolutional coded. 44 bps x 2 x 30 min x 60 sec = 158,400 bits.</li> </ul> <p>Implementation</p> <p>Similar CCD memories provide low power, lightweight DSU's for probe/DTU and image requirements. These memories replace Pioneer 10/11 DSU.</p>
New equipment																																											
PLSI	36																																										
Additional equipment	<u>18</u>	44																																									
Deleted equipment																																											
IPP	<u>15</u>	15																																									
Net new commands (PLSI)		<u>29</u>																																									
ACS		11																																									
Magnetometer boom																																											
Propulsion		6																																									
EPDS		6																																									
Probe		<u>24</u>																																									
Required additional pulse commands		77																																									
Available spares		<u>34</u>																																									
Total additional capacity required		43																																									

## 6. RADIATION EXPOSURE

A small periapsis distance at Jupiter ( $r_p = 1.8 R_J$ ) is selected for the spacecraft bus primarily to limit the relay communication range between entry probe and bus to distances of less than 80,000 km. This choice also has the advantage of reducing the retargeting maneuver which must be performed to deflect the bus spacecraft from planetary impact after probe separation, and achieving high efficiency of orbit insertion. However, this choice also imposes the penalty of exposing the spacecraft to high energetic-particle flux during passage through the inner part of the Jovian radiation belt. Subsequent passages will occur at much larger distances, if after insertion into Jupiter orbit a major (posigrade) apoapsis maneuver is performed. Typically, the subsequent periapsis passages occur at 10 to 15  $R_J$ , i. e., in a much less severe radiation environment.

### 6.1 ESTIMATED ELECTRON AND PROTON FLUENCES EXPERIENCED BY ORBITER AND PROBE

An updated version of the ARC Jupiter Radiation Model (October 1974) was used in estimating the radiation exposure of the entry probe and of the bus during the critical initial passage. This model takes into account results of the Pioneer 10 Jupiter encounter and incorporates the D2 Jupiter Magnetic Field Model.\* Figure 6-1 shows the flux of electrons ( $E > 3$  MeV) as function of Jupiter distance according to the updated ARC model.

Only preliminary results of the Pioneer 11 encounter were available at the time of this writing but these results indicate that the extrapolations to lower altitudes is probably conservative. Reported results from the U.C.S.D. trapped radiation detector indicate that below the Pioneer 10 periapsis the energetic electron fluxes level off so that the peak flux seen by Pioneer 11 at  $L = 1.7$  is about the same as the Pioneer 10 flux at  $L = 2.9$ . The high energy proton flux apparently does rise below the Pioneer 10 periapsis but not as steeply as the extrapolation.

---

\* E. J. Smith, et al., "The Planetary Magnetic Field and Magnetosphere of Jupiter: Pioneer 10," J. Geophys. Res., vol. 79, pp 3501-3513, 1974.

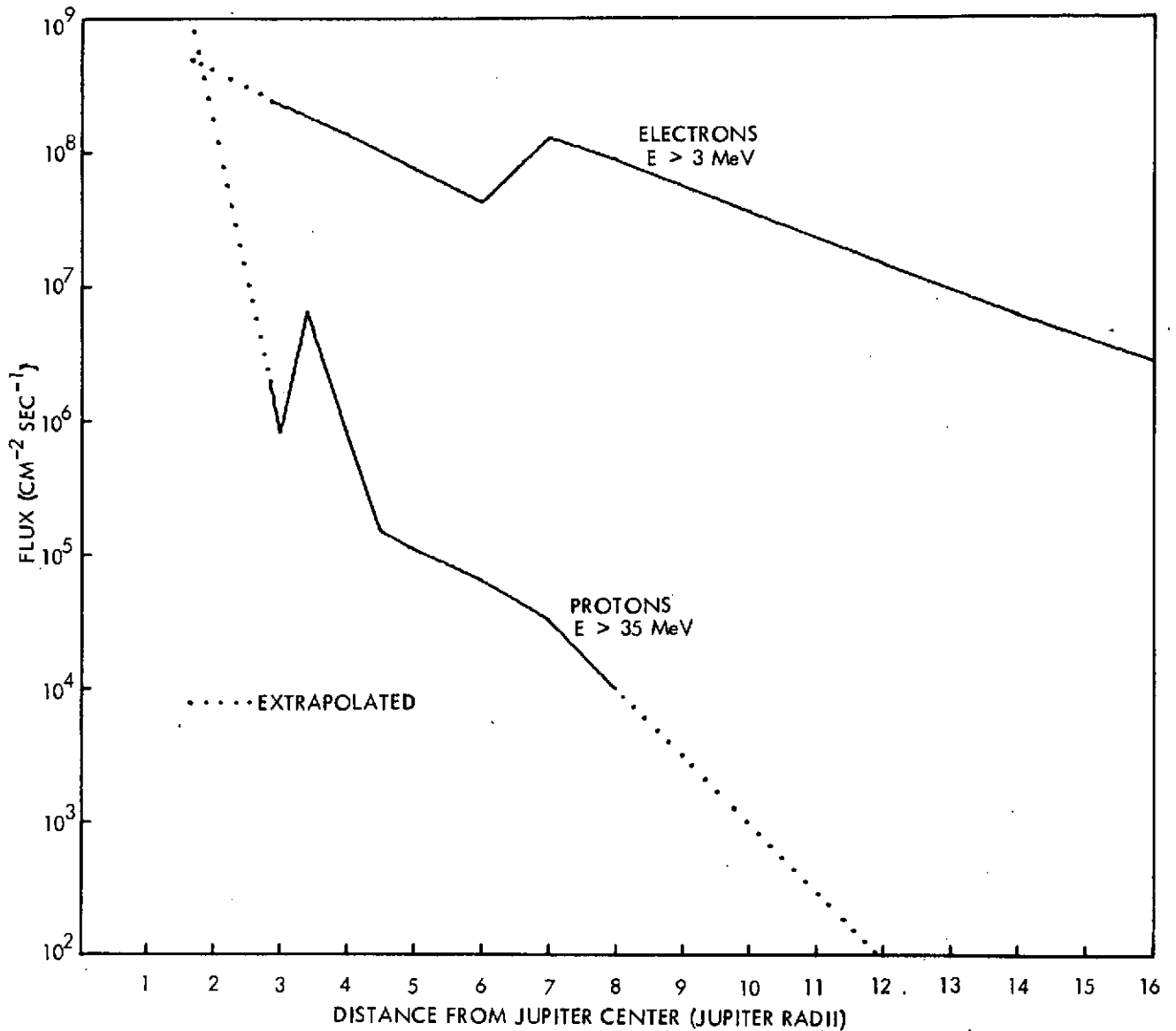


Figure 6-1. Jupiter High Energy Particle Flux in Equatorial Plane

The fluence obtained in a given orbit depends on the phase of the position of the spacecraft at periapsis relative to the orientation of Jupiter's magnetic dipole. This phase is defined as the time the spacecraft is at periapsis and is measured by the angle between Jupiter System III zero longitude and the intersection between the Jupiter equatorial plane and the ecliptic plane. Zero phase occurs when the intersection and the System III zero coincide. Figure 6-2 shows the corresponding fluences calculated for the orbiter as functions of periapsis distance. Fluences are shown for periapsis positions down to  $r_p = 1.8 R_J$ .

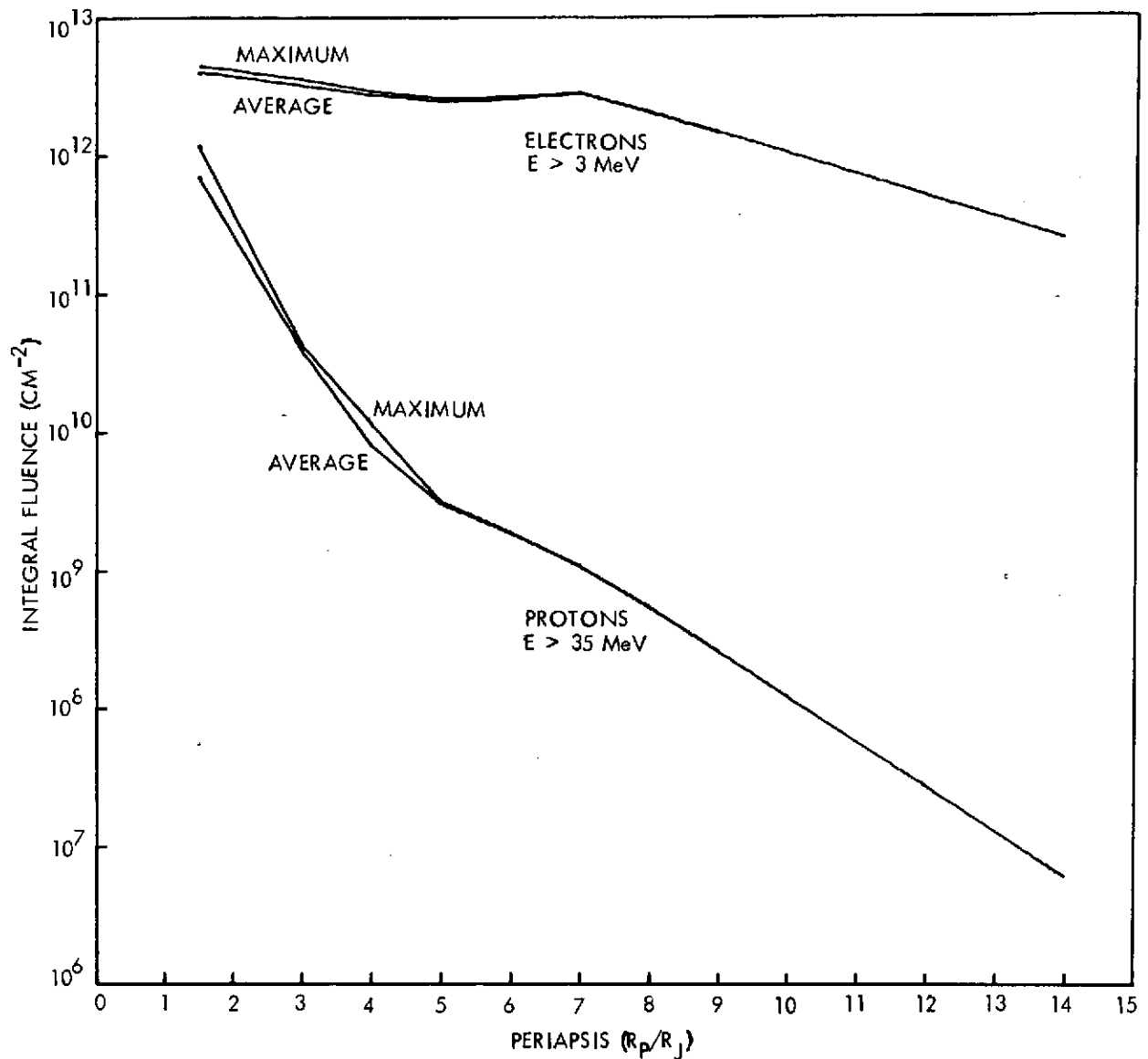


Figure 6-2. Jupiter Orbiter Fluence

Maximum fluences occurring in the worst case, when the periapsis passage is at the longitude of the offset Jovian magnetic dipole, differ only insignificantly from fluences averaged over all phasing conditions, down to the altitudes indicated in the graph.

The fluences for the orbiter are shown and include both the maximum fluence, as well as an average over the phase. Fluences are shown for periapsides positions down to  $R_p = 1.8 R_J$ . Note the effect of phase is not very striking down to these altitudes.

The Pioneer 10 fluences were estimated in a previous study\* to be  $6 \times 10^{12}$  electron/cm<sup>2</sup> for  $E > 3$  MeV and  $2 \times 10^{10}$  proton/cm<sup>2</sup>. Although these were computed using the preliminary Jupiter radiation belt model, we note that they are very close to what would be expected from comparison with Figure 6-2 at  $R_p/R_J = 2.85$ . The most significant difference between the fluence/orbit for the orbiter with periapsis below 2.85 and the fluence received by Pioneer will be the large increase in high energy proton fluence. This result, however, is based on the extrapolation of the proton model to lower L values.

Estimates of the radiation exposure of the entry probe at 7-degree entry angle are shown in Figure 6-3 as function of the phase. Note that the electron fluence varies little with phase. The proton fluence varies by about one order of magnitude between  $10^{11}$  and  $10^{12}$  protons/cm<sup>2</sup>.

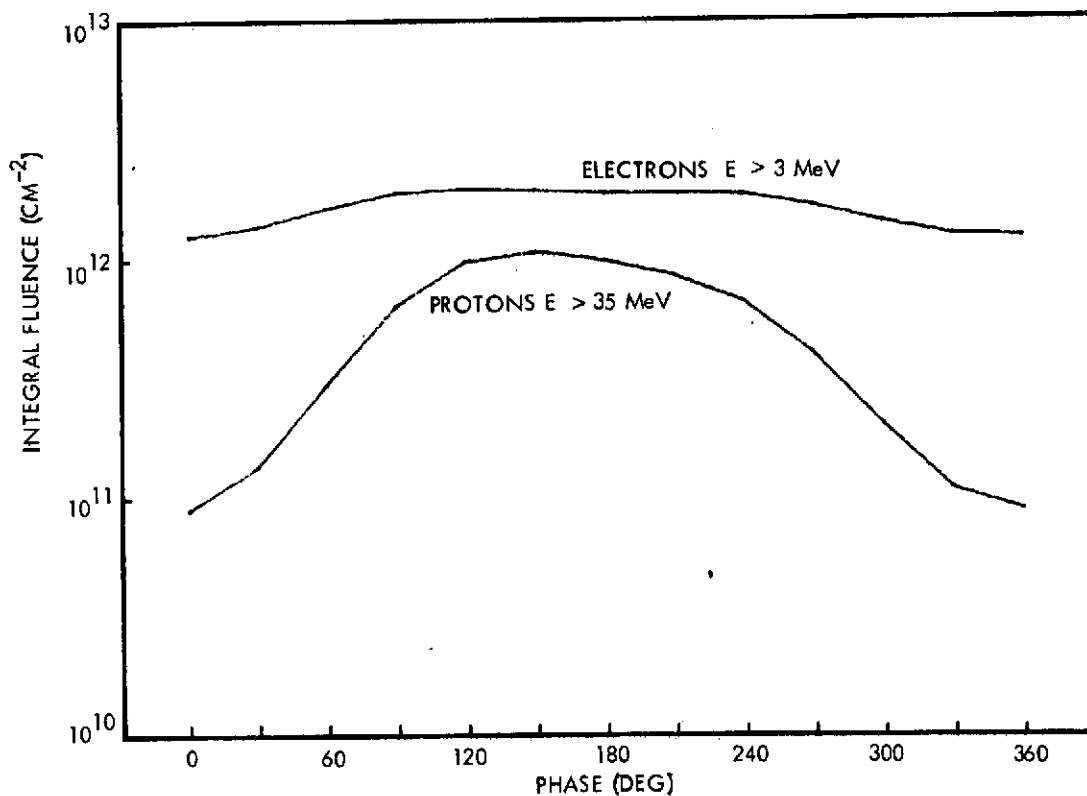


Figure 6-3. Jupiter Probe Fluence 7-Degree Entry Angle - Equatorial Plane

\* Final Report on Radiation Study for Mariner-Jupiter-Saturn Project, "26451-6004-RU-00, TRW Systems Group, Redondo Beach, California, July 18, 1974.

## 6.2 DEGRADATION EFFECTS DUE TO RADIATION EXPOSURE

An analysis of degradation effects on critical components exposed to these fluences was performed by TRW Systems as a result of effects observed on Pioneer 10.

The equivalent 3 MeV electron, equivalent 20 MeV proton fluences, as well as the electron and proton doses, were computed at several components in the orbiter and probe. The components chosen for degradation analysis were typical Pioneer 10 components and in some cases were known to be relatively sensitive to radiation. Two different glasses which might be used in scientific instruments have been included. The list of components along with criteria for "onset" and "complete" degradation are shown in Table 6-1.

Table 6-1. Criteria for Degradation Analysis

Components Examined	Assembly	Effect Type	Degradation Criteria Used	
			Onset	Complete
MOSFET	DTU	Ionization	One gate of 14 failed in test	All gates failed in test
Fiber Optics	SRA	Ionization	25% transmission decrease	50% transmission decrease
7940 Glass Corning	Possible science instrument	Ionization	25% transmission decrease for 0.076 cm thickness	50% transmission decrease for 0.076 cm thickness
Glass (Pb silicate)	Possible science instrument	Ionization	25% transmission decrease for 0.076 cm thickness	50% transmission decrease for 0.076 cm thickness
P/N Detector	SRA	Displacement	25% decrease in gain	50% decrease in gain
Transistors 2N2222	Receiver, DTU, CDU	Ionization and Displacement	25% change in $\beta$	50% change in $\beta$
2N2907A				
2N2920				
	DDU, CDU			

The sensitivity of an electronic component to radiation depends to a large extent on the circuit application of the component. The estimated doses and fluence levels shown in the table are based on the assumption that the component would be used in the same circuit as in Pioneer 10/11. In all cases tabulated, except the transistors, the complete degradation

The radiation dose at components on the probe was computed under the same shielding and entry conditions as the probe equivalent fluence estimates. The results are shown in Table 6-3, compared to the estimated degradation doses. Notice that ordinary Pb silicate

Table 6-3. Worst Case Dose at Components in Probe and Degradation Dose (150-degree phase)

Component	Dose at Components (rads)			Degradation Dose (rads)	
	Electron Contribution	Proton Contribution	Total	Onset	Complete
MOSFET	$1.1 \times 10^4$	$7 \times 10^4$	$8.1 \times 10^4$	$1.1 \times 10^5$	$1.1 \times 10^6$
Fiber Optics	↑	↑	↑	$5.6 \times 10^5$	$1.4 \times 10^6$
Glass (7940 Corning)				$3 \times 10^8$	$7 \times 10^8$
Glass (Pb silicate)				$1.5 \times 10^6$	$3.3 \times 10^6$
Transistors *	↓	↓	↓		
2N2222				$9 \times 10^4$	$2.6 \times 10^5$
2N2907A				$6 \times 10^4$	$1.7 \times 10^5$
2N2920				$3 \times 10^4$	$9 \times 10^4$

\* Collector current = 1 mA

glass is 200 times more vulnerable to radiation damage than the 7940 Corning glass, but that neither will suffer as much as 25 percent degradation behind  $1.5 \text{ g/cm}^2$ . Only in the case of the transistors is an onset of degradation predicted for the worst case entry phase and minimum shielding. Proton effects again predominate.

### 6.2.2 Orbiter Degradation

The equivalent 3 MeV electron fluence for the orbiter was computed using estimates of component shielding within the DTU and the SRA from the referenced study. \* The equivalent fluence per orbit is shown for an orbit with periapsis at  $R_p = 1.8 R_J$ .

As in the case of the probe the results in Table 6-4 show that proton effects predominate and that no displacement degradation is

\* Final Report on Radiation Study for Mariner-Jupiter-Saturn Project, " 26451-6004-RU-00, TRW Systems Group, Redondo Beach, California, July 18, 1974.

expected for these components for one orbit. For 40 orbits with the same periapsis, however, onset of displacement damage would be expected if recovery effects are neglected.

Table 6-4. Equivalent 3 MeV Electron Fluence at Components for Orbiter ( $R_p/R_J$ ) = 1.8 and Degradation Fluence

Component	Equivalent 3 MeV Electron Fluence ( $\text{cm}^{-2}$ )			Degradation Fluence	
	Electron Contribution	Proton Contribution*	Total	Onset	Complete
P/N Detector	$2.4 \times 10^{11}$	$1.7 \times 10^{12}$	$1.9 \times 10^{12}$	$2 \times 10^{13}$	$8 \times 10^{14}$
Transistors**					
2N2222	$3.8 \times 10^{11}$	$1.2 \times 10^{12}$	$1.5 \times 10^{12}$	$6 \times 10^{13}$	$1.8 \times 10^{14}$
2N2907A	$3.8 \times 10^{11}$	$1.2 \times 10^{12}$	$1.5 \times 10^{12}$	$6 \times 10^{13}$	$1.8 \times 10^{14}$
2N2920	$3.8 \times 10^{11}$	$1.2 \times 10^{12}$	$1.5 \times 10^{12}$	$10^{14}$	$3 \times 10^{14}$

\* Proton contribution = 77 x equivalent 20 MeV proton fluence

\*\* Collector current = 1 mA

The orbiter dose/orbit is shown in Table 6-5 for  $R_p = 1.8 R_J$ . Protons play a more important role than electrons for the ionization effects except for the transistors. The exception is due to the fact that the transistor shielding in the DTU is significantly greater than the

Table 6-5. Orbital Dose ( $R_p/R_J$ ) = 1.8 and Degradation Dose

Component	Dose/Orbit (rads)			Degradation Dose (rads)	
	Electron Contribution	Proton Contribution	Total	Onset	Complete
MOSFET	$2.7 \times 10^4$	$2.8 \times 10^5$	$3.1 \times 10^5$	$1.1 \times 10^5$	$1.1 \times 10^6$
Fiber Optics	$2.5 \times 10^4$	$8.7 \times 10^4$	$1.1 \times 10^5$	$5.6 \times 10^5$	$1.4 \times 10^6$
Glass* (7940 Corning)	$4.5 \times 10^4$	$6.5 \times 10^4$	$1.1 \times 10^5$	$3 \times 10^8$	$7 \times 10^8$
Glass* (Pb silicate)	$4.5 \times 10^4$	$6.5 \times 10^4$	$1.1 \times 10^5$	$1.5 \times 10^6$	$3.3 \times 10^6$
Transistors**					
2N222	$9.1 \times 10^3$	$2.6 \times 10^3$	$1.2 \times 10^4$	$9 \times 10^4$	$2.6 \times 10^5$
2N2907A	$9.1 \times 10^3$	$2.6 \times 10^3$	$1.2 \times 10^4$	$6 \times 10^4$	$1.7 \times 10^5$
2N2920	$9.1 \times 10^3$	$2.6 \times 10^3$	$1.2 \times 10^4$	$3 \times 10^4$	$9 \times 10^4$

\*  $1.5 \text{ g/cm}^2$  shield assumed

\*\* Collector current = 1 mA

shielding of the other components shown. Increased local shielding will be very effective in reducing the dose due to protons.

The effects due to ionization on the orbiter appear to be the most serious, particularly when 40 orbits are considered.

### 6.2.3 Recovery Effects

The orbiter data shown in the previous pages are for a single orbit only. It would, however, be an overestimate of the damage to assume that the degradation produced after N orbits is N times the degradation per orbit. It is now known that most of the degradation produced on Pioneer 10 has completely recovered. Recovery of some parameters were observed to begin within several hours of periapsis. In Figures 6-4, 6-5, and 6-6 some of the recovery effects observed on Pioneer 10 are shown. The effects of annealing have not been examined, but will play an important role in the ability of the orbiter to withstand the Jupiter environment. At the present time insufficient work has been performed on the practical utilization of the annealing effects in materials for extended space missions. An understanding of the kinetics of the annealing process can result in significant shield weight savings in cases where annealing can be predicted in advance or where the annealing process can be deliberately accelerated.

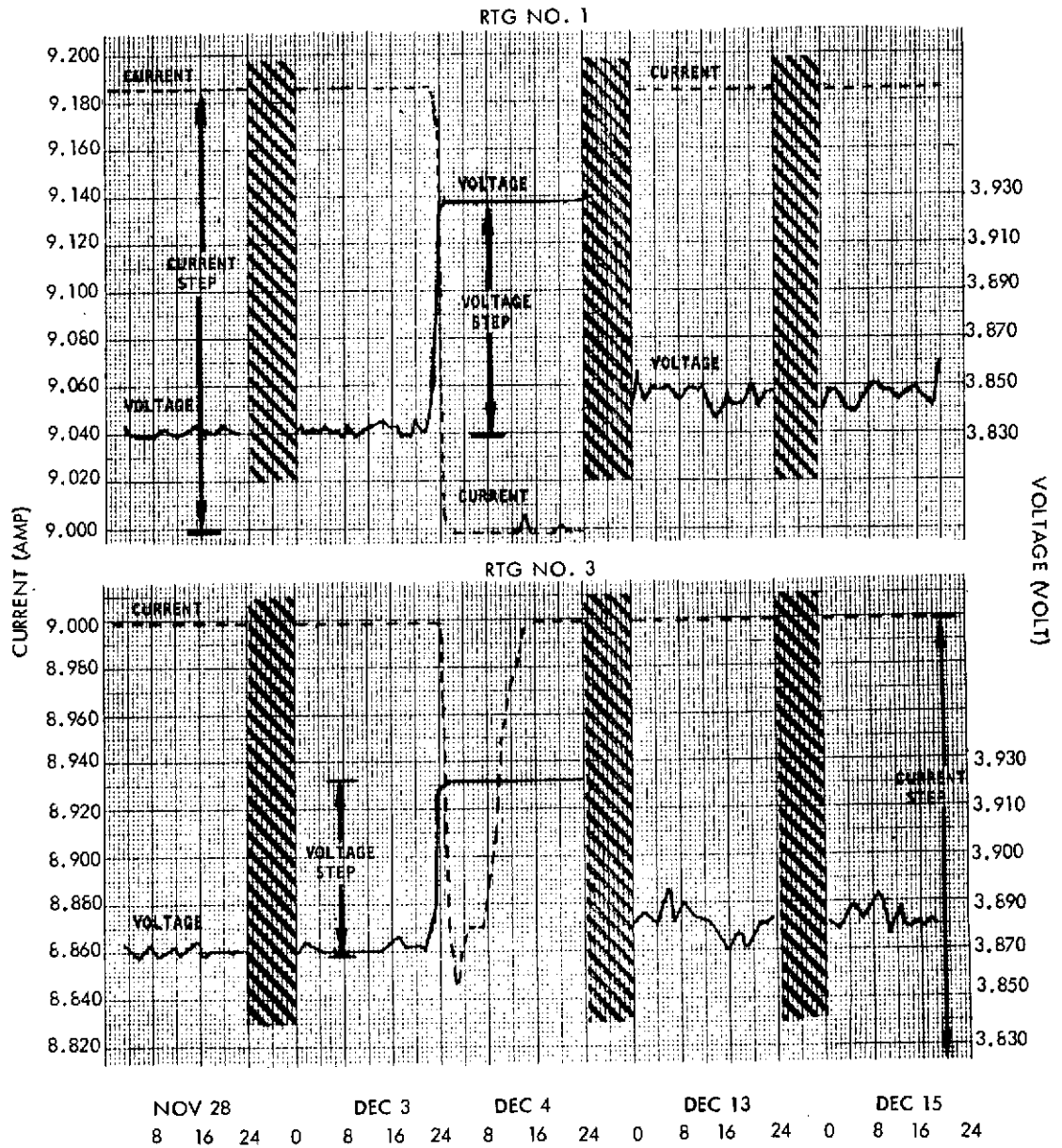


Figure 6-4. Pioneer 10 Recovery of Telemetered RTG Parameters

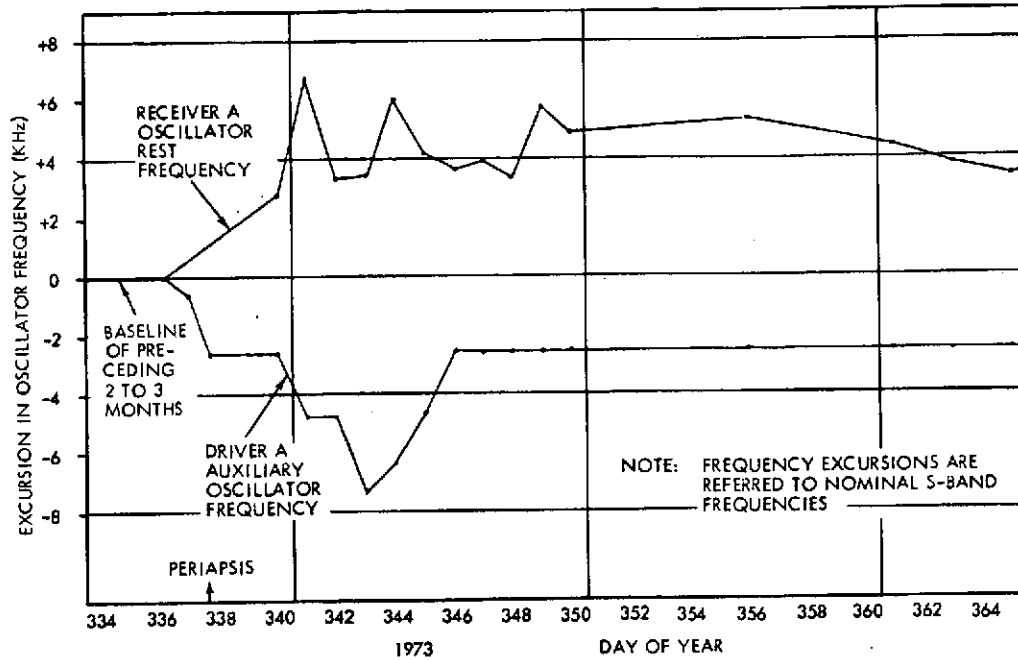


Figure 6-5. Pioneer 10 Recovery of Oscillator Frequency Changes

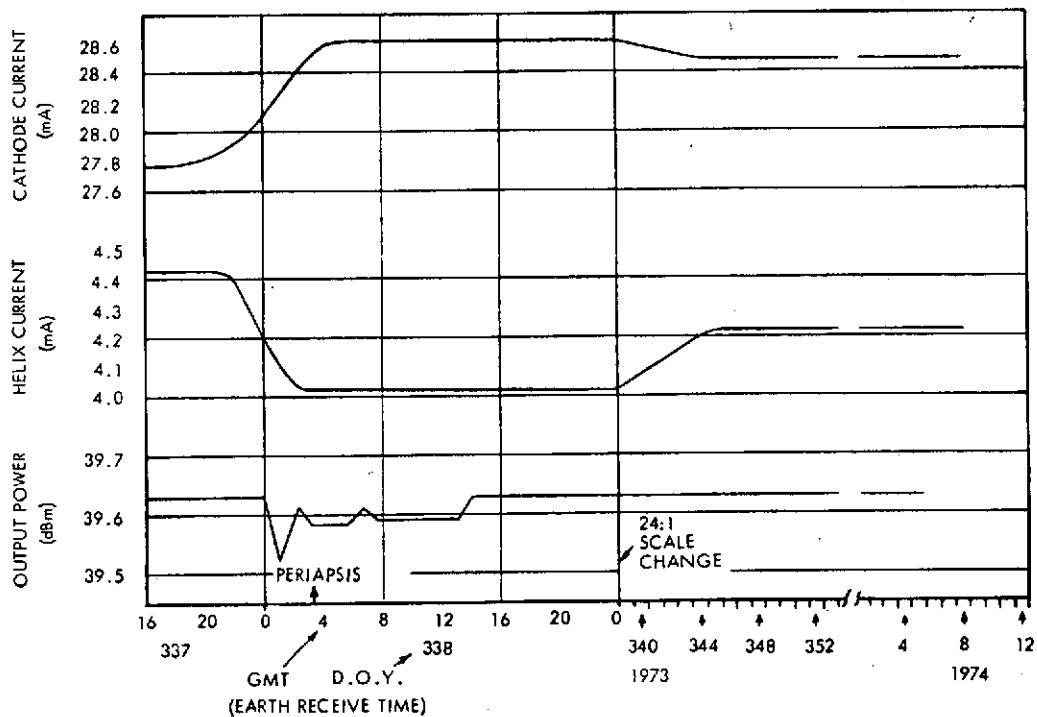


Figure 6-6. Pioneer 10 Recovery of Telemetered TWTA Parameters

## 6-3 RADIATION SUMMARY

Results of preliminary analysis are summarized as follows:

### 1) Probe

- Time-of-entry has a significant effect on fluence
- Proton effects dominate
- With reasonable hardening precautions no severe damage problems are expected.

### 2) Orbiter

- Ionization effects appear to be most serious
- Proton effects will be greater than on Pioneer 10
- Additional radiation hardening of critical components will probably be required. Current application of sensitive electronic components should be reviewed.
- Scientific components, e.g., detectors that must be exposed to severe radiation require special attention
- Annealing effects must still be further assessed.

## 7. SCHEDULE

The schedule for Pioneer Jupiter Orbiter (PJO) for the 1980 launch opportunity allows a comfortable 32 months, starting in the middle of FY 1978. It does not require any parts procurement activity prior to Phase C/D start.

The prototype uses existing flight quality boxes and the Pioneer H structure, supplemented with newly designed equipment, fabricated using short-lead commercial parts. The prototype will be used for system level qualification tests. These tests precede the flight spacecraft integration.

The flight spacecraft uses newly fabricated boxes and for these boxes requiring box level qualification, the qualification unit is refurbished to flight spare status.

Also shown are needs dates for the probe proof test model and flight unit. One month is allowed between the end of acceptance tests and the start of launch site operations. This provides for transportation and also for a deliberate contingency. The probe requires a Phase C/D start of 1 January 1978.

The PJO<sub>p</sub> spacecraft schedule (coordinated with probe schedule) is shown in Figure 7-1.



APPENDIX A  
EQUIPMENT STATUS

Component	S/N	Configuration	Current Status	Critical Parts	Recommended Action	Remarks
<u>Antenna</u>						
Diplexer	E001	Engr Model	Pending verification		Test unit	
	E002	Engr Model	Pending verification		Test unit	
	001	Qual	High magnetics		Pending requirements review	
	002	Proto	High magnetics		Pending requirements review	Installed on proto s/c
	003	Proto	High magnetics		Pending requirements review	Installed on proto s/c
	008	Flight	Pending verification		OK to use	Flight G spare
	009	Flight	Flightworthy		OK to use	Flight G spare
FMM	001	Proto	Pending verification		Update to flight status	Installed on proto s/c
	002	Life Test	Pending verification		Test unit	
	003	Life Test	Pending verification		Test unit	
HG/MG Antenna	006	Flight	Flightworthy		OK to use	Flight G spare
	001	Proto	Outstanding EO's		Update to flight status	
Omni Antenna	---	Structural Model	Pending verification		Test unit	Delivered to NASA/ARC
	E001	Engr Model	Pending verification		Test unit	
Antenna Cable Set	003	Proto	High VSWR		Update to flight status	
	E001	Engr Model	Pending verification		Test unit	
Transfer Switch	001	Proto	Pending verification		Update to flight status	
	004	Flight	Flightworthy		OK to use	Flight G spare
Pin Puller Assembly	E001	Engr Model	Pending verification		Test unit	
	001	Qual	Pending verification		Update to flight status	
	002	Proto	Pending verification		Update to flight status	
	004	Proto	Pending verification		Update to flight status	Installed on proto s/c
	007	Flight	Flightworthy		OK to use	Flight G spare
	008	Flight	Flightworthy		OK to use	Flight G spare
	267	Flight	Flightworthy		OK to use	Flight G spare
<u>Attitude Control</u>						
CEA	E001	Engr Model	Pending verification		Test unit	
	001	Qual	Outstanding EO's		Update to flight status	
	002	Proto	Outstanding EO's		Update to flight status	
DSA	003	Flight	Flightworthy		OK to use	Flight G spare
	E001	Engr Model	Pending verification		Test unit	
	E002	Engr Model	Pending verification		Test unit	
SRA	001	Qual	Pending verification		Update to flight status	
	002	Proto	Pending verification		Update to flight status	Installed on proto s/c
	003	Proto	Pending verification		Update to flight status	Installed on proto s/c
SRA Shade	008	Flight	Flightworthy		OK to use	Flight G spare
	E001	Engr Model	Pending verification	Lens and mirror	Test unit	
	001	Qual	High magnetics		Pending status check	May be disassembled
SSA	002	Proto	Low transmissibility		Pending status check	May be disassembled
	003	Flight	Flightworthy		OK to use	Flight G spare
	002	Flight	Flightworthy		OK to use	
SSA	003	Flight	Flightworthy		OK to use	
	004	Flight	Flightworthy		OK to use	
	E001	Engr Model	Pending verification		Test unit	
	001	Qual	Pending verification		Update to flight status	
	002	Proto	Pending verification		Update to flight status	
	005	Flight	Flightworthy		OK to use	Flight G spare

Component	S/N	Configuration	Current Status	Critical Parts	Recommended Action	Remarks
<u>Attitude Control (Continued)</u>						
CEA Fuse Mod	Vari-ous	Engr Model Qual Proto Flight	Pending verification		Classify and update as required	Quantity of 10
<u>Communication</u>						
Conscan Signal Processor	E001001	Engr Model Qual	Pending verification Outstanding EO's		Test unit Update to flight status	
	002	Proto	Outstanding EO's		Update to flight status	
	005	Flight	Flightworthy		OK to use	Flight G spare
Receiver No. 1	E001002	Engr Model Proto	Pending verification Outstanding EO's	Crystals	Test unit Update to flight status	Redundant Rx S/N 001
	006	Flight	Flightworthy		OK to use	Flight G spare Redundant Rx S/N 003
Receiver No. 2	001	Qual	Outstanding EO's	Crystals	Update to flight status	
	003	Proto	Outstanding EO's		Update to flight status	Redundant Rx S/N 001
	007	Flight	Flightworthy		OK to use	Flight G spare Redundant Rx S/N 003
RF Cable Assembly	Vari-ous	Engr Model Proto Qual Flight	Pending verification		Classify and update as required	Quantity of 26
Transmitter Driver	E001001	Engr Model Qual	Pending verification Outstanding EO's	TCXO	Test unit Update to flight status	
	002	Proto	Outstanding EO's		Update to flight status	Installed on proto s/c
	003	Proto	Outstanding EO's		Update to flight status	Installed on proto s/c
	004	Flight	Flightworthy		OK to use	Flight G spare
TWTA	E001001	Engr Model Qual	Pending verification Non-operable	TWT	Test unit Repair and certify	Installed on proto s/c
	002	Proto	Pending verification		Update to flight status	
	003	Proto	Pending verification		Update to flight status	Installed on proto s/c
	005	Flight	Flightworthy		OK to use	Flight G spare
<u>Data Handling</u>						
DDU	E001001	Engr Model Qual	Pending verification Outstanding EO's		Test unit Update to flight status	
	002	Proto	Outstanding EO's		Update to flight status	
	003	Proto	Pending verification		Update to flight status	
	008	Flight	Flightworthy		OK to use	Flight G spare
DSU	E001001	Engr Model Qual	Pending verification Outstanding EO's		Test unit Update to flight status	
	002	Proto	Outstanding EO's		Update to flight status	
	003	Flight	Flightworthy		OK to use	Flight G spare
DTU	E001001	Engr Model Qual	Pending verification Outstanding EO's		Test unit Update to flight status	
	002	Proto	Outstanding EO's		Update to flight status	Installed on proto s/c
	005	Flight	Flightworthy		OK to use	Flight G spare
DTU/Exp Plug	002	Proto	Pending verification		Update to flight status	
	005	Flight	Flightworthy		OK to use	Flight G spare
	006	Flight	Flightworthy		OK to use	Flight G spare

Component	S/N	Configuration	Current Status	Critical Parts	Recommended Action	Remarks
<u>Data Handling (Continued)</u>						
DTU Prog Conn (264498-1)	E001 001	Engr Model Qual	Pending verification Pending verification		Test unit Update to flight status	Installed on Qual DTU
	002	Proto	Pending verification		Update to flight status	Installed on Proto DTU
	005	Flight	Flightworthy		OK to use	Installed on DTU S/N 0
DTU Prog Conn (264499-1)	E001 001	Engr Model Qual	Pending verification Pending verification		Test unit Update to flight status	Installed on Qual DTU
	002	Proto	Pending verification		Update to flight status	Installed on Proto DTU
	005	Flight	Flightworthy		OK to use	Installed on DTU S/N 0
<u>Electrical Distribution</u>						
CDU	E001 001	Engr Model Qual	Pending verification Outstanding EO's	Ordnance Capacitors	Test unit Update to flight status	
	002	Proto	Outstanding EO's		Update to flight status	
	004	Flight	Flightworthy		OK to use	Flight G spare
CDU Fuse Mod	Vari- ous	Engr Model Qual Proto Flight Test unit	Pending verification		Classify and update as required	Quantity of 10
Interconnection Harness	E001 001	Engr Model Proto	Pending verification Pending verification		Test unit Update to flight status	Installed on Proto s/c
Mag Boom Cable	E001 001	Engr Model Proto	Pending verification Outstanding EO's		Test unit Update to flight status	
Meteoroid Exp. Harness	E004 001	Engr Model Proto	Pending verification Pending verification		Test unit Update to flight status	
Ordnance Harness A	E001 001	Engr Model Proto	Pending verification Pending verification		Test unit Update to flight status	Installed on Proto s/c
RTG Cable W06	E001 002	Engr Model Proto	Pending verification Pending verification		Test unit Update to flight status	
	003	Flight	Pending verification		Update to flight status	
	005	Flight	Flightworthy		OK to use	Flight G spare
	006	Flight	Flightworthy		OK to use	Flight G spare
RTG Cable W07	E001 E002 002	Engr Model Engr Model Proto	Pending verification Pending verification Pending verification		Test unit Test unit Update to flight status	
	003	Flight	Pending verification		Update to flight status	Flight G spare
	005	Flight	Flightworthy		OK to use	Flight G spare
	006	Flight	Needs repair		Repair and certify	
-Y Outrigger Harness	E001 001	Engr Model Proto	Pending verification Pending verification		Test unit Update to flight status	Installed on Proto s/c
+Y Outrigger Harness	E001 001	Engr Model Proto	Pending verification Pending verification		Test unit Update to flight status	Installed on Proto s/c
<u>Electrical Power</u>						
Battery	E001 001	Engr Model Qual	Pending verification Pending verification	Battery Cells	Test unit Test unit	
	002	Proto	Pending verification		Test unit	
	003	Life Test	Pending verification		Test unit	
	004	Life Test	Pending verification		Test unit	
	006	Flight	Pending verification		Test unit	Flight F spare
	009	Flight	Flightworthy		Test unit	Flight G spare

Component	S/N	Configuration	Current Status	Critical Parts	Recommended Action	Remarks
<u>Electrical Power (Continued)</u>						
CTRF	E001 001	Engr Model Qual	Pending verification Outstanding EO's		Test unit Update to flight status	
	002	Proto	Outstanding EO's		Update to flight status	
	004	Flight	Flightworthy		OK to use	Flight G spare
PCU	E001 001	Engr Model Qual	Pending verification Outstanding EO's		Test unit Update to flight status	
	002	Proto	Outstanding EO's		Update to flight status	
	005	Flight	Flightworthy		OK to use	Flight G spare
Inverter	E001 E002 001	Engr Model Engr Model Qual	Pending verification Pending verification Outstanding EO's		Test unit Test unit Update to flight status	
	002	Proto	Outstanding EO's		Update to flight status	Installed on Proto s/c
	003	Proto	Outstanding EO's		Update to flight status	
	008	Flight	Flightworthy		OK to use	Flight G spare
Shunt Radiator	E001 001	Engr Model Qual	Pending verification Out of spec		Test unit Update to flight status	Installed on Proto s/c
	004	Flight	Flightworthy		OK to use	Flight G spare
	005	Flight	Flightworthy		OK to use	Flight G spare
Battery Cable	002	Proto	Pending verification		Update to flight status	
Batt Fuse Mod	Vari- ous	Engr Model	Pending verification		Classify and update as required	Quantity of 9
		Qual				
		Proto				
		Flight Life Test				
CTRF Fuse Mod	Vari- ous	Engr Model	Pending verification		Classify and update as required	Quantity of 75
		Qual				
		Proto				
		Flight Test Unit				
Inv Fuse Mod	Vari- ous	Engr Model	Pending verification		Classify and update as required	Quantity of 20
		Qual				
		Proto				
		Flight Test Unit				
PCU Fuse Mod	Vari- ous	Engr Model	Pending verification		Classify and update as required	Quantity of 10
		Qual				
		Proto				
		Flight Test Unit				
<u>Propulsion</u>						
Line and Heater Assembly +Y	001	Proto	Pending verification		Update to flight status	Installed on Proto s/c
	002	Qual	Pending verification		Update to flight status	
	005	Flight	Flightworthy		OK to use	Flight G spare
Line and Heater Assembly -Y	002	Proto	Pending verification		Update to flight status	Installed on Proto s/c
	003	Qual	Pending verification		Update to flight status	
	006	Flight	Flightworthy		OK to use	Flight G spare
PSA	E001 001	Engr Model Qual	Pending verification Pending verification		Test unit Update to flight status	
	002	Proto	Pending verification		Update to flight status	Installed on Proto s/c
	005	None	Kitted parts		Inventory	

Component	S/N	Configuration	Current Status	Critical Parts	Recommended Action	Remarks
<u>Propulsion (Continued)</u>						
TCA	001	Qual	Outstanding EO's	Propellant Valve and Temperature Sensor	Update to flight status	Installed on Proto s/c Flight G spare { Only one valve available
	002	Qual	Outstanding EO's		Update to flight status	
	005	Proto	Outstanding EO's		Update to flight status	
	007	Flight	Flightworthy		OK to use	
	013	None	Kitted parts		Inventory	
	014	None	Kitted parts		Inventory	
	015	Test Unit			Test Unit	
	016	Test Unit			Test Unit	
	017	Test Unit			Test Unit	
	018	Test Unit		Test Unit		
<u>Structure</u>						
RTG Dampers 122639-1	001	Proto	Pending verification		Update to flight status	Installed on Proto s/c
	004	Flight	Flightworthy		OK to use	Flight G spare
122639-2	005	Proto	Pending verification		Update to flight status	Installed on Proto s/c
	007	Flight	Flightworthy		OK to use	Flight G spare
Mag. Boom Damper 122639-3	009	Proto	Pending verification		Update to flight status	Installed on Proto s/c
	010	Flight	Flightworthy		OK to use	Flight G spare
Wobble Damper	005	Flight	Flightworthy		OK to use	Flight G spare
RTG Guide Rod	-	Flight	Flightworthy		OK to use	Quantity of 1
Bolt Cutter Assembly	Vari- ous	Flight	Flightworthy		OK to use	Quantity of 46
S/C Structure	001	Proto	Pending Verification		Update to Flight Status	
<u>Thermal</u>						
Louver Assembly	037	Flight	Open Discrepancy		Repair and certify OK to use OK to use	
	050	Flight	Flightworthy			
	053	Flight	Flightworthy			
<u>Miscellaneous</u>						
Attenuators	Vari- ous	Engr Model Qual Proto Flight	Pending verification		Classify and update as required	Quantity of 27
Ground Strap	001	Proto	Pending verification		Update to flight status	
Inv. Osc. Disable IFJ	E001	Engr Model	Pending verification		Test unit	Flight G spare
	001	Proto	Pending verification		Update to flight status	
	003	Flight	Flightworthy		OK to use	
O-d. In-Flight Jumper #1 "B"	E001	Engr Model	Pending verification		Test unit	Installed on Proto s/c
	002	Proto	Pending verification		Update to flight status	
Rapid Cmd IFJ	E001	Engr Model	Pending verification		Test unit	
	001	Proto	Pending verification		Update to flight status	
	004	Flight	Flightworthy		OK to use	
Shunt Regulator Cable	E001	Engr Model	Pending verification		Test unit	Installed on Proto s/c
	001	Proto	Pending verification		Update to flight status	

**APPENDIX B**

**TRW'S MULTIMISSION  
BIPROPELLANT PROPULSION SYSTEM**

**February 1975**

## **DEMONSTRATED**

**DEVELOPMENT AND QUALIFICATION OF A MULTI-START BIPROPELLANT PROPULSION SYSTEM WHICH PROVIDES PROPULSIVE IMPULSE FOR VELOCITY CHANGE AND COLD GAS FOR STABILIZATION CONTROL.**

## TYPICAL PROGRAM TASKS

- o DEFINED PROPULSION SUBSYSTEM DESIGN REQUIREMENTS WHICH SATISFIED THE VEHICLE CRITERIA
- o PERFORMED TRADEOFF ANALYSIS OF ALTERNATE CONFIGURATIONS AND SELECTED THE PREFERRED CONFIGURATION
- o DEFINED FUNCTIONAL, MECHANICAL AND ELECTRICAL INTERFACES
- o IDENTIFIED AND MANAGED ALL SUBCONTRACT TRANSACTIONS REQUIRED TO SUPPORT THE PROGRAM
- o PERFORMED DETAILED ANALYSIS OF THE PROPULSION SYSTEM CONFIGURATION
- o PREPARED AND RELEASED MANUFACTURING DRAWINGS FOR THE PROCUREMENT AND/OR FABRICATION OF TEST AND PRODUCTION HARDWARE
- o PREPARED A MANUFACTURING PLAN WHICH IDENTIFIED THE MANUFACTURING CYCLE OF ALL PARTS AND MATERIALS
- o PROVIDED MANUFACTURING SERVICES FOR THE FABRICATION, INTEGRATION AND NON-REACTIVE TEST OF THE BI-PROPELLANT PROPULSION SUBSYSTEM
- o PREPARED TEST PLANS, SPECIFICATIONS AND PROCEDURES FOR THE DEVELOPMENT, DESIGN VERIFICATION, QUALIFICATION AND ACCEPTANCE TESTS
- o CONDUCTED COMPONENT AND SUBSYSTEM DEVELOPMENT, DESIGN VERIFICATION, QUALIFICATION AND ACCEPTANCE TESTS
- o PERFORMED TEST DATA REVIEW AND PREPARED TEST REPORTS
- o CONDUCTED CONCEPTUAL, DEVELOPMENTAL AND CRITICAL DESIGN REVIEWS IN ACCORDANCE WITH THE PROGRAM REQUIREMENTS

# PROPULSION SUBSYSTEM

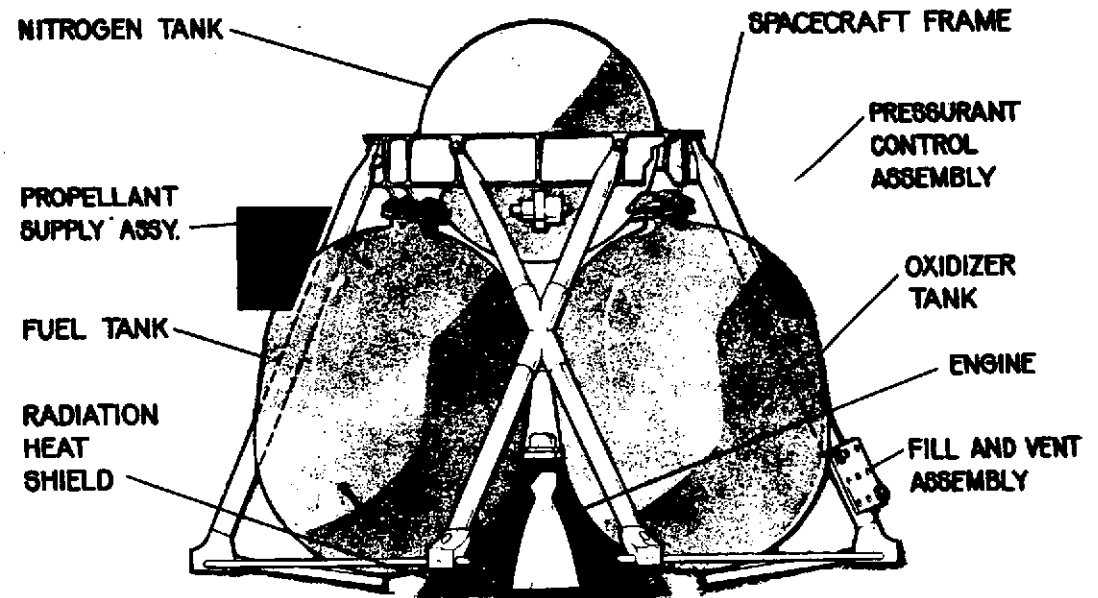
SUBSYSTEM WEIGHT - 190

UNLIMITED MULTI-START SYSTEM  
3000 STARTS DEMONSTRATED

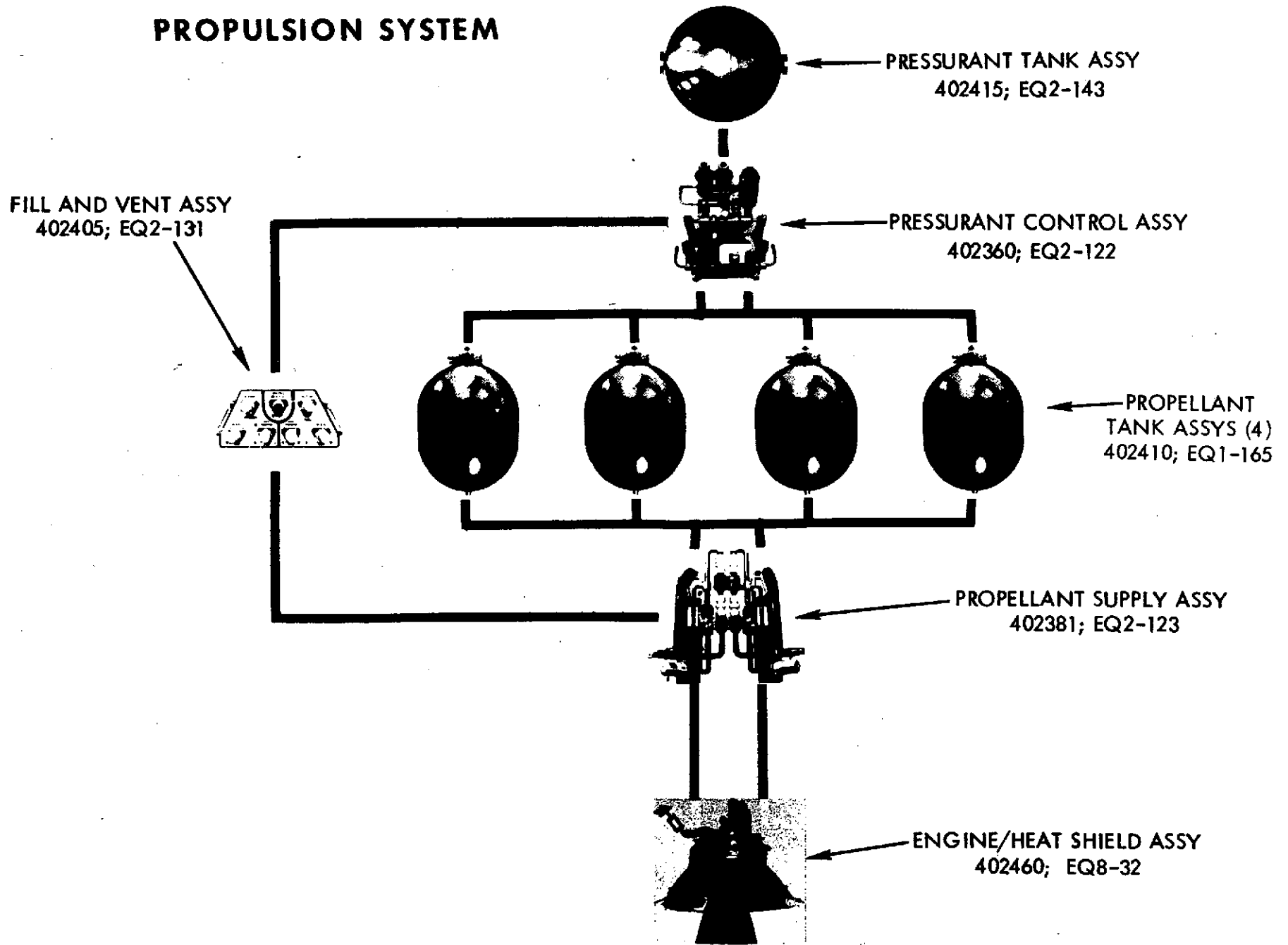
RADIATION COOLED ALL-COLUMBIUM ENGINE ASSEMBLY-  
OVER 12,000 SECONDS HOT FIRING DEMONSTRATED  
TANKAGE LIMITED DURATION 4250 SECONDS

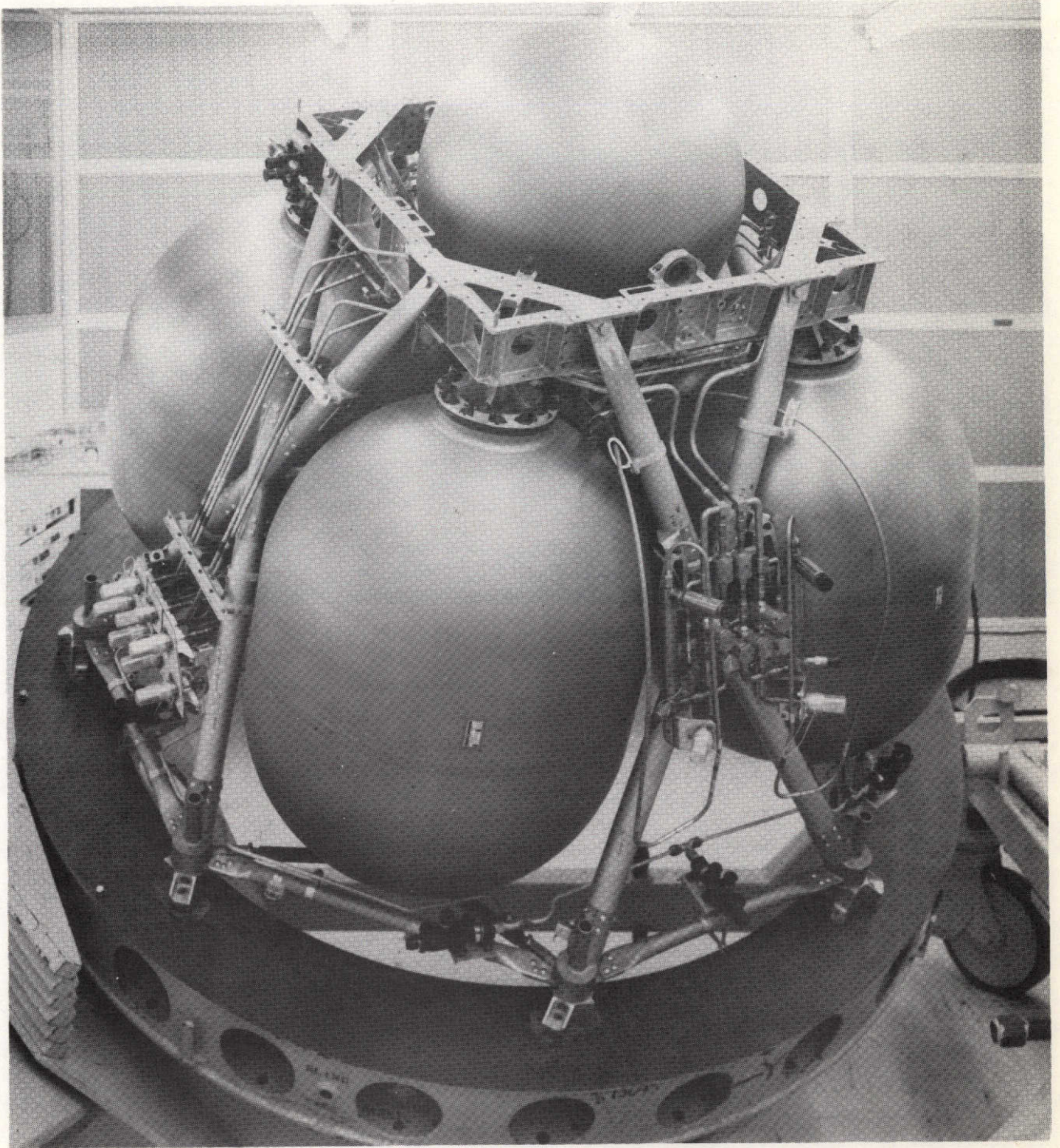
HYPERGOLIC PROPELLANT COMBINATION  
800 LBS  $N_2O_4$  AND 490 LBS MMH

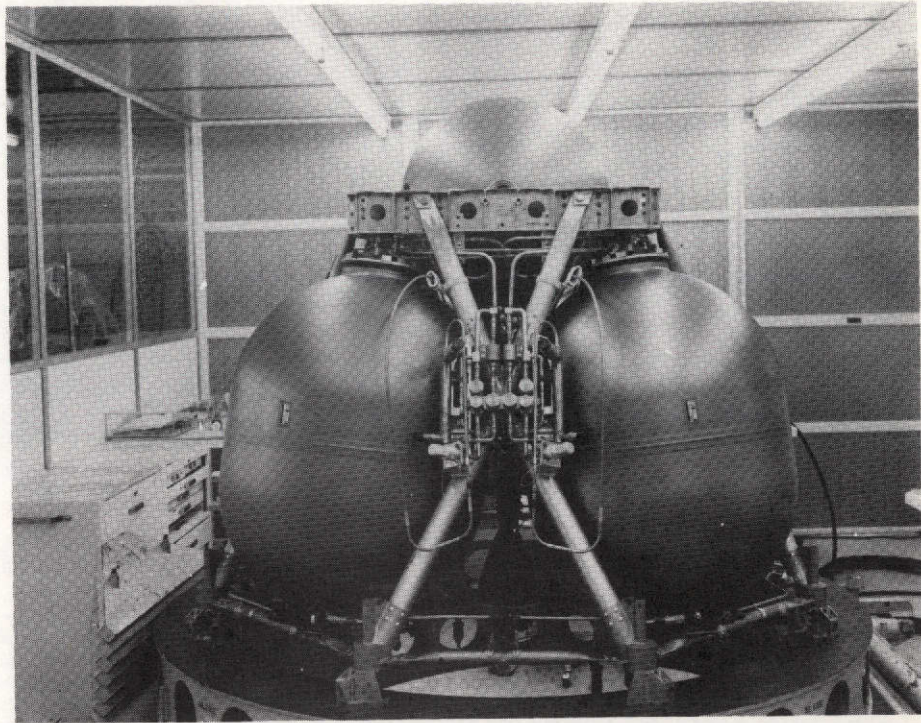
B-3



# PROPULSION SYSTEM

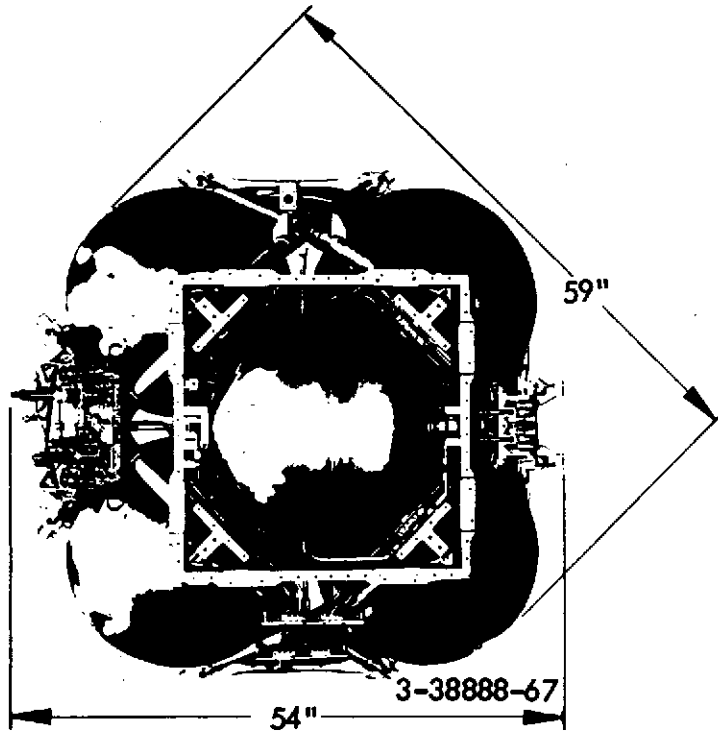




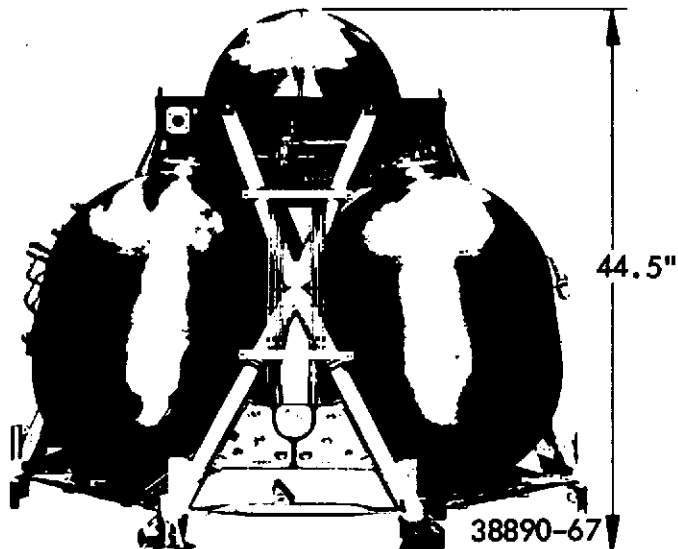


# BIPROPELLANT PROPULSION SYSTEM

## DESIGN AND PERFORMANCE CHARACTERISTICS



B-7

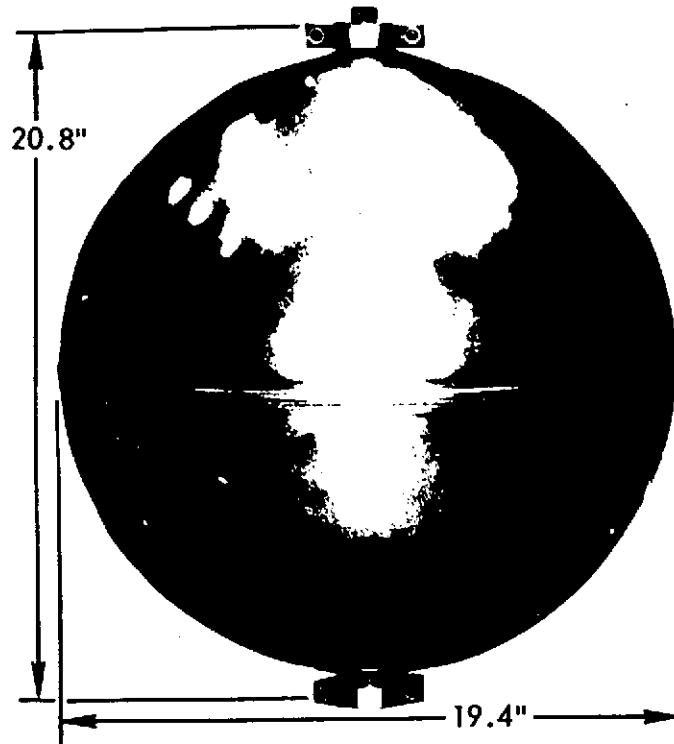


TOTAL IMPULSE	372,000 LB <sub>F</sub> - SEC
SPECIFIC IMPULSE (NOMINAL)	295 LB <sub>F</sub> - SEC/LB <sub>M</sub>
VACUUM THRUST	88 LB <sub>F</sub>
PROPELLANT MIXTURE RATIO	1.64±.04 (NTO/MMH)
PROPELLANT UTILIZATION	97.8%
TOTAL PROPELLANT RESIDUALS	28 LB <sub>M</sub>
CUTOFF IMPULSE	2.0±0.2 LB <sub>F</sub> - SEC
RESTART CAPABILITY	50,000 CYCLES
TEMPERATURE RANGE:	
OPERATIONAL	30-90 F
STORAGE	25-120 F
WEIGHT:	
DRY	190 LB <sub>M</sub>
WET	1523 LB <sub>M</sub>
TOTAL ALLOWABLE LEAKAGE	50X10 <sup>-5</sup> SCC/SEC He

**TRW**  
SYSTEMS GROUP

# PROPULSION SYSTEM

## PRESSURANT TANK ASSEMBLY

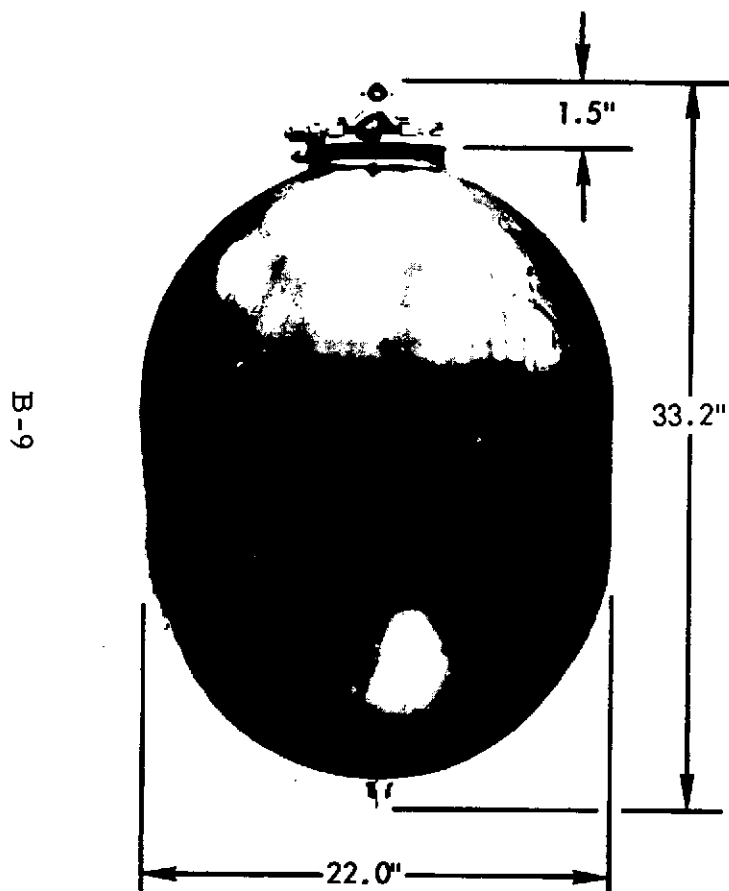


38888-67

MATERIAL:	6Al 4V TITANIUM
VOLUME:	3475 CU. IN.
WEIGHT - EMPTY:	44.0 LBS MAX
WEIGHT - FULL (4000 PSIG GN <sub>2</sub> ):	77.3 LBS
OPERATING PRESSURE:	4000 PSIG
PROOF PRESSURE:	6192 PSIG
BURST PRESSURE:	8000 PSIG
OPERATING TEMPERATURE RANGE:	-20° TO +150°F
STORAGE TEMPERATURE RANGE:	-100 TO +150 F
CYCLE LIFE:	500 CYCLES
LEAKAGE:	1X10 <sup>-7</sup> SCC/SEC He AT 4000 PSIG
INSTRUMENTATION:	FLIGHT TELEMETRY TEMPERATURE TRANSDUCER GROUND MONITOR TEMPERATURE TRANSDUCER

# PROPULSION SYSTEM

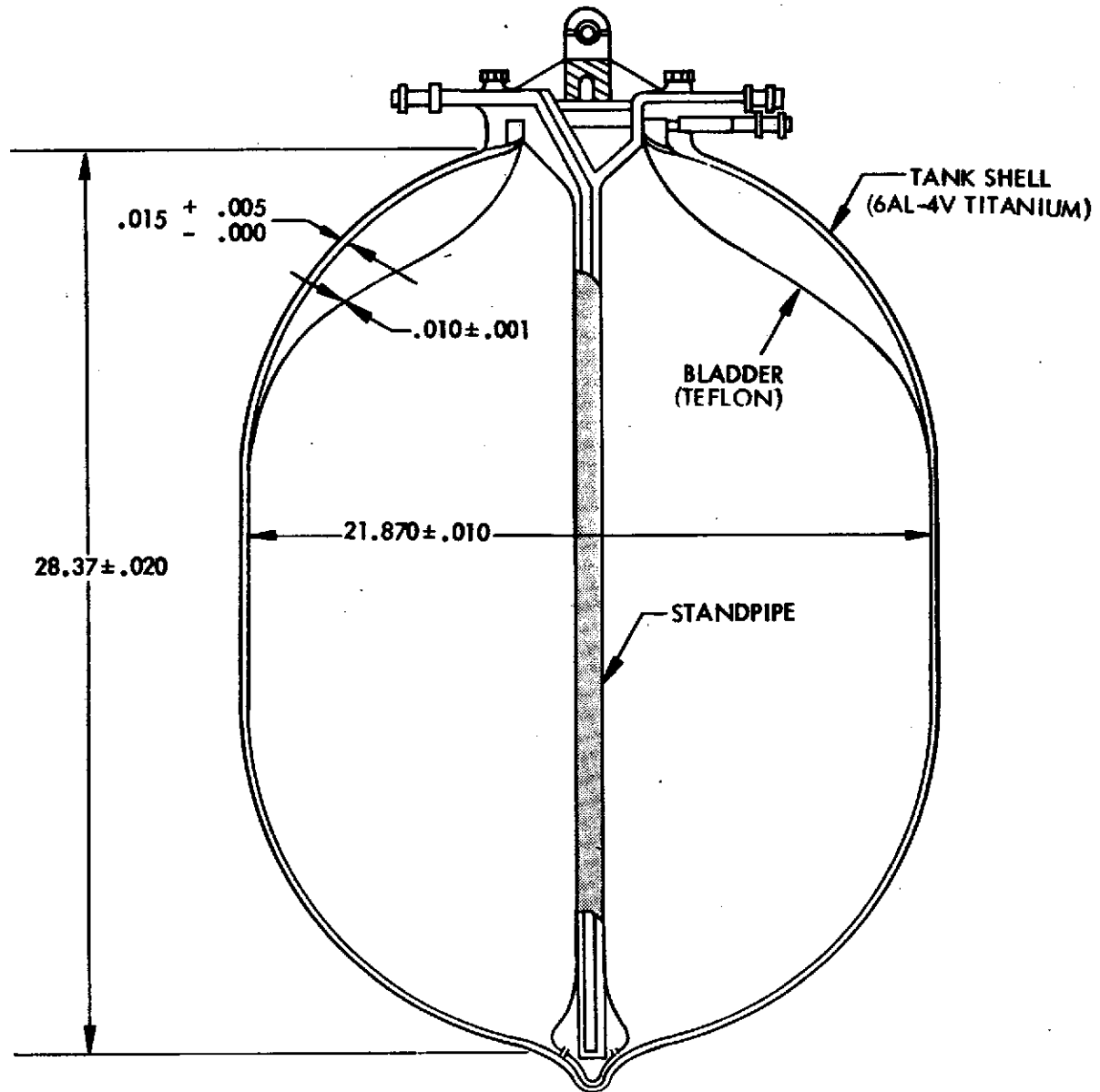
## PROPELLANT TANK ASSEMBLY



56259-68

MATERIALS:	6Al4V TITANIUM TANK WITH TEFLON BLADDER
VOLUME	7870 CU. IN. MIN.
WEIGHT	16.4 LBS
OPERATING PRESSURE:	220 PSIG
PROOF PRESSURE:	330 PSIG
BURST PRESSURE:	440 PSIG
OPERATING TEMPERATURE:	30 - 90 F
STORAGE TEMPERATURE:	-65 TO 150 F
BLADDER CYCLE LIFE:	4 CYCLES
LEAKAGE:	
EXTERNAL	1X10 <sup>-3</sup> SCC/SEC He AT 220 PSIG
INTERNAL (BLADDER)	ZERO LIQUID LEAKAGE 350 SCC/HR He AT 5 PSIG
EXPULSION EFFICIENCY:	99.4%

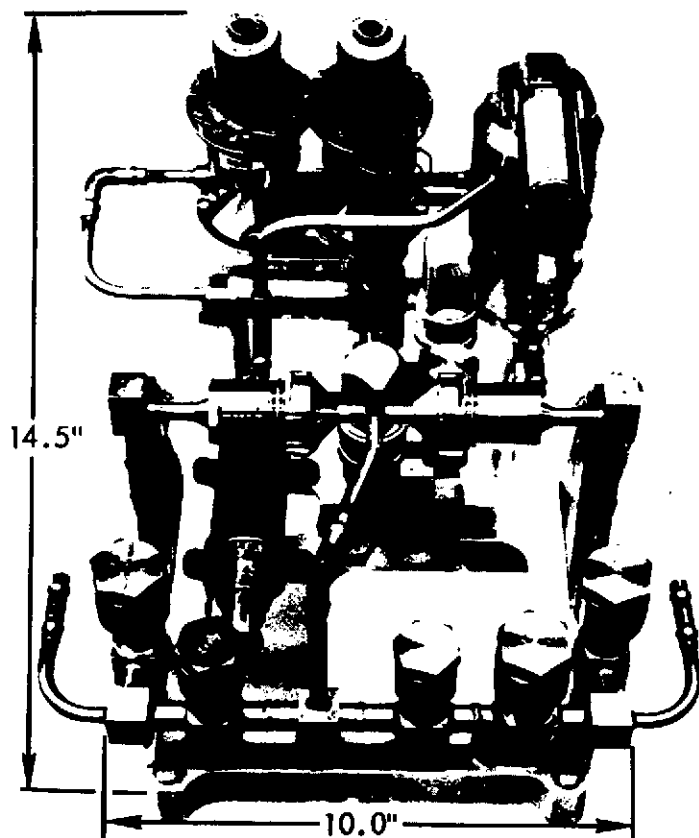
# PROPELLANT TANK ASSY



B-10

# PROPULSION SYSTEM

## PRESSURANT CONTROL ASSEMBLY



B-11

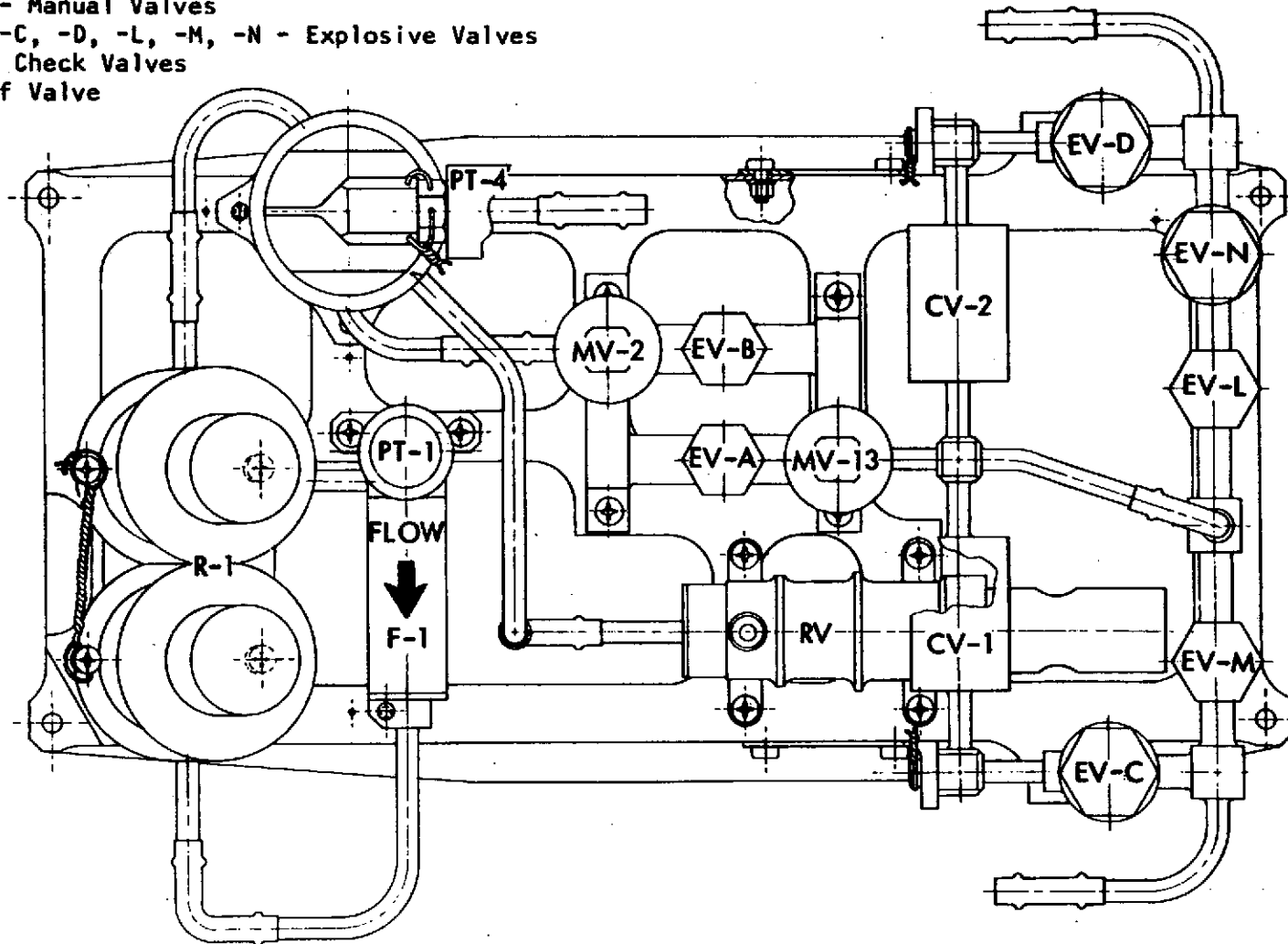
OPERATING PRESSURE:	
HI PRESSURE SIDE (INLET)	4000 PSIG
LO PRESSURE SIDE (OUTLET)	214±6 PSIG
PROOF PRESSURE:	
HI PRESSURE SIDE	6680 PSIG
LO PRESSURE SIDE	500 PSIG
BURST PRESSURE:	
HI PRESSURE SIDE	8000 PSIG
LO PRESSURE SIDE	600 PSIG
OPERATING TEMPERATURE:	0-100 F
STORAGE TEMPERATURE:	0-120 F
NOMINAL FLOWRATE (ENGINE + ACS)	0.011 LBS/SEC GN <sub>2</sub>
NOMINAL PRESSURE DROP:	6.0 PSID GN <sub>2</sub>
EXTERNAL LEAKAGE:	2X10 <sup>-5</sup> SCC/SEC AT 4000 PSIG
WEIGHT:	12.7 LBS

55915-68

**TRW**  
SYSTEMS GROUP

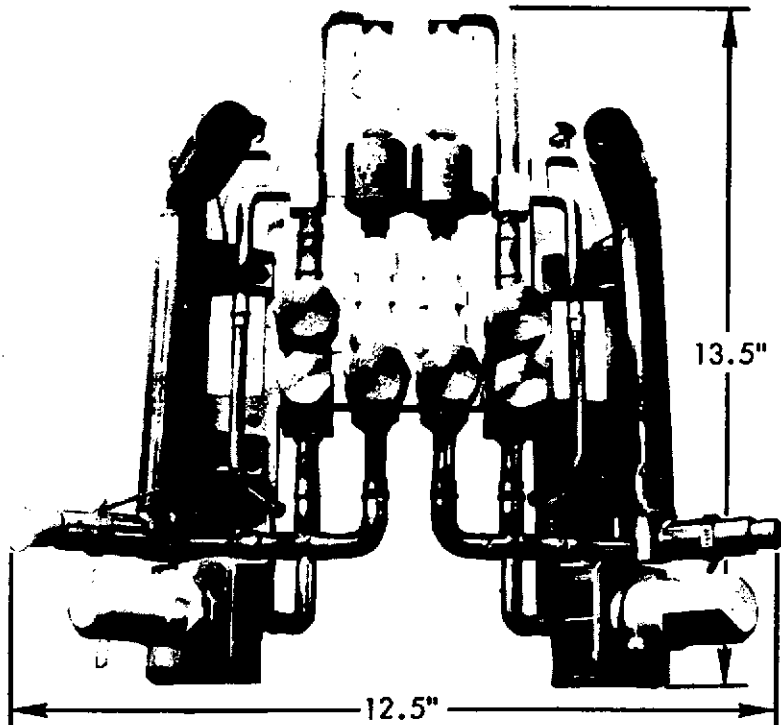
## PRESSURANT CONTROL ASSY

- R-1 - Regulator
- PT-1, -4 - Pressure Transducers
- F-1 - Gas Filter
- MV-2, -13 - Manual Valves
- EV-A, -B, -C, -D, -L, -M, -N - Explosive Valves
- CV-1, -2 - Check Valves
- RV - Relief Valve



# PROPULSION SYSTEM

## PROPELLANT SUPPLY ASSEMBLY

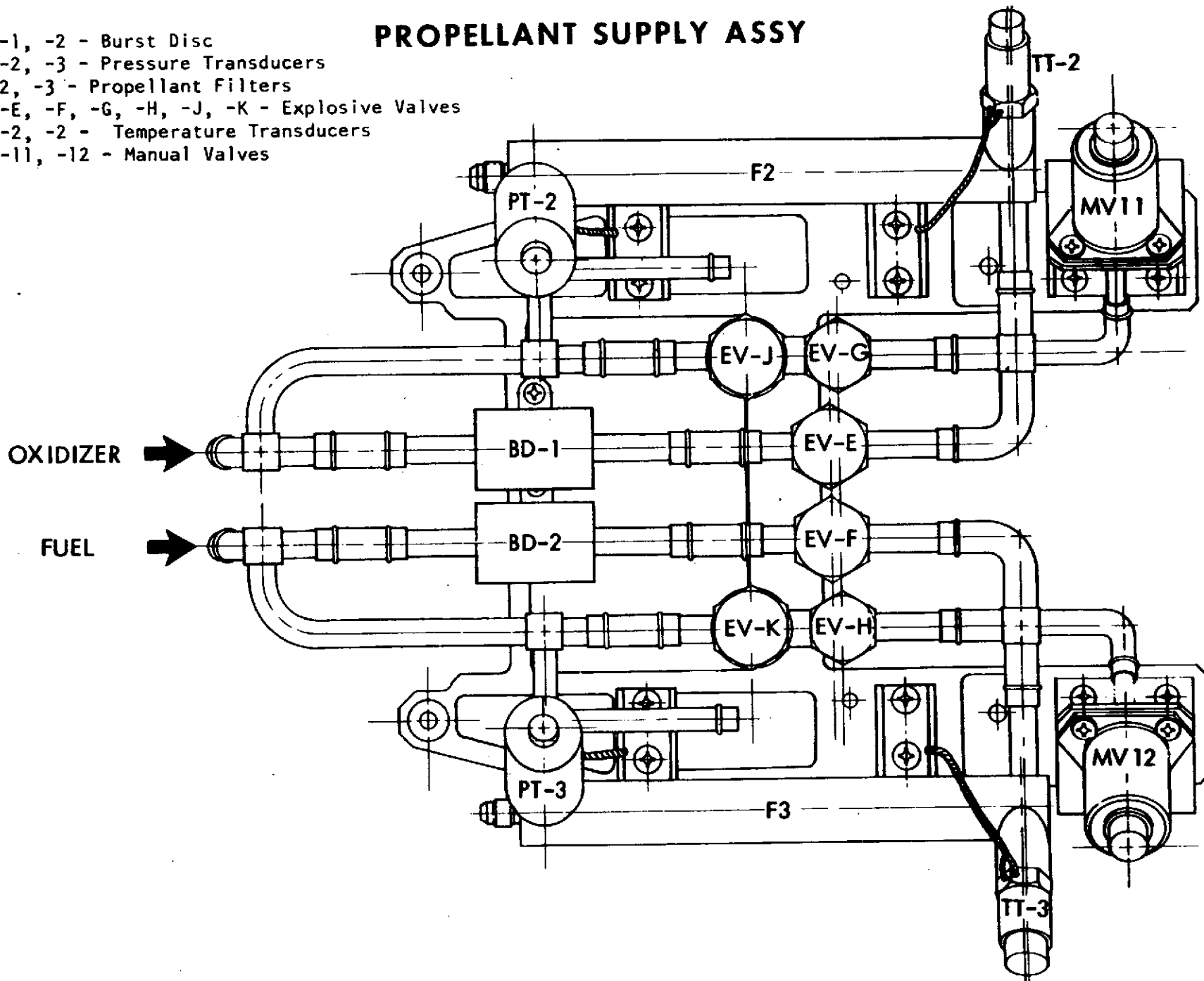


55911-68

OPERATING PRESSURE:	300 PSIG
PROOF PRESSURE:	500 PSIG
BURST PRESSURE:	600 PSIG
OPERATING TEMPERATURE:	30-90 F
STORAGE TEMPERATURE:	0-120 F
NTO	0.209 LBM/SEC
MMH	0.131 LBM/SEC
NOMINAL PRESSURE DROP:	7.0 PSID
LEAKAGE:	
EXTERNAL	6.0X10 <sup>-5</sup> SCC/SEC He AT 300 PSIG
	ZERO LIQUID LEAKAGE
INTERNAL	1X10 <sup>-7</sup> SCC/SEC He AT 300 PSID
WEIGHT:	7.4 LBS

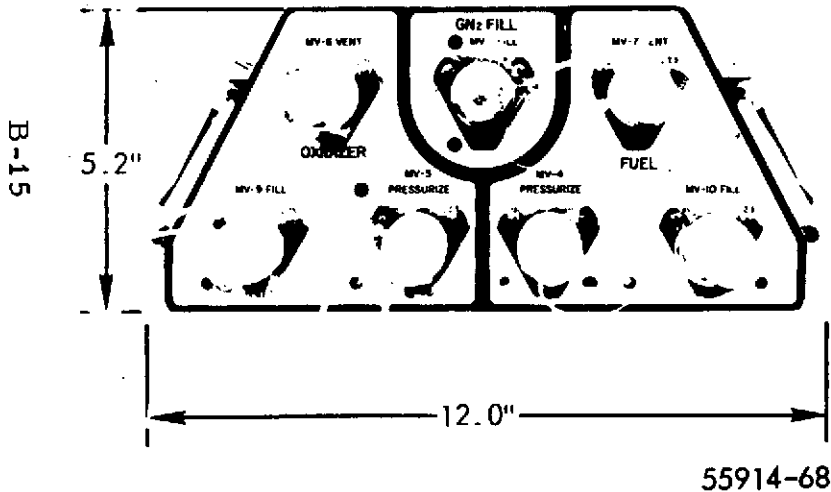
# PROPELLANT SUPPLY ASSY

- BD-1, -2 - Burst Disc
- PT-2, -3 - Pressure Transducers
- F-2, -3 - Propellant Filters
- EV-E, -F, -G, -H, -J, -K - Explosive Valves
- TT-2, -3 - Temperature Transducers
- MV-11, -12 - Manual Valves



B-14

# PROPULSION SYSTEM FILL AND VENT ASSEMBLY



**OPERATING PRESSURE:**

HI PRESSURE INTERFACE (GN<sub>2</sub>)      4000 PSIG  
 LO PRESSURE INTERFACE (PROPELLANTS)    240 PSIG

**PROOF PRESSURE:**

HI PRESSURE INTERFACE                    6680 PSIG  
 LO PRESSURE INTERFACE                    575 PSIG

**BURST PRESSURE:**

HI PRESSURE INTERFACE                    8000 PSIG  
 LO PRESSURE INTERFACE                    690 PSIG

**OPERATING TEMPERATURE:**

0-100 F

**STORAGE TEMPERATURE:**

0-120 F

**EXTERNAL LEAKAGE:**

HI PRESSURE                                 $8 \times 10^{-7}$  SCC/SEC    He  
 LO PRESSURE                                 $8 \times 10^{-7}$  SCC/SEC    He

**MANUAL VALVES CYCLE LIFE:**

100 CYCLES

**WEIGHT:**

2.8 LBS

**MSSPS/AGE INTERFACES:**

HI PRESSURE NITROGEN FILL VALVE  
 PROPELLANT TANK FILL VALVES  
 PROPELLANT TANK VENT VALVES

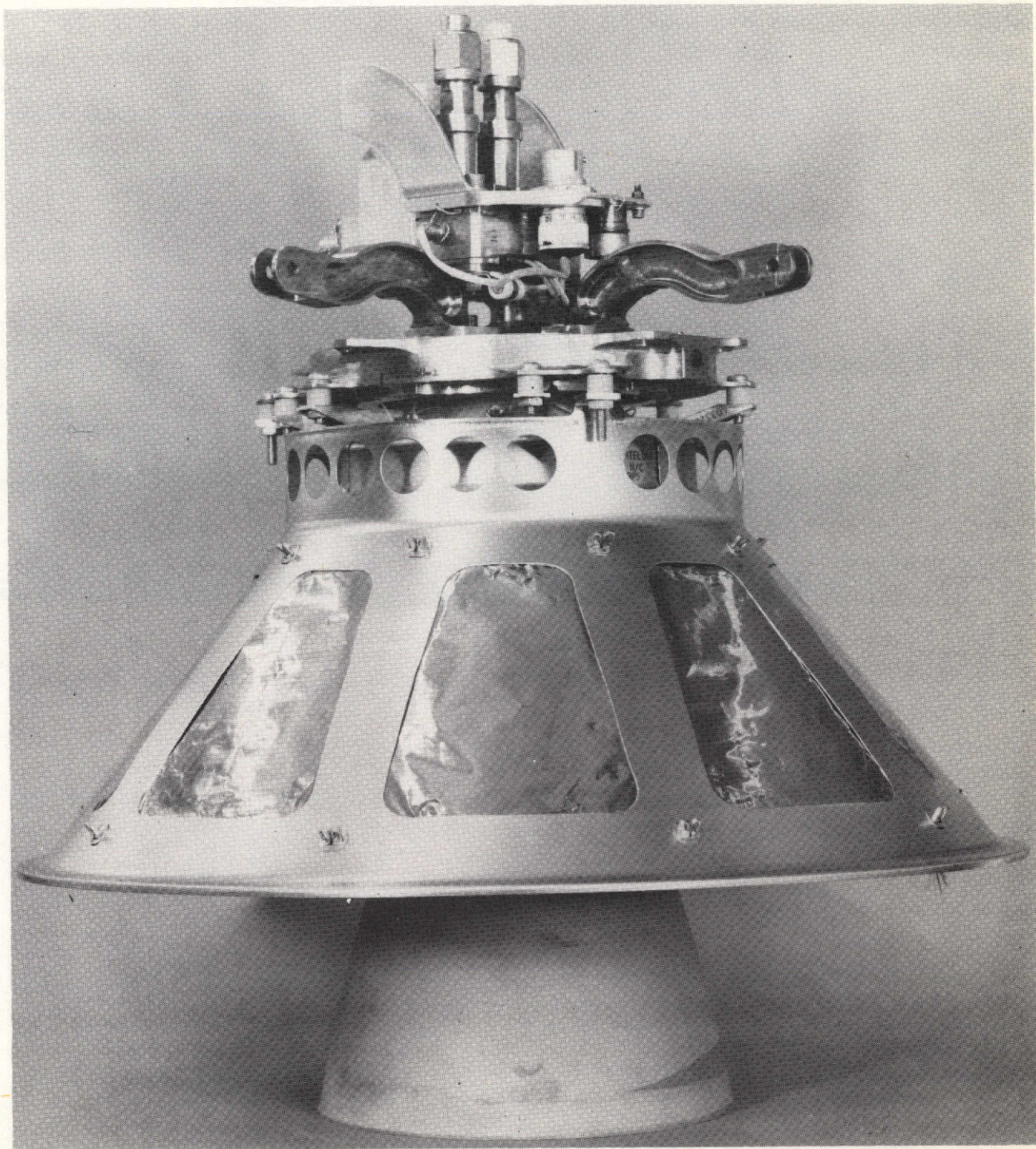
## PROPULSION SYSTEM

### ENGINE ASSEMBLY DESIGN AND PERFORMANCE CHARACTERISTICS



50617-68

THRUST (NOMINAL)	88 LBS
CHAMBER PRESSURE:	91 PSIA
EXPANSION AREA RATIO:	52:1
PROPELLANTS:	NTO/MMH
MIXTURE RATIO:	1.64±.04
SPECIFIC IMPULSE: (3σ MINIMUM)	292 SECS
PROPELLANT TEMPERATURE RANGE:	30 TO 90 F
PROPELLANT SUPPLY PRESSURE:	185±5 PSIA
THRUST VECTOR OFFSET	.050 INCH MAXIMUM
MINIMUM FIRING DURATION	0.1 SECOND
RESTART CAPABILITY:	5 MINIMUM
GIMBAL ANGLE:	±5°
SERVICE LIFE:	4,550 SECS
QUAL REQMT (3X SERVICE LIFE):	13,650 SECS
ACTUAL DEMONSTRATED LIFE:	25,000 SECS
DEMONSTRATED IMPULSE CAPABILITY	2.2 MILLION LB - SECS
WEIGHT (INCLUDING HEAT SHIELD):	10.3 LB <sub>M</sub> MAXIMUM
POWER REQUIREMENTS:	
VALVE	12 WATTS AT 24 VDC
HEATER	8 WATTS AT 24 VDC



## **ELECTRICAL/TELEMETRY REQUIREMENTS**

### **ELECTRICAL**

- o ACTUATION OF EXPLOSIVE VALVES (13)
- o BIPELLANT VALVE OPERATION
- o ENGINE HEATER AND THERMOSWITCH CIRCUIT
- o OPERATION OF PNEUMATIC SUBSYSTEM VALVES FOR ACS CONTROL

### **TELEMETRY**

- o PRESSURE TRANSDUCERS
- o THERMISTORS

**PROPELLANT IMMERSION  
SURFACE MOUNTED**